UNIVERSITÀ DEGLI STUDI DI PADOVA

DIPARTIMENTO DI INGEGNERIA CIVILE EDILE E AMBIENTALE

HYDRAULICS AND COASTAL ENGINEERING LABORATORY,
AALBORG UNIVERSITY, DK

CORSO DI LAUREA MAGISTRALE IN INGEGNERIA CIVILE

Tesi di Laurea Magistrale

Experimental investigation on caisson breakwater sliding

Indagine sperimentale sullo scorrimento di una diga a cassoni

Relatore
Ch.mo Prof. Piero Ruol

Correlatori
Dott. Ing. Luca Martinelli
Prof. Ing. Thomas Lykke Andersen

Laureando
Paolo Martin

Anno Accademico 2012/2013

Acknowledgments

I would like to express gratitude for the patient guidance of supervisors Thomas Lykke Andersen and Jørgen Harck Nørgaard at Aalborg University, as well as Adrian Batacui and Radu Catalin Ciocan for having work together in this project as a real team. I would like to acknowledge the staff at the laboratory facilities of the Civil Engineering Department of Aalborg University, Niels Drustrup and Kim Borup, for their crucial help during test setup model testing. Finally a special thanks goes to my Professors at Padova University, Piero Ruol and Luca Martinelli, for their support and willingness in the final part of work.

Contents

Contents 5

I Introduction 7

1 Introduction 9
1.1 Introduction to project and project objectives . . . 9
1.2 Definition and current status of caisson breakwaters . . . 9
1.3 Most frequent failure modes for caisson breakwaters . . . 12

II Model testing 13

2 Plan for Model Testing 15
2.1 Flume setup . . . 17
2.2 Model and Setup . . . 17
2.3 Foundation of the breakwater . . . 20
2.4 Pressure transducers . . . 21
2.5 Wave Gauges . . . 22
2.6 The friction coefficient . . . 23

III Test results and analysis 25

3 Wave generation and analysis 27
3.1 Wave generation . . . 27
3.2 Wave analysis . . . 28

4 Pressure Profiles and Forces 31
4.1 Horizontal Force . . . 34
4.2 Uplift Force . . . 36
4.3 Overturning Moment . . . 38
4.4 Location of maximum pressure . . . 42
4.5 Setups comparison . . . 43

5 Displacements and Rotation 45
5.1 Rocking analysis . . . 46
5.2 Sliding analysis . . . 47
5.3 Expected sliding distance . . . 51
5.4 Qualitative dynamic response . . . 54

IV Conclusions 59

6 Uncertainties and Errors 61

7 Conclusion 63
7.1 Answers to the research questions . . . 63
7.2 Suggestions for improvement . . . 64

V Literature **65**

Bibliography **67**

VI Appendix **69**

A Analytical models **71**
A.1 Breaking wave height 72
A.2 Forces acting on the caisson 74
A.3 Scaling 75

B Result Plots **77**

C MATLAB scripts **97**
C.1 Main program 97
C.2 Wave length calculation 105
C.3 Convertion from Volts to Pressure for the front wall of the caisson 106
C.4 Convertion from Volts to Pressure for the bottom surface of the caisson . 109
C.5 Goda forces compared with measured forces 112

Part I

Introduction

1 Introduction

1.1 Introduction to project and project objectives

This project presents the conducting and the results of scaled, physical model tests for the purpose of analyzing the forces acting on a caisson breakwater and the sliding that these forces may produce.
For the purpose of data gathering, several parameters are varied in order to assess their influence on the behavior of the structure and on the acting forces. These parameters include water depth, wave height, wave breaking, wave period and mass of the caisson. An experimental setup is presented, along with a description of the materials and instrumentation used. Then, a series of tests are conducted where parameters are varied and the response of the structure recorded. The data collected from the tests is then processed. A comparison is made between the forces found in the experiment and the forces obtained by using wave load formulas, as well as the caisson displacements compared with an existing model used to predict the sliding distance. Also, some research objectives are formulated.
In a separate chapter, sources of errors and uncertainties, as well as solutions to avoid or compensate are presented.

1.2 Definition and current status of caisson breakwaters

Caisson breakwaters are vertical wall structures meant to protect coastlines and harbors from the damaging or even destructive wave actions. They are also used for protection of navigation channels and beaches against sediment transportation.

They are composed by three main parts: the superstructure, the substructure and the rubble mound foundation.
The superstructure is composed of a parapet wall and deck; the parapet wall is meant to reduce overtopping over the structure while the deck serves as a roadway or a pavement. The substructure is built out of caissons; a caisson is an open reinforced concrete box with a bottom slab and outer walls. A large caisson is usually divided into several inner cells by partition walls in order to reduce the span length of the outer walls. The footings at the front and back heels of the caisson have the role of increasing the contact surface between the caisson and the foundation, thus increasing the load-transfer area.
The rubble mound foundation acts like a buffer between the substructure and the sea bed, spreading the vertical load from the substructure over a wide area of sea bed. Other than this, it protects the foot of the caisson (seaward side) against instability, with a row of foot protection blocks and a front armor layer. Therefore the rubble mound foundation consists in the already specified armour layer, a core and, if necessary, a filter layer, with smaller stone diameters going deeper.

Vertical wall breakwaters are massive structures and they resist to waves thanks to gravity, reflecting them completely or partially. They are preferred to rubble-mound breakwaters in no-breaking wave situations.
In general, there are several types of vertical wall breakwaters.

First category is represented by the conventional caisson breakwaters with vertical front. They are built in a specific construction site, to whom is followed the transfer, through buoyancy, to the location where they have to be placed. In fact the inner structure is

cellular, as explained before, which is then filled by sand when the positioning begins, so it can be easily removed in case of mainteinance works or relocations.

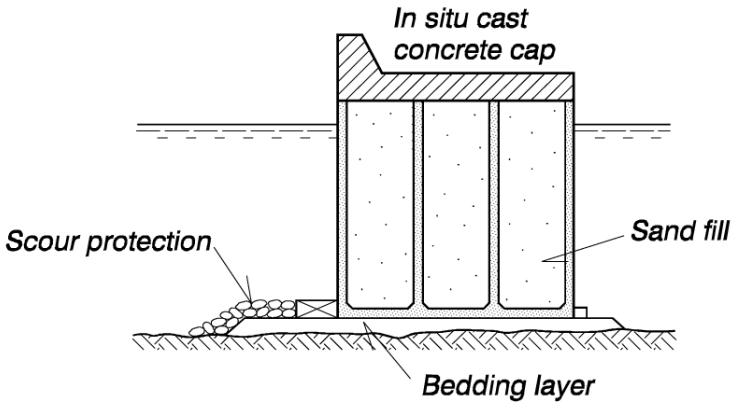

Figure 1.1. Conventional caisson breakwater with vertical wall. CEM [2012]

Another category, similar to the first one, is represented by vertical composite caisson breakwaters, lying on a thick layer of rubble-mound foundation. They are tipically used for waves with smaller amplitude than those in the first case.

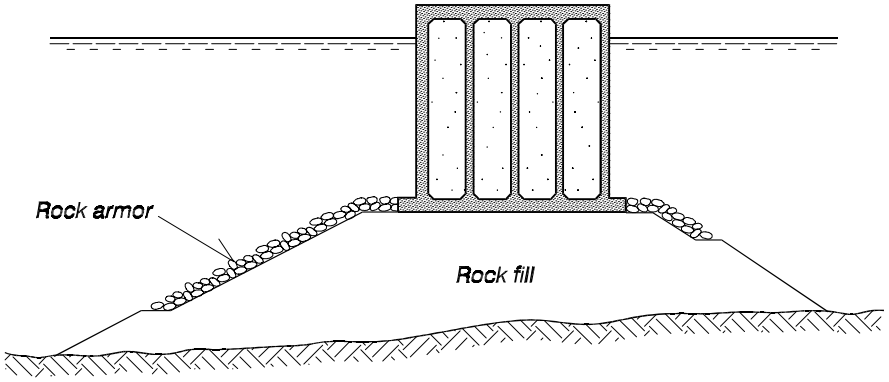

Figure 1.2. Vertical composite caisson breakwater. CEM [2012]

When greater stresses for the structure may occur, horizontal composite caisson breakwaters can be used. They present a front wall covered by armor units or a rubble-mound structure.

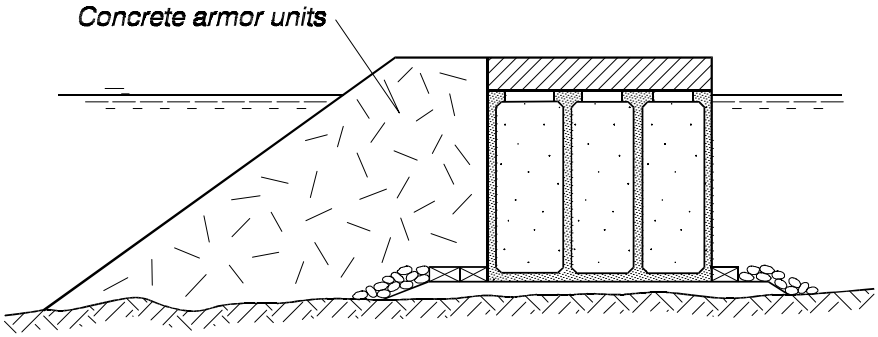

Figure 1.3. Horizontal composite caisson breakwater. CEM [2012]

In order to induce less reflection, perforated front wall caisson breakwaters are a good solution.

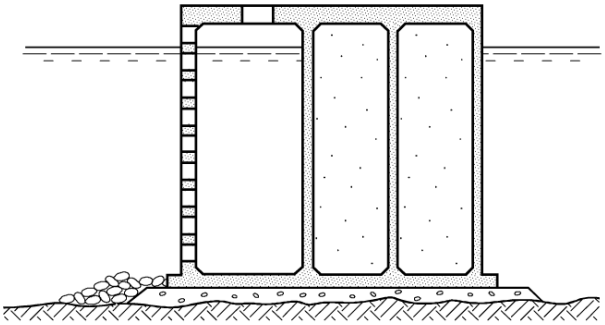

Figure 1.4. Perforated front wall caisson breakwater. CEM [2012]

Another category is that of blockwork breakwaters, applied only if there is a rock seabed or a very strong soil, due to very high foundation loads. Their use is almost ceased.

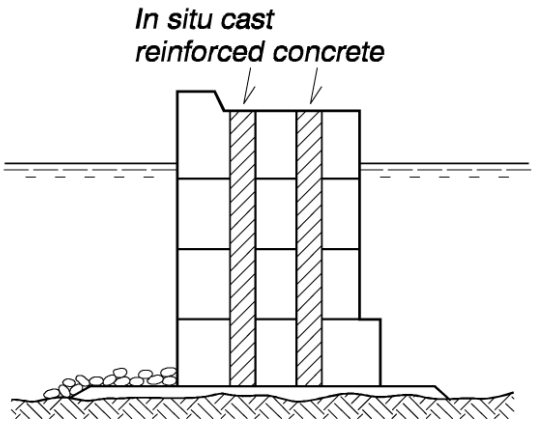

Figure 1.5. Blockwork breakwater. CEM [2012]

It is again possible to build vertical wall breakwaters of Cofferdam type, with sheet piles joined toghether in such a way that they create huge cilinders, later filled with concrete.

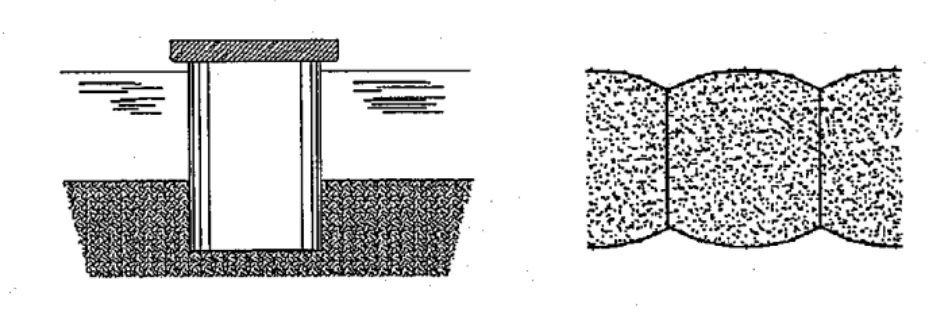

Figure 1.6. Cofferdam barrier. CEM [2012]

1.3 Most frequent failure modes for caisson breakwaters

According to Goda and Takagi [2000], based on the occurrence frequency observed in Japan, sliding represents one of the most important failure types for caisson breakwater on rubble mound foundation. The observed occurrence frequency is illustrated below, in Table 1.1.

Table 1.1. Occurence frequency. [Goda and Takagi, 2000]

Most occured	Failure type
1	Sliding of caissons
2	Displacement of concrete blocks and large rubble stones armoring a rubble foundation mound
3	Breakage and displacement of armor units in the energy-dissipating mound in front of a caisson
4	Rupture of front walls and other damage on concrete sections of a caisson
5	Failure in the foundation and subsoil

Considering that sliding is the most frequent failure mode, it is very important to document and study it in order to create tools for better understanding the phenomena involved. It is the purpose of this report to identify areas where more information is needed in the research on the sliding of caissons, and add to the work that has been done.

The present project will analyze the sliding failure mode, but in the tests that will be performed in this project sliding and overturning are expected to occur. These two failure types are illustrated separately in Figure 1.7.

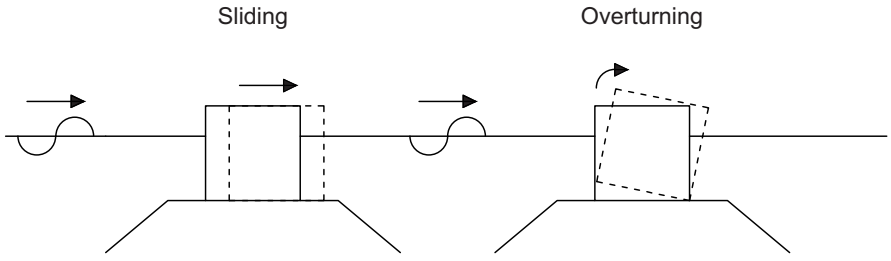

Figure 1.7. Possible failure modes.

These investigations will be the main goal of the present project. A similar scaled model will be used but with load measuring equipment both on the moving and fixed part of the model, thus it will be possible to discuss the influence sliding has on the wave loads. The wave types will also be varied, the present project will use regular and irregular types for both breaking and non-breaking waves.

Part II

Model testing

2 Plan for Model Testing

This part of the project will describe how the scaled model will be tested in the laboratory, illustrate its dimensions and explain the reasons for varying different parameters.
The scaled model is build and tested in one of Aalborg University's wave flumes. The setup for the tests and the model are presented in section 2.2. It is important to note that the model is equipped with both a fixed and a movable section. The movable section allows for sliding and is equipped with displacement-measuring gauges.

The parameters varied during the tests are:

Mass Since vertical breakwaters use their own weight to resist wave loads, the mass is very important in determining stability. This being said, three different values will be used for the laboratory tests, one over the threshold where sliding is expected to occur, and two othes that will allow sliding to occur. Values for the expected mass at sliding are calculated using the method presented in appendix A.2. The initial estimation for the mass is done using the Goda formula for wave forces, using a non-breaking wave. Because of the short duration of impulsive loads and their rare occurrence, existing breakwaters are designed using this formula and safety coefficients. If the design wave forces were estimated using formulas for impulsive loads, the weight of the caisson would need to be much higher.

Still Water Level Each mass will be tested against three different water levels. The values for the highest SWL were chosen in order to obtain a large wave height, thus the highest possible forces on the caisson wall. The intermediate and lowest SWL were chosen so that there is significant difference from the first SWL, but relatively little difference between them. These SWLs were chosen in order to observe the increase of wave forces caused by a relatively small increase in water level versus the increase caused by a significant increase. SWL influences the wave height at which breaking occurs, and it is important to consider also because currently, due to different factors, the sea-levels are rising, with the risk of future cost to populations and activities in coastal areas. By analogy to a real prototype, the difference between SWL two and three simulates a water level increase of 0.5 m at a scale of $1 : 42.5$.

Wave height and period Wave heights and periods are calculated using the method explained in Appendix A. Non-breaking, breaking and irregular waves will be generated during model testing. This variety is useful for validating the formulas used and verifying the methods adopted. The steeper waves that are necessary for wave-breaking tests will be generated using the Stream function. Irregular waves simulate the wave expected in a storm, using a JONSWAP spectrum with a chosen peak enhancement factor, 3.3 in this case, significant wave height and peak period, which will be detailed later on.

Next, a test programme is established, taking into consideration the variations mentioned before. The test programme can be seen in Table 2.1. Each test consists of 60 waves, which will allow for a sufficient amount of sliding to occur. For the irregular wave tests, in the columns H and T, the significant wave height and peak period are shown.

Table 2.1. Test programme for model testing.

Test	Mass[kg]	SWL[m]	H[m]	T[s]	Observation
1.1.1	113	0.35	0.10	1.12	non-breaking
1.1.2	113	0.35	0.20	1.53	non-breaking
1.1.3	113	0.35	0.27	2	breaking
1.1.4	113	0.35	H_s=18	T_p=1.53	irregular wave test
1.2.1	113	0.33	0.10	1.12	non-breaking
1.2.2	113	0.33	0.20	1.53	non-breaking
1.2.3	113	0.33	0.25	2	breaking
1.2.4	113	0.33	H_s=18	T_p=1.53	irregular wave test
1.3.1	113	0.25	0.10	1.12	non-breaking
1.3.2	113	0.25	0.20	1.53	non-breaking
1.3.3	113	0.25	0.20	2	breaking
1.3.4	113	0.25	H_s=18	T_p=1.53	irregular wave test
2.1.1	123	0.35	0.10	1.12	non-breaking
2.1.2	123	0.35	0.20	1.53	non-breaking
2.1.3	123	0.35	0.27	2	breaking
2.1.4	123	0.35	H_s=18	T_p=1.53	irregular wave test
2.2.1	123	0.33	0.10	1.12	non-breaking
2.2.2	123	0.33	0.20	1.53	non-breaking
2.2.3	123	0.33	0.25	2	breaking
2.2.4	123	0.33	H_s=18	T_p=1.53	irregular wave test
2.3.1	123	0.25	0.10	1.12	non-breaking
2.3.2	123	0.25	0.20	1.53	non-breaking
2.3.3	123	0.25	0.20	2	breaking
2.3.4	123	0.25	H_s=18	T_p=1.53	irregular wave test
3.1.1	103	0.35	0.10	1.12	non-breaking
3.1.2	103	0.35	0.20	1.53	non-breaking
3.1.3	103	0.35	0.27	2	breaking
3.1.4	103	0.35	H_s=18	T_p=1.53	irregular wave test
3.2.1	103	0.33	0.10	1.12	non-breaking
3.2.2	103	0.33	0.20	1.53	non-breaking
3.2.3	103	0.33	0.25	2	breaking
3.2.4	103	0.33	H_s=18	T_p=1.53	irregular wave test
3.3.1	103	0.25	0.10	1.12	non-breaking
3.3.2	103	0.25	0.20	1.53	non-breaking
3.3.3	103	0.25	0.20	2	breaking
3.3.4	103	0.25	H_s=18	T_p=1.53	irregular wave test

Due to the limited number of pressure transducers, in order to have comparable results from the fixed and moving part of the scaled-model, during the tests previously presented, the pressure-measuring gauges will be kept on one part at a time, with 5 gauges on the other part for validation.

2.1 Flume setup

The physical model was built in the Shallow Water Wave Flume at the Hydraulics and Coastal Engineering Laboratory of Aalborg University. The dimensions are 25 m of length, 1.5 m of width and 1 m of depth. The flume is equipped with a piston-type wave generator and with 5 porous walls, which permits to avoid the generation of cross waves. Due to an active absorption system, reflected waves are damped, based on data coming from a series of wave gauges next to the paddle of the generator.

In figures 2.1 and 2.2 it is shown the flume setup for the tests, with the position of the breakwater model, the wave gauges, the porous walls and the wave generator.

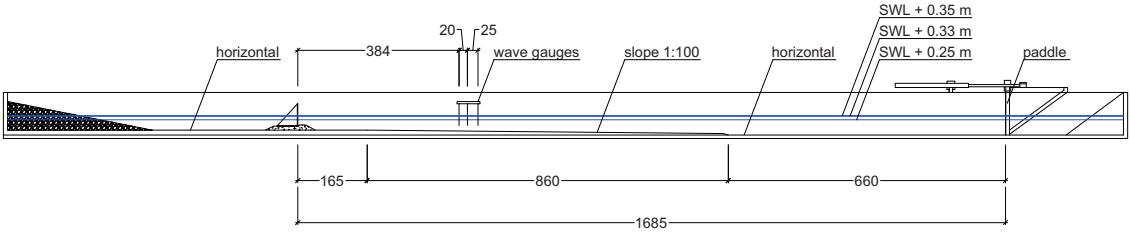

Figure 2.1. Flume setup for the tests. Longitudinal view. (annotations in [mm])

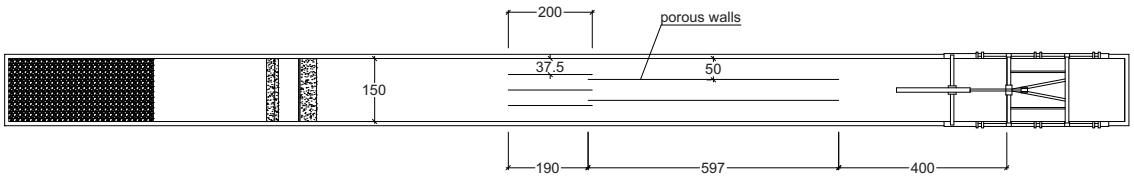

Figure 2.2. Flume setup for the tests. Top view. (annotations in [mm])

2.2 Model and Setup

The model that will be used for the experimental part of this project will be illustrated here with it's exact dimensions and gauges positions.
First it's important to say that the model is divided into three parts, two fixed parts and a moving one, as illustrated in figure 2.3 and 2.4. One of the fixed parts and the moving part will have pressure gauges on them in the same configuration, in order to observe the difference in wave loads between a moving and a fixed structure.

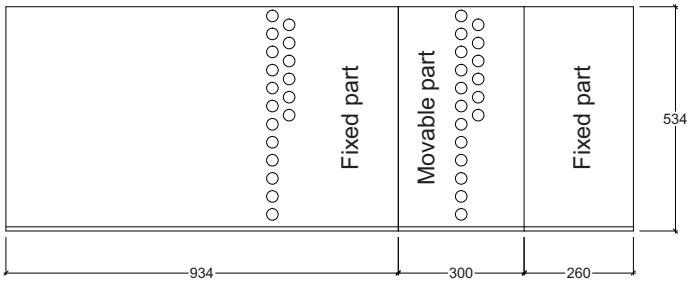

Figure 2.3. General overview of the model. Frontal view.

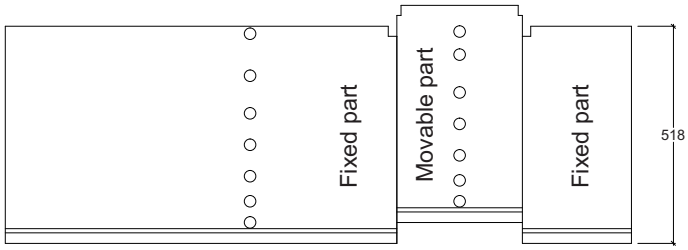

Figure 2.4. General overview of the model. Top view.

In Figure 2.5 the model is illustrated in 3 dimensions in order to give a better overview of its main components.

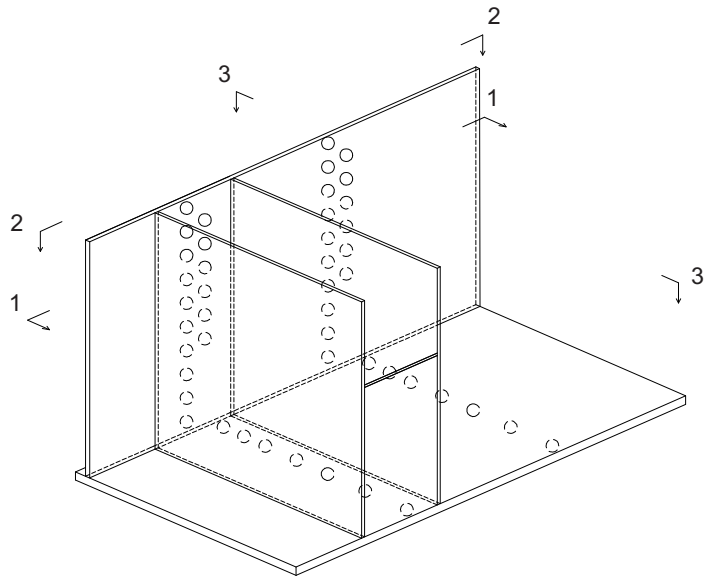

Figure 2.5. General perspective view of the model.

In figure 2.6, the exact positions of the measuring devices is illustrated on the fixed and moving parts of the model.

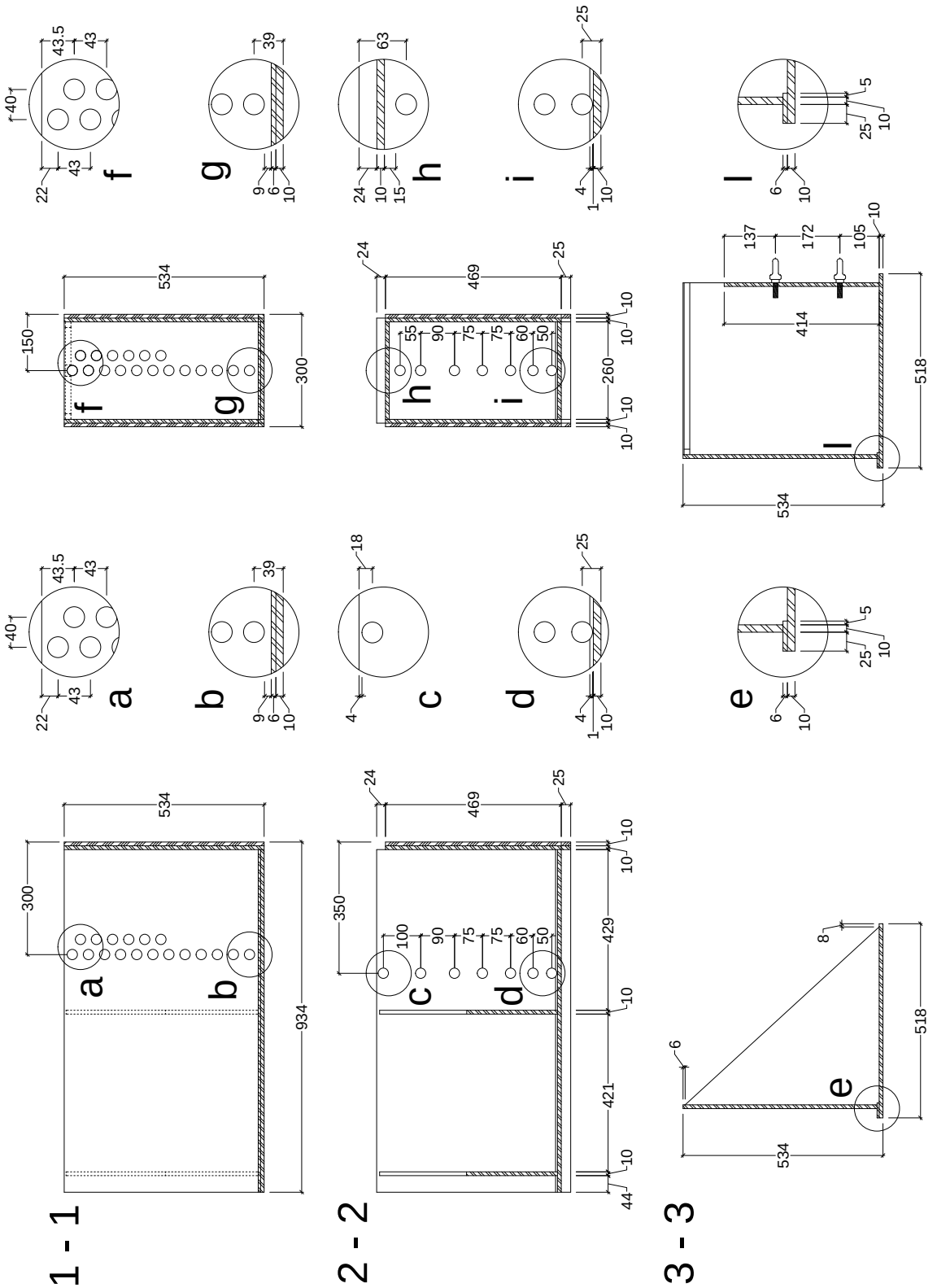

Figure 2.6. Gauges positions and elements dimensions.

The pressure gauges, shown in the previous figure as circles, are used to measure the exact wave load profile which will later be compared to the theory load profile. Also, to aid in the comparison between the moving and fixed parts, the transducers will be moved during the test. This process will be later described in more details.
The displacement measuring devices will be attached to the moving part in 2 points and thus the rotation of the moving part can be also calculated. The exact positions are illustrated in Figure 2.6.

2.3 Foundation of the breakwater

The study of the foundation is not the main focus of this project, therefore only the main aspects will be presented in this chapter.
Two types of rocks and a foot protection block were chosen and the specifications are reported in the table 2.2.

Table 2.2. Material specifications

Position	W_{50} [g]	Size [mm]	ρ [t/m^3]
Foot protection blocks	98	59x35x18	2.66
Core/filter material	0.46	D_{50} = 5.6	2.62
Front armor layer	8.85	D_{50} = 14.7	2.81

W_{50}	median weight of the armor stone
D_{50}	median diameter of the armor stone
ρ	density of the armor stone

The diameters of the three types of stones, given the mean weight, were calculated with the equation:

$$D_{n50} = \left(\frac{W_{50}}{\rho}\right)^{\frac{1}{3}} \tag{2.1}$$

D_{n50}	nominal diameter of the armor stone

The dimensions of the foundation are reported in the figure 2.7:

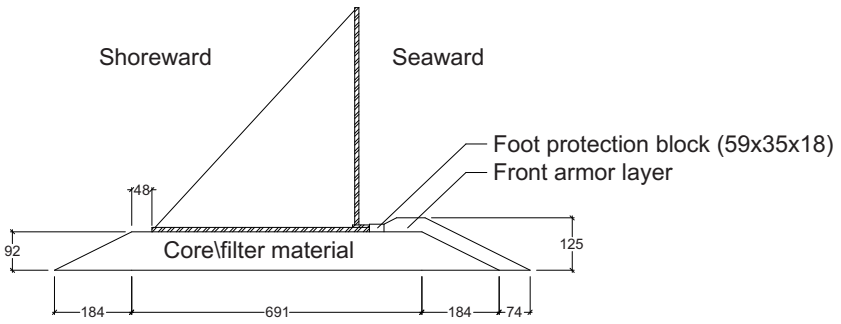

Figure 2.7. Gauges Positions and Elements Dimensions.

2.4 Pressure transducers

The pressure gauges used in this project are Druck PMP Unik 5000 and they are located as shown in the Figure 2.6.

The pressure transducers are tested before being mounted on the scaled model, by submersion under a column of water. After fixing them, calibrations are performed each time the transducers change position. Three measurements are taken:

- Measurement 1 The flume is left empty and the signals from the pressure transducers are recoded for 1 minute. The average of this recording is taken as zero-pressure, or pressure in-air.
- Measurement 2 Water is introduced into the flume. The water level is brought to the top of the caisson and another 1 minute recording is taken.
- Measurement 3 The water level is increased by 10 more centimeters, so the SWL is 10 cm above the caisson. A recording is then performed.

A linear fit is applied to the measurements, defining a calibration function, as shown in (2.2), where X represents the recorded value in Volts, and Y represents the corresponding pressure p(z), calculated using (2.3). Parameters a and b are the slope and the increment of the polynomial respectively, ρ is the water density, g is the gravitational acceleration, and z is de depth of water.

$$Y = aX + b \tag{2.2}$$

$$p(z) = \rho g z \tag{2.3}$$

A picture with the caisson having the pressure transducers mounted on it is shown below, in Figure 2.8.

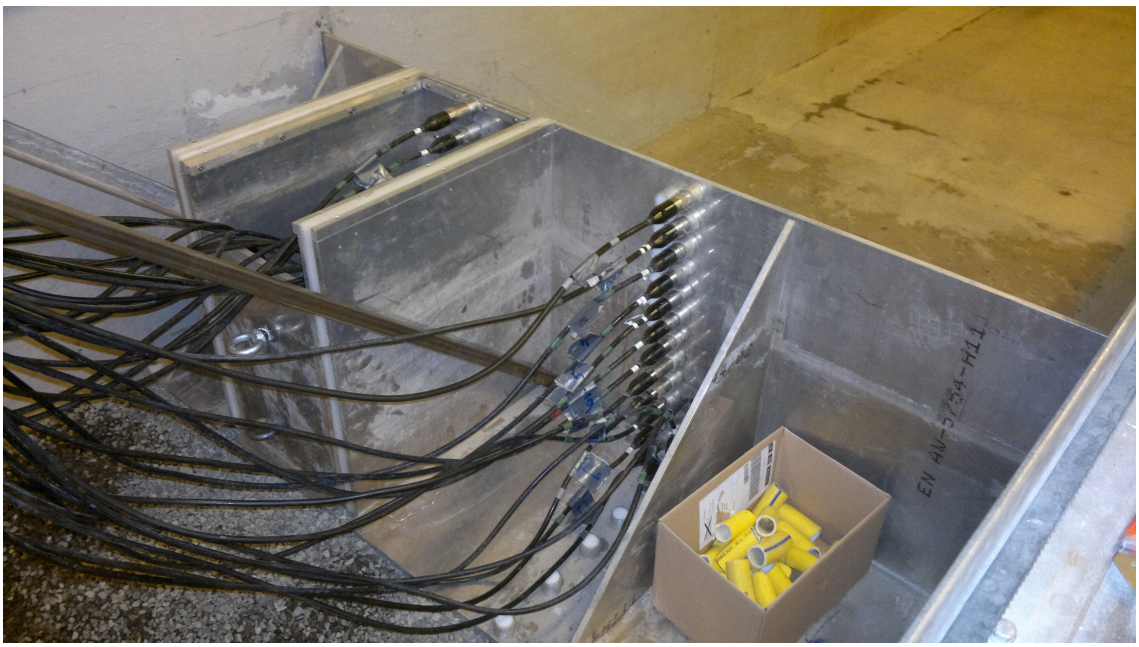

Figure 2.8. Picture of pressure-gauges.

2.5 Wave Gauges

Three waves gauges were placed in the flume, in order to measure the incident waves, which are not exactly the same as specified to the wave generator, and to separate them from the reflected waves.

The position of the waves gauges were chosen referring to Goda and Suzuki [1976]. Experiments showed that, to have reliable results, the gap between the wave gauges has to be larger than $0.1\times$ the maximum wave length of the incident wave, and smaller than $0.4\times$ the minimum wave length of the incident waves.
This can be seen in the Figure 2.9.

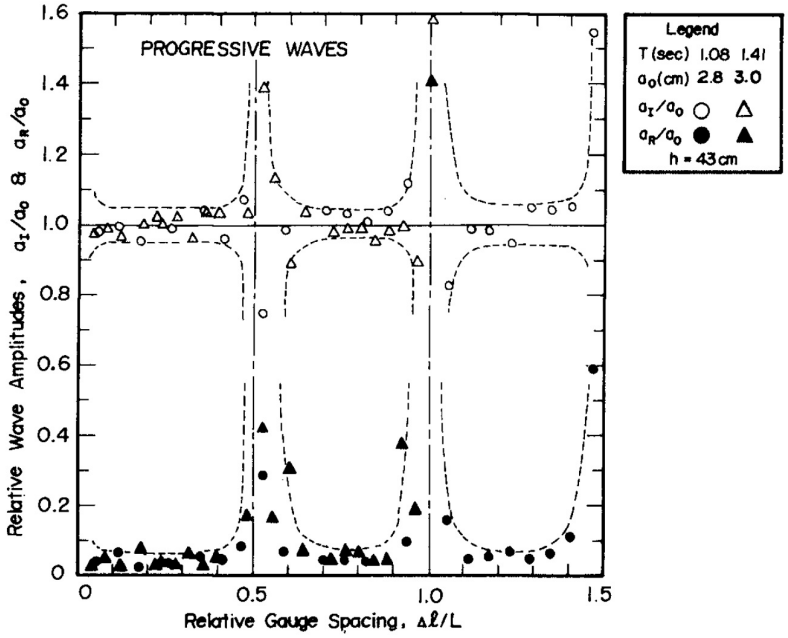

Figure 2.9. Relative wave gauges spacing, for progressive waves. [Goda and Suzuki, 1976]

With regard to the space between the vertical wall and the first wave gauge, the closest to the caisson, the only assumption is to guarantee, for the regular tests, a minimum distance of $0.2\times$ the maximum wave length of the incident wave, as it is shown in the Figure 2.10.

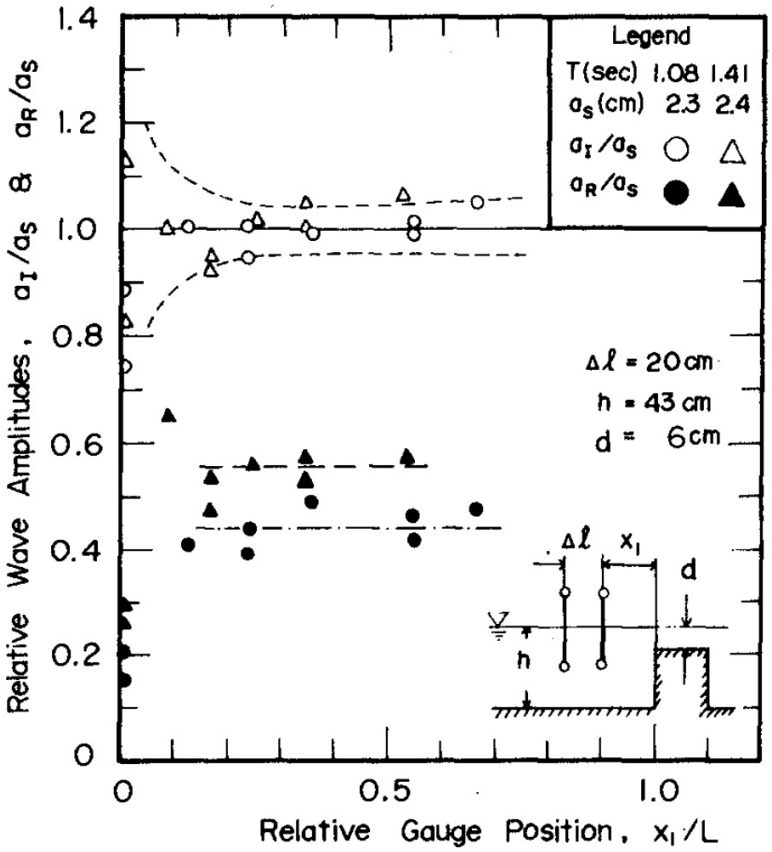

Figure 2.10. Relative wave gauge positioning with respect to the caisson. [Goda and Suzuki, 1976]

For the irregular tests, the minimum recommended distance is $1\times$ the maximum wave length of the incident wave.

The chosen array of wave gauges is reported in Figure 2.1.

2.6 The friction coefficient

The friction coefficient μ is very important for the sliding function, shown in equation (5.2). This coefficient is determined by dividing the force needed to drag the caisson over the foundation by the weight of the caisson. This coefficient is found to vary depending on the weight of the caisson, and whether the foundation is dry or wet. Changes in the positioning of the individual components of the foundation may explain why the coefficient changes. Also the friction coefficient can 'vary with the load duration' [Burcharth, Andersen, and Meinert, 2008]. To study this phenomenon, the flume is filled as in the experiment, and the weight changed. Table 2.3 shows the different parameters changed. For each weight, three measurements are taken and averaged. In Figure 2.11, it can be seen that μ increases proportional to the weight.

Table 2.3. Friction coefficient over wet foundation.

Weight [kg]	Friction coefficient [-]
103	0.446
113	0.451
123	0.471
133	0.518

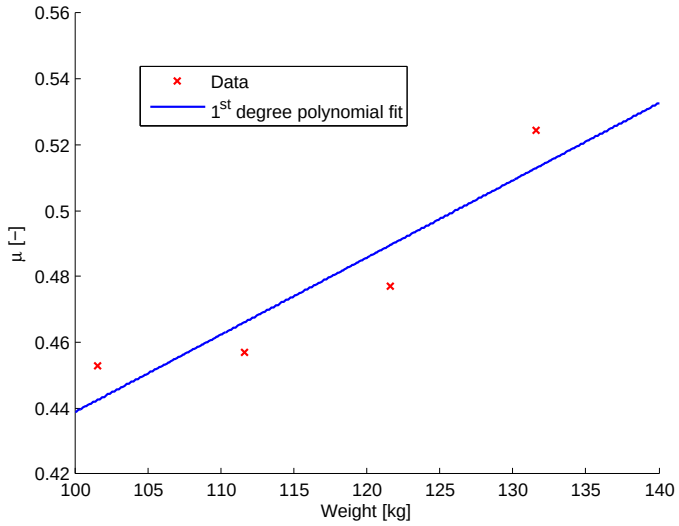

Figure 2.11. Friction coefficient measurements and fit.

Part III

Test results and analysis

3 Wave generation and analysis

3.1 Wave generation

Experiments were performed with the AWASIS system, developed at Aalborg University. According with the manufacturer, irregular waves were generated with the White Noise Filtering Method, a non-deterministic method which permits to obtain long time series without the repetition of the signal and with no discontinuities in the energy spectrum, compared to an InvFFT method.
The chosen power spectrum for irregular waves is JONSWAP (JOint North Sea WAve Project), which is typically used for seas with limited fetch. The peak enhancement parameter is $\gamma = 3.3$.

In figure 3.1 an example of the JONSWAP energy-spectrum is presented.

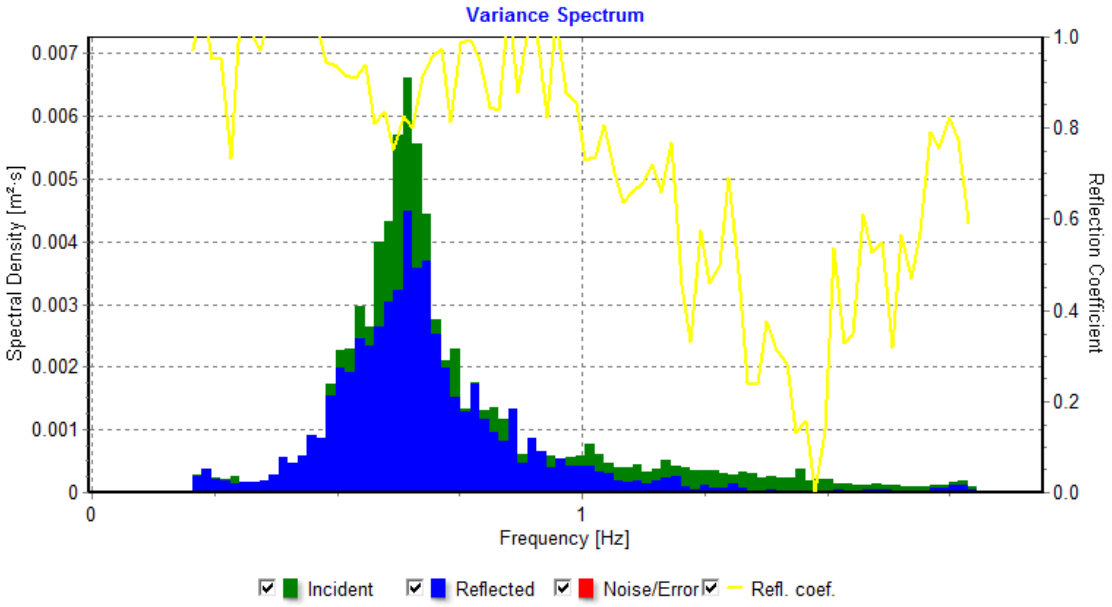

Figure 3.1. Example of a JONSWAP spectrum for an irregular waves test.

In the data acquisition configuration, the calibration functions were added for all the channels needed, in some case also the offset was inserted.
The pressure transducers were calibrated at 3 different water depths, as previously described in Chapter 2.4, while the 2 rotational potentiometers were calibrated recording the voltage referring to a complete turn of the wheel of the instrument. The wave gauges can be set in 2 positions, corresponding to a relative difference of 10 cm, therefore the same water depth was used for the calibration at the 2 different positions.
An example of a channel configuration is illustrated in Figure 3.2.

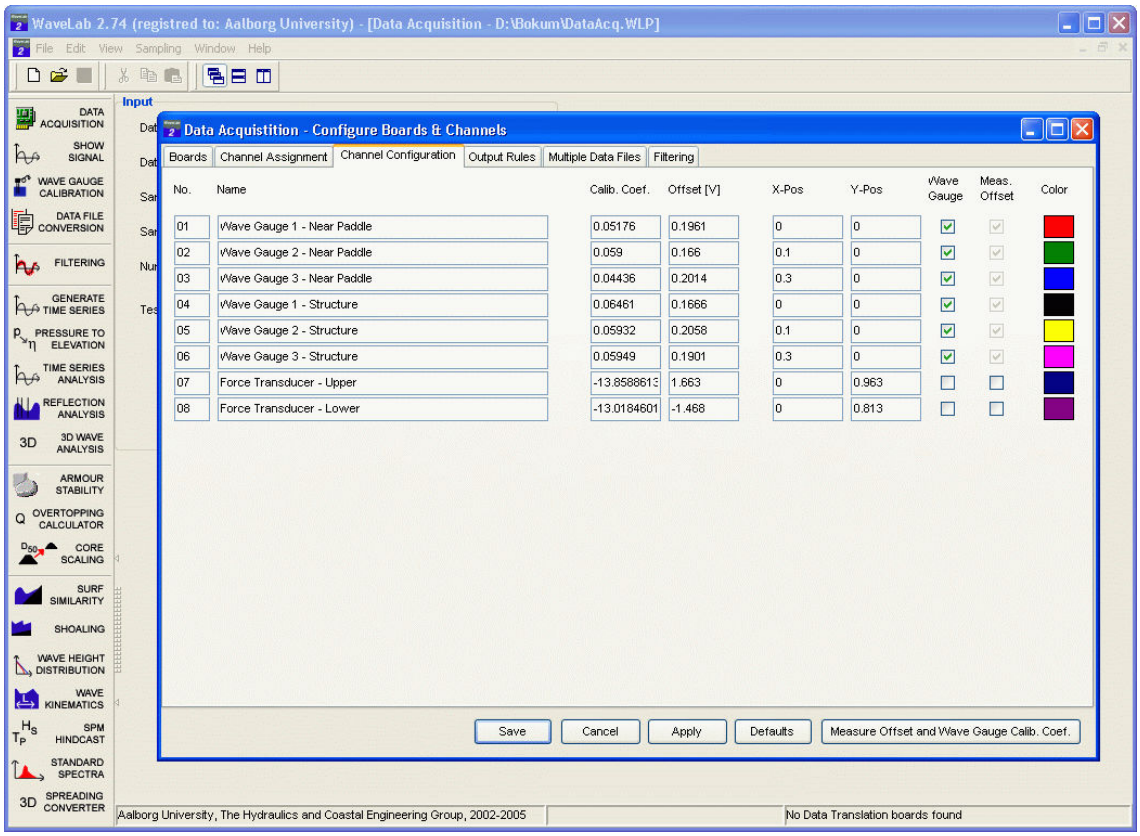

Figure 3.2. Example of the configuration Boards and Channels window.

3.2 Wave analysis

A wave analysis is needed after the tests are performed. In this project the WaveLab software was used, created at the Aalborg University. The program is based on the Mensard and Funke prescriptions, separating the incident spectra from the reflected spectra through a 'least squares method'.
From the time domain analysis was then possible to calculate the values of period and wave height for different return periods.

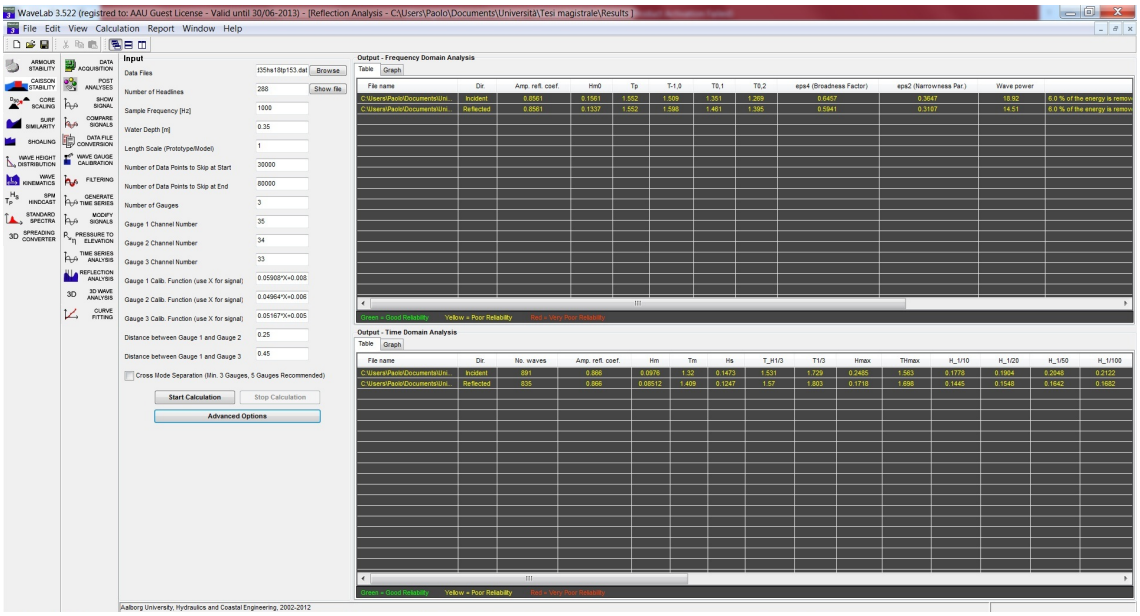

Figure 3.3. Wave analysis in the frequency domain and in the time domain, for an irregular waves test. Tables.

Figure 3.4. Wave analysis in the frequency domain and in the time domain, for an irregular waves test. Graphs.

A syntesis of the results for different probability of occurrence can be seen in the Table 3.1. For some large wave heights, the reflection analysis did not always return reliable results, due to a probable overtopping of the wave gauges, and this effect can be seen from the discrepancy between the specified wave height and the recorded wave height.

Table 3.1. Reflection analyisis (time domain)

Test	Observation	specified H[m]	Hm[m]	Hs[m]	$H_{1/20}$[m]
1.1.1	non-breaking	0.10	0.09	0.10	0.11
1.1.2	non-breaking	0.20	0.14	0.17	0.20
1.1.3	breaking	0.27	0.13	0.15	0.17
1.1.4	irregular wave test	H_s=18	0.09	0.13	0.16
1.2.1	non-breaking	0.10	0.07	0.08	0.08
1.2.2	non-breaking	0.20	0.14	0.16	0.19
1.2.3	breaking	0.25	0.18	0.19	0.20
1.2.4	irregular wave test	H_s=18	0.09	0.13	0.17
1.3.1	non-breaking	0.10	0.09	0.09	0.09
1.3.2	non-breaking	0.20	0.16	0.18	0.20
1.3.3	breaking	0.20	0.19	0.21	0.23
1.3.4	irregular wave test	H_s=18	0.09	0.13	0.17
2.1.1	non-breaking	0.10	0.09	0.10	0.10
2.1.2	non-breaking	0.20	0.12	0.16	0.18
2.1.3	breaking	0.27	0.13	0.18	0.20
2.1.4	irregular wave test	H_s=18	0.09	0.12	0.15
2.2.1	non-breaking	0.10	0.09	0.09	0.10
2.2.2	non-breaking	0.20	0.15	0.18	0.20
2.2.3	breaking	0.25	0.17	0.19	0.22
2.2.4	irregular wave test	H_s=18	0.09	0.14	0.18
2.3.1	non-breaking	0.10	0.09	0.10	0.11
2.3.2	non-breaking	0.20	0.18	0.21	0.22
2.3.3	breaking	0.20	0.16	0.20	0.21
2.3.4	irregular wave test	H_s=18	0.10	0.15	0.19
3.1.1	non-breaking	0.10	0.09	0.10	0.10
3.1.2	non-breaking	0.20	0.12	0.16	0.18
3.1.3	breaking	0.27	0.11	0.13	0.15
3.1.4	irregular wave test	H_s=18	0.09	0.12	0.15
3.2.1	non-breaking	0.10	0.10	0.10	0.10
3.2.2	non-breaking	0.20	0.17	0.19	0.21
3.2.3	breaking	0.25	0.17	0.20	0.22
3.2.4	irregular wave test	H_s=18	0.10	0.14	0.19
3.3.1	non-breaking	0.10	0.08	0.08	0.09
3.3.2	non-breaking	0.20	0.16	0.18	0.20
3.3.3	breaking	0.20	0.15	0.18	0.21
3.3.4	irregular wave test	H_s=18	0.10	0.15	0.20

4 Pressure Profiles and Forces

The first step in analysing the forces is comparing the measured forces on the caisson with the forces predicted using the Goda formula, as described in Equation (A.18), in Appendix A. This is the method proposed by H.Oumeraci, A.Kortenhaus, Allsop, de Groot, Crouch, Vrijling, and Voortman [2001]. First the pressures at the corners of the structure are extrapolated, and numerical integration over the height of the caisson is applied to determine this force.

The pressures at the top and bottom of the vertical plate and back of the horizontal plate are obtained by linear extrapolation. Extrapolation needs to be performed in each corner, because there is a distance between the corner where the pressure is needed and the nearest pressure transducer. The regions where extrapolation is performed are shown in Figure 4.1, which represents a cross-section of the caisson.

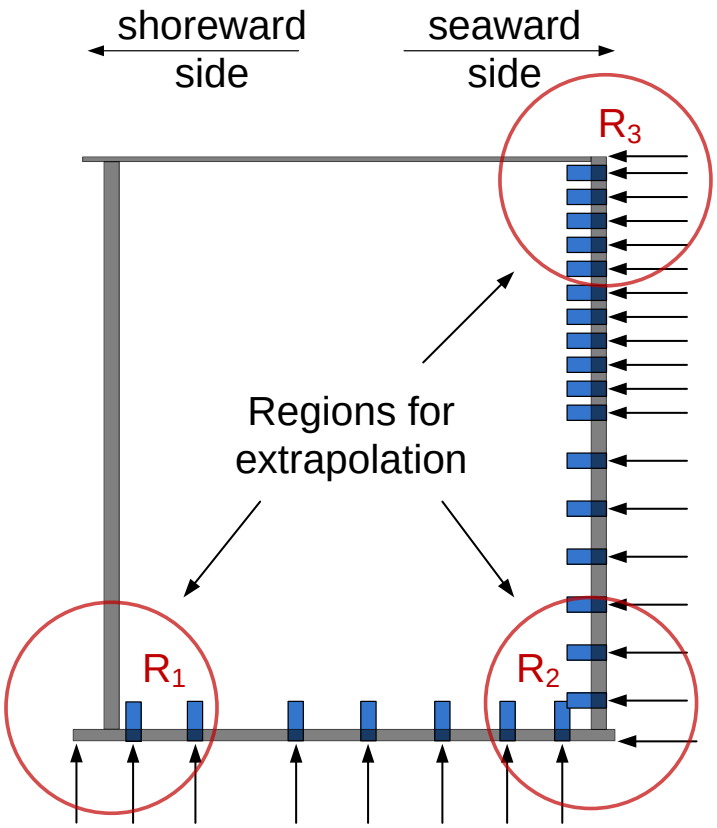

Figure 4.1. Corners for extrapolation.

For region R_1, the extrapolation is done using Equation (4.1) and for region R_3 using Equation (4.2). The parameters are drawn in Figures 4.2 and 4.3.

$$p_{26} = p_{25} - \frac{p_{24} - p_{25}}{x_{25}} x_{26} \tag{4.1}$$

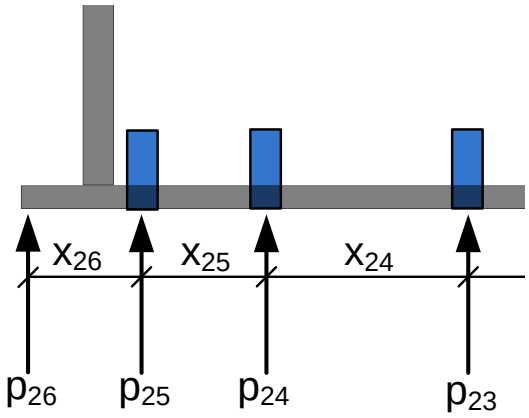

Figure 4.2. Extrapolation for region R_1.

$$p_0 = p_1 - \frac{p_2 - p_1}{y_2} y_1 \tag{4.2}$$

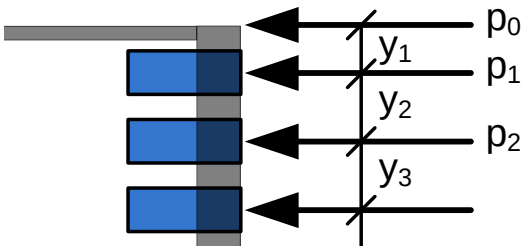

Figure 4.3. Extrapolation for region R_3.

Region R_2 is located around the front corner of the caisson. $p_{18,u}$ is set equal to p_{18}, which is calculated in Equation (4.3). The parameters used in this equation are illustrated using Figure 4.4.

$$p_{18} = p_{17} - \frac{p_{16} - p_{17}}{y_{17}} y_{18} \tag{4.3}$$

$$p_{18,u} = p_{18} \tag{4.4}$$

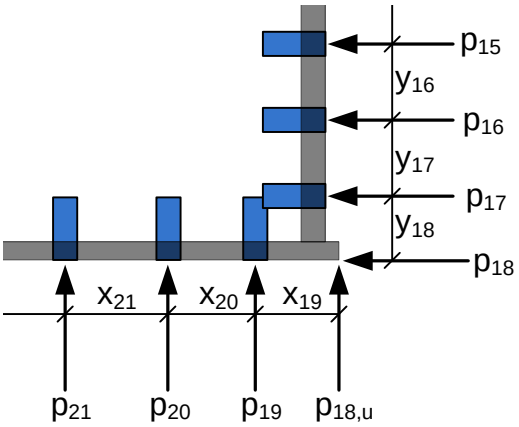

Figure 4.4. Extrapolation for region R_2.

The numerical integration method used in this report aproximates the area under the graph as the area of a trapezoid. The procedure is detailed below, with Figure 4.5 graphical explanation.

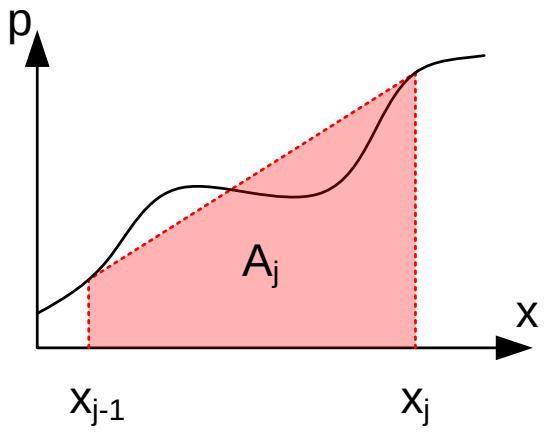

Figure 4.5. Numerical integration - trapezoid method.

Equation (4.5) shows how the area in Figure 4.5 is obtained. A_j is the approximation obtained for the area under the graph.

$$A_j = \int_{x_{j-1}}^{x_j} p(x)dx \approx (x_j - x_{j-1})\frac{p(x_j) + p(x_{j-1})}{2} \tag{4.5}$$

The sum of areas thus obtained represents the force, F, (4.6) and (4.7). The same procedure is applied to the uplift force. The procedure for obtaining the overturning moment is explained in Appendix 4.3.

$$F = \int_0^{\infty} p(x)dx \tag{4.6}$$

$$F \approx \sum_{j=0}^{n} (x_j - x_{j-1}) \frac{p(x_j) + p(x_{j-1})}{2} \tag{4.7}$$

Where:

x_j	length coordinate
$p(x_j)$	recorded pressure
A_j	area obtained by numerical integration
n	number of numerical integration points

Figure 4.6 shows an example of a pressure profile from one of the tests, at the instance the maximum uplift force acts.

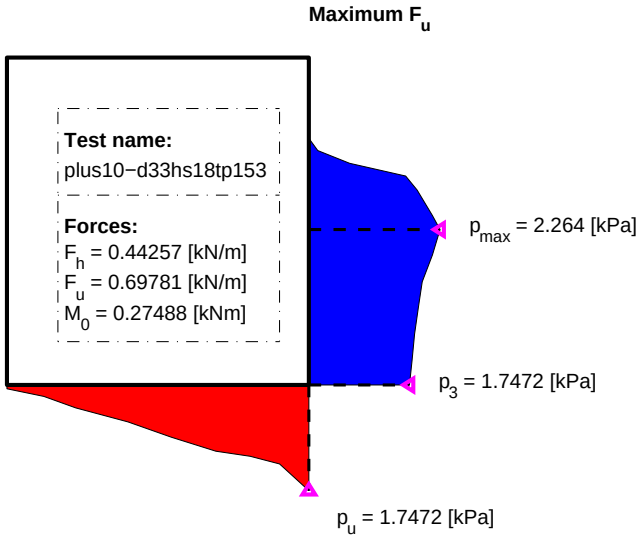

Figure 4.6. Pressure profile example.

4.1 Horizontal Force

There is a difference between the expected forces and the measured horizontal forces, as seen in Table 4.1. It is evident that, for non-breaking wave tests, highlighted in blue, the Goda theory estimates quite well the experimental data. While for breaking wave tests, indicated in red, these are largely underestimated.

Table 4.1. Horizontal force comparison.

d	H	T	Observation	Goda [N/m]	Measured [N/m]
25	10	1.12	non-breaking	166.4	136
25	20	1.53	non-breaking	681.6	544.6
25	20	2	breaking	679.8	930.4
33	10	1.12	non-breaking	163.6	138.7
33	20	1.53	non-breaking	535.6	406.7
33	25	2	breaking	663.3	853.8
35	10	1.12	non-breaking	193.1	153.9
35	20	1.53	non-breaking	460.2	553.1
35	27	2	breaking	628.3	1561.1

As it can be observed in Figure 4.6, there is a significant difference between the pressure at the lowest point on the vertical wall (p_3), and the uplift pressure (p_u). Using the Goda formulas from Appendix A.2 for this case, the following values are found:

$$p_1 = 1.72kPa \tag{4.8}$$

$$p_3 = 1.37kPa \tag{4.9}$$

$$p_u = 1.27kPa \tag{4.10}$$

For a better illustration and validation of results, the Goda force is plotted against the results in Figure 4.7. The circles represent data points, and a 45° line is added as an aid. Red marks the tests with no wave breaking, and blue marks the tests where breaking occures.

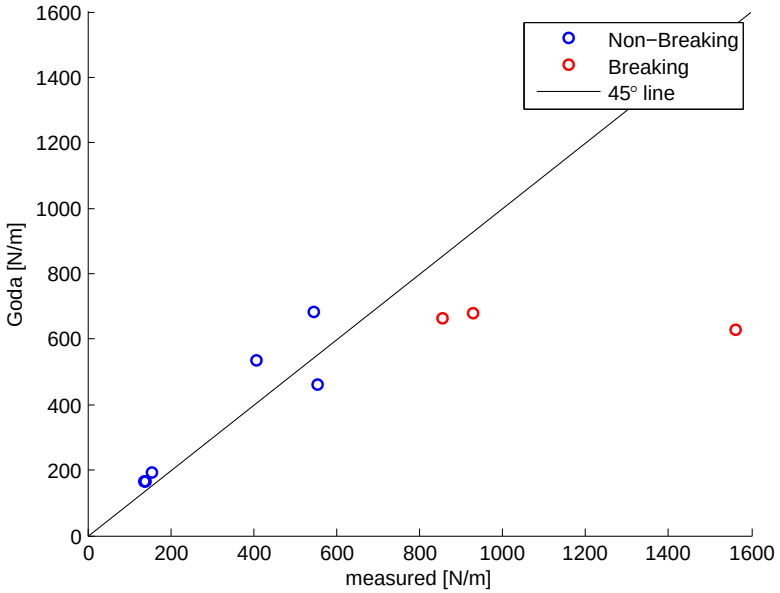

Figure 4.7. Goda force compared with measured force.

Another way to show the difference between the predictions and results is plotting the measured forces against the ratio between the measured and predicted. This is shown in Figure 4.8, where the red marks represent the situations with no wave breaking, and

the blue marks the situations with breaking. The horizontal black line represents the situation where the two parameters are equal.

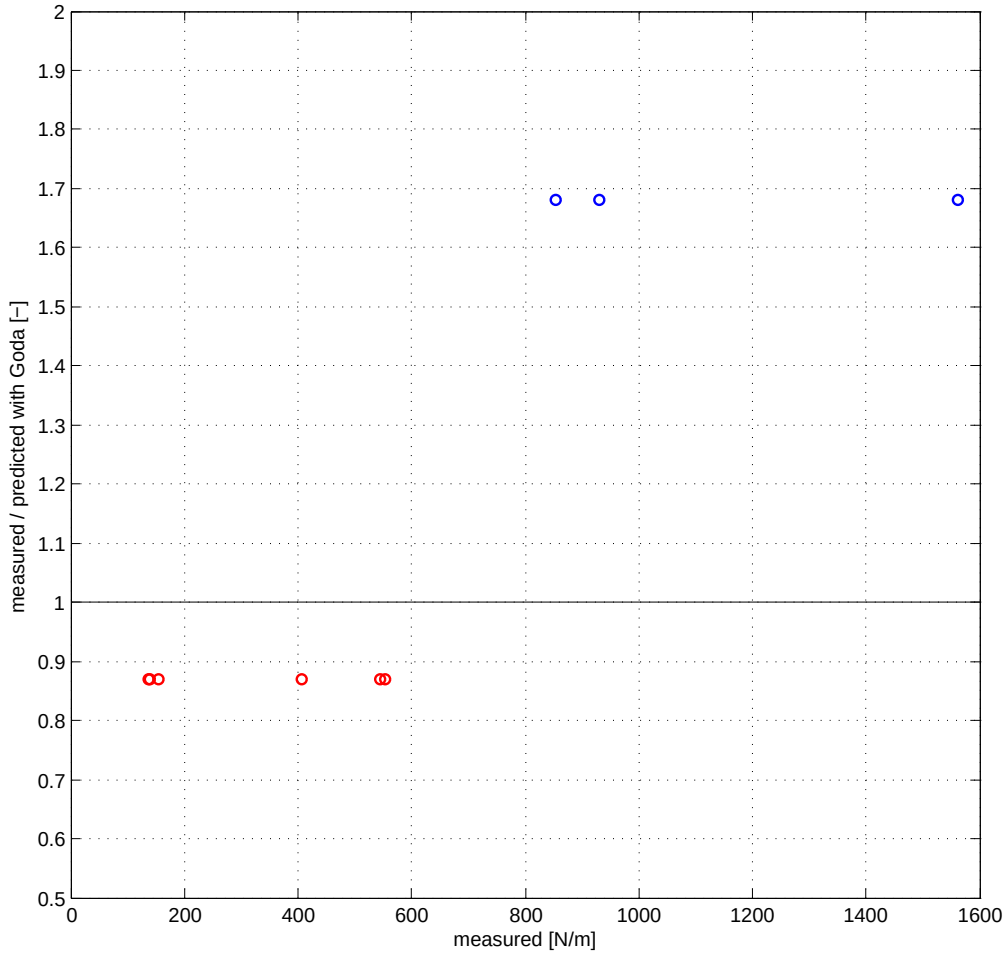

Figure 4.8. Comparison between the predictions and measurements for the total horizontal force.

4.2 Uplift Force

The uplift force measured in the test is obtained by integrating the uplift pressures over the bottom of the caisson. The theoretical values are calculated using the method described in H.Oumeraci et al. [2001], and detailed in Appendix A. Table 4.2 and Figure 4.9 show the comparison made between the measured forces and the theoretical ones.

Table 4.2. Uplift force comparison.

d	H	T	Observation	Goda [N/m]	Measured [N/m]
25	10	1.12	non-breaking	130.8	72.8
25	20	1.53	non-breaking	364.4	141.0
25	20	2	breaking	403.7	334.4
33	10	1.12	non-breaking	93.9	51.2
33	20	1.53	non-breaking	271.7	174.4
33	25	2	breaking	352.1	352.6
35	10	1.12	non-breaking	98.8	55.7
35	20	1.53	non-breaking	233.4	171.3
35	27	2	breaking	326.5	346.4

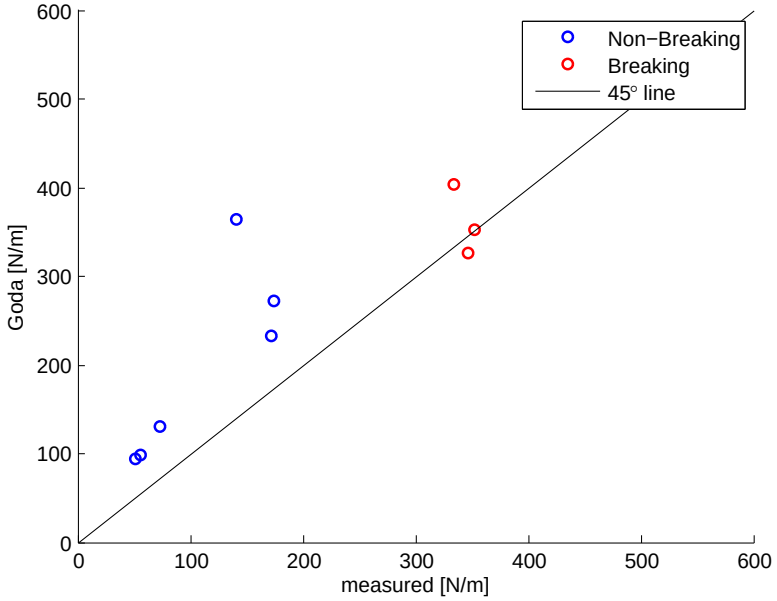

Figure 4.9. Comparison of uplift forces.

It should be noted that, for the tests where rotation occured, the measured uplift forces are higher than in corresponding tests with no rotation. When analyzing the pressure profiles from these tests, it can be seen that, once rotation occurs, a pressure developes at the heel of the caisson, contributing to the overall value of the uplift force. This can be seen in Figure 4.10. The influence of this pressure at the heel of the caisson may be overestimated due to the positioning of pressure transducers around this area. Near to the back of the caisson, the distance between consecutive transducers is increased. Between consecutive transducers, the pressure profile is assumed to follow a linear interpolation. In conclusion, increasing this length over which the pressures are interpolated makes the length over which the pressures are integrated larger and, in turn, exagerating their contribution to the overall uplift force. Another explaination would be that, because of the big waves that often caused overtopping and the nature of the foundation material, a set-up of water level might have occured during the test, accounting for this increased pressure around the heel.

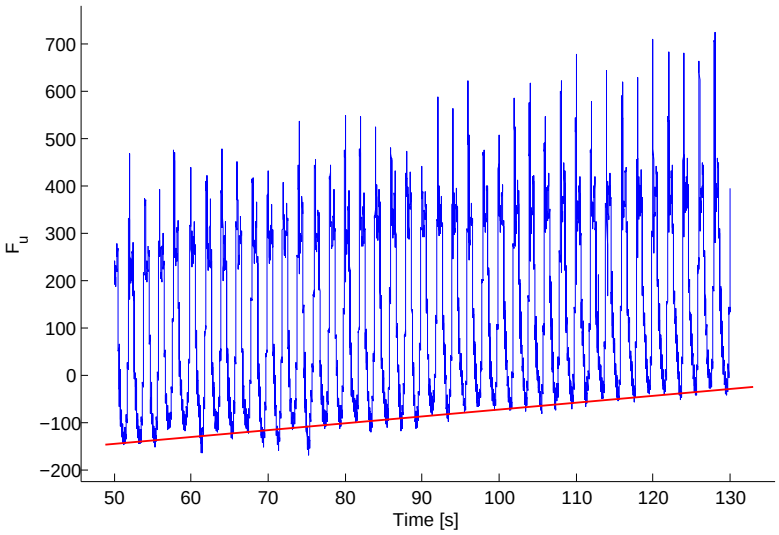

Figure 4.10. Change in uplift force.

4.3 Overturning Moment

The overturning moments are calcuated using the method described in the following.

$$M_{tot} = M_1 + M_2 \tag{4.11}$$
$$M_1 = F_h y_{Fh} \tag{4.12}$$
$$M_2 = F_v x_{Fv} \tag{4.13}$$
$$\tag{4.14}$$

Where:

M_{tot}	total overturning moment around heel
M_1	moment due to horizontal force
M_2	moment due to vertical force
F_h	horizontal force
F_v	vertical (uplift) force
y_{Fh}	vertical coordinate of F_h from the bottom
x_{Fv}	horizontal coordinate of F_v from the heel

Figure 4.11 better shows the parameters used to calculate the moments.

It can be seen in Table 4.3 and Figure 4.12 that, for the tests performed, there is a relative small difference between the predicted and measured overturning moments for no-breaking waves, while in tests where wave breaking occurs, the overturning moment calculated using the forces obtained by Goda's formula is smaller than the values recorded in the experiment.

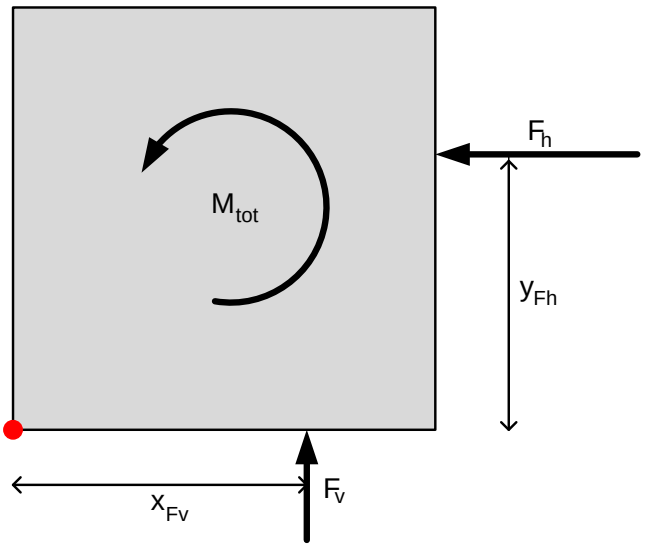

Figure 4.11. Forces contributions to overturning moment.

Table 4.3. Overturning moments comparison.

d	H	T	Observation	Goda [N/m]	Measured [N/m]
25	10	1.12	non-breaking	52.7	40.2
25	20	1.53	non-breaking	177.5	133.8
25	20	2	breaking	187.4	320.5
33	10	1.12	non-breaking	46.7	41.4
33	20	1.53	non-breaking	144.1	120
33	25	2	breaking	183.8	293.9
35	10	1.12	non-breaking	53.2	42.9
35	20	1.53	non-breaking	126.1	189.0
35	27	2	breaking	175.5	589.9

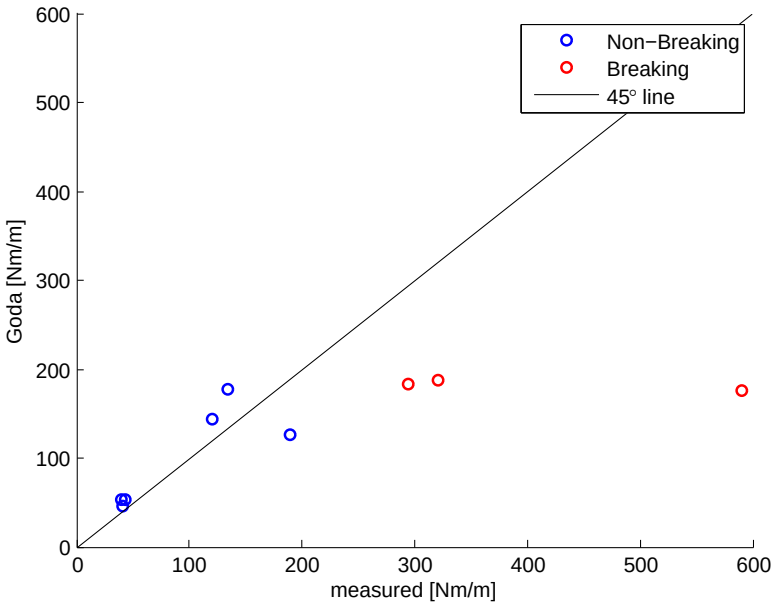

Figure 4.12. Comparison of overturning moments.

Frequency analysis

A frequency analysis has been performed in order to underline the importance of sampling frequency. This was done by processing the data gained from the experiments, which was recorded at a frequency of 1000$[Hz]$.
Figures 4.13 and 4.14 illustrate the difference for cutting the recording frequency in half, from 1000$[Hz]$ to 500$[Hz]$, while the last plot, Figure 4.15, shows the readings for a much lower frequency, of 100$[Hz]$.

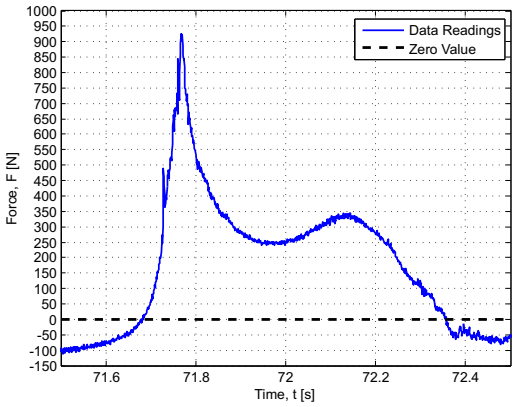

Figure 4.13. Frequency 1000$[Hz]$.

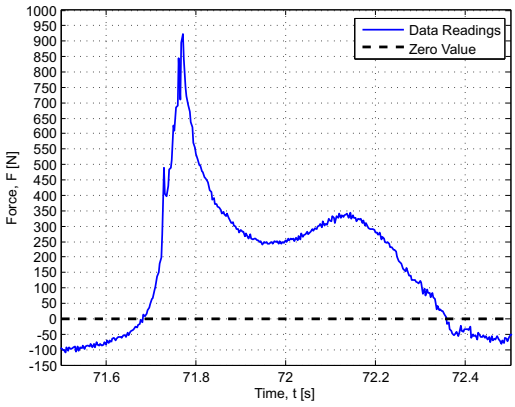

Figure 4.14. Frequency 500$[Hz]$.

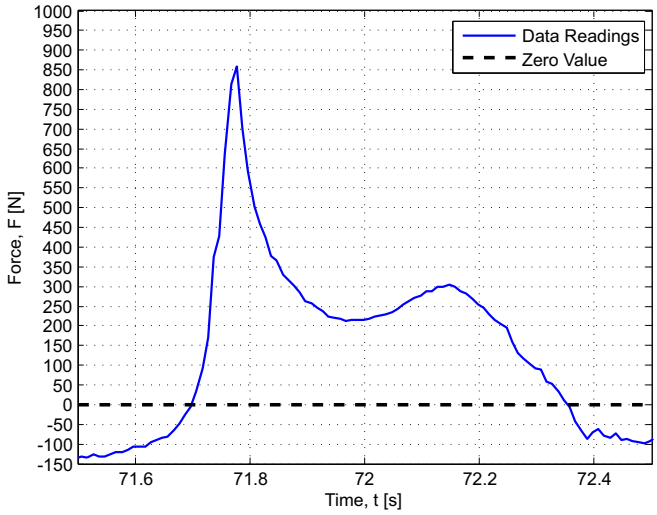

Figure 4.15. Frequency $100[Hz]$.

It can be seen from the figures that by reducing the sampling frequency will clearly result in a difference in maximum recorded forces. In Table 4.4, the results from the frequency analysis are shown.

Table 4.4. Frequency Analisys.

Frequency $[Hz]$	Force $[N]$	Difference from $1000[Hz]$ [%]
1000	924.9	-
500	923	0.20
333	921	0.42
250	902.6	2.41
166	877.8	5.17
125	874	5.50
111	864.9	6.48
100	858.6	7.16

As it can be seen in the results from Table 4.4, as the frequency is increased towards $1000[Hz]$ the difference in the maximum recorded force between two consecutive frequencies is decreasing. This decreasing is a sign of convergence, as also shown in Figure 4.16.

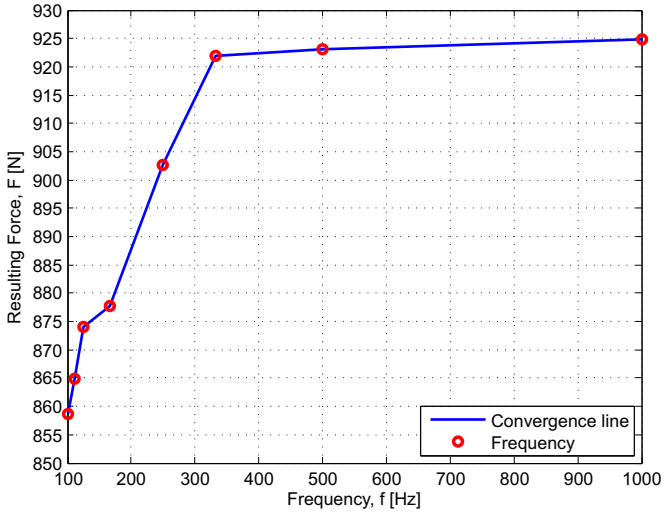

Figure 4.16. Frequency Convergence.

Although this difference in recorded forces can occur due to water drops hitting the pressure transducers at high speed, this is not our case since there are no significant solitary peaks in the readings. It can be concluded that by using a sampling frequency of $1000[Hz]$ the recordings are able to catch the highest forces exerted by the waves over the caisson and that the frequency is not high enough to record water-drops travelling at high speed and also not low enough to miss the highest forces.

4.4 Location of maximum pressure

In the analysis of wave pressure distribution it is important to note the location of the maximum horizontal pressure p_{max}. Table 4.5 shows the location of the maximum pressure as proposed by different studies. Kisacik, Troch, and Bogaert [2012] relates the location of p_{max} to the water depth in front of the caisson d, and proposes an expression based on wave steepness. This study is based on experiments using different wave breaking types (slightly breaking, breaking with small air trap, breaking with large air trap, and broken waves).

Table 4.5. Location of maximum pressure. [Kisacik et al., 2012]

Article	p_{max}
Richert (1968)	Below the SWL
Partenscky (1988)	$0.7H_b$ above SWL
Chan and Melville (1988)	$z/L = 0.05 - 0.07$
Hull and Muller (2002)	At the SWL
Kisacik et. al (2012)	Above SWL for slightly breaking waves Slightly below SWL for breaking waves with large air trap

A plot of the location of the p_{max} is showed in Figure 4.17, where z/h is plotted against wave steepness. In the table, z represents the vertical coordinate of the maximum

pressure and h represents the water depth in front of the caisson. Wave steepness is defined as $S = 2\pi\frac{H}{gT^2}$, where H and T are the wave height and period respectively. For simplicity, the location of p_{max} for a test is obtained by averaging the top 20 values obtained during that test. Values for non-breaking waves are also plotted.

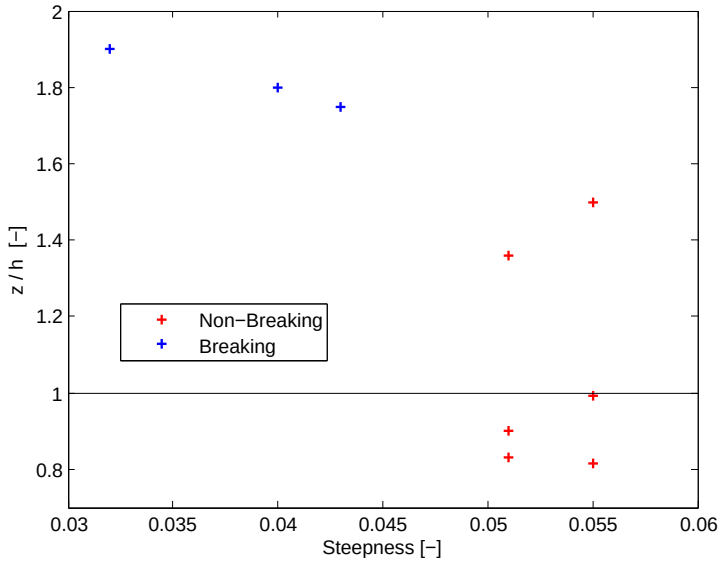

Figure 4.17. Location of p_{max} in relation to wave steepness.

The number of data points collected in the present study are not enough to draw a definite conclusion. From the data available it can be seen that there is some variation in the location where the pressures are obtained. The results are in agreement to the conclusion of Kisacik et al. [2012], that bigger waves in shallower water produce a higher location for p_{max}. However the results fail to closely fit Expression (4.15), proposed for breaking waves, where L_0 represents the deep water wave length, while it is in the better agreement with Partenscky (1988) from Table 4.5.

$$\frac{z}{h} = -23.2\frac{H}{L_0} + 1.4 \tag{4.15}$$

4.5 Setups comparison

A short discussion concerning the validation of the two setups is presented. In this section the following is defined:

- *Setup I*: 18 pressure transducers on the vertical wall of the fixed part and 7 on the bottom. 5 kept for reference on the movable part, which is fixed for this setup.
- *Setup II*: 18 pressure transducers on the vertical wall of the movable part, 7 on the bottom, 5 kept for reference on the fixed part. The movable part is weighted and allowed to move.

In *Setup II*, during the tests where the movable part has its largest mass, the five reference transducers and their counterparts record very similar pressures, proving that the setup is suitable. However, there is a discrepancy between *Setup I* and *Setup II*, when forces are

analysed. Contrary to expectations, the forces on the movable part when displacement occurs are sometimes larger than the fixed part. The two causes considered for this situation are either possible errors during calibration of pressure transducers in *Setup I*, better detailed later in another chapter, or rocking of the movable part, investigated in section 5.1.

5 Displacements and Rotation

The analysis of displacements and rotation consists first of showing the measured displacements of the movable section at different weight, water depth and wave height, then of comparing the obtained results with those existing in literature, trying to explain possible differences.

Sliding failure occurs when a strong horizontal force produced by a wave exceeds the difference between the weight of the caisson in water and the uplift force, generated from the same wave, times the friction coefficient.
Together with the displacement of the caisson, also an overturning movement can be observed. As pointed out in Chapter 1, overturning is not a frequent failure mode, but it can be studied to give a better comprehension of the phenomena, since a rocking movement appears in all the tests.

An example of a displacement and rotation analysis is illustrated in Figure 5.1. The area marked with red will be detailed and discussed later.
Rotation is calculated using Equation (5.1), where D1 and D2 are the two displacements recorded by the rotational potentiometers, respectively the upper one and the lower one, and b is the distance between the measuring points.

$$r = \arctan \frac{|D1 - D2|}{b} \tag{5.1}$$

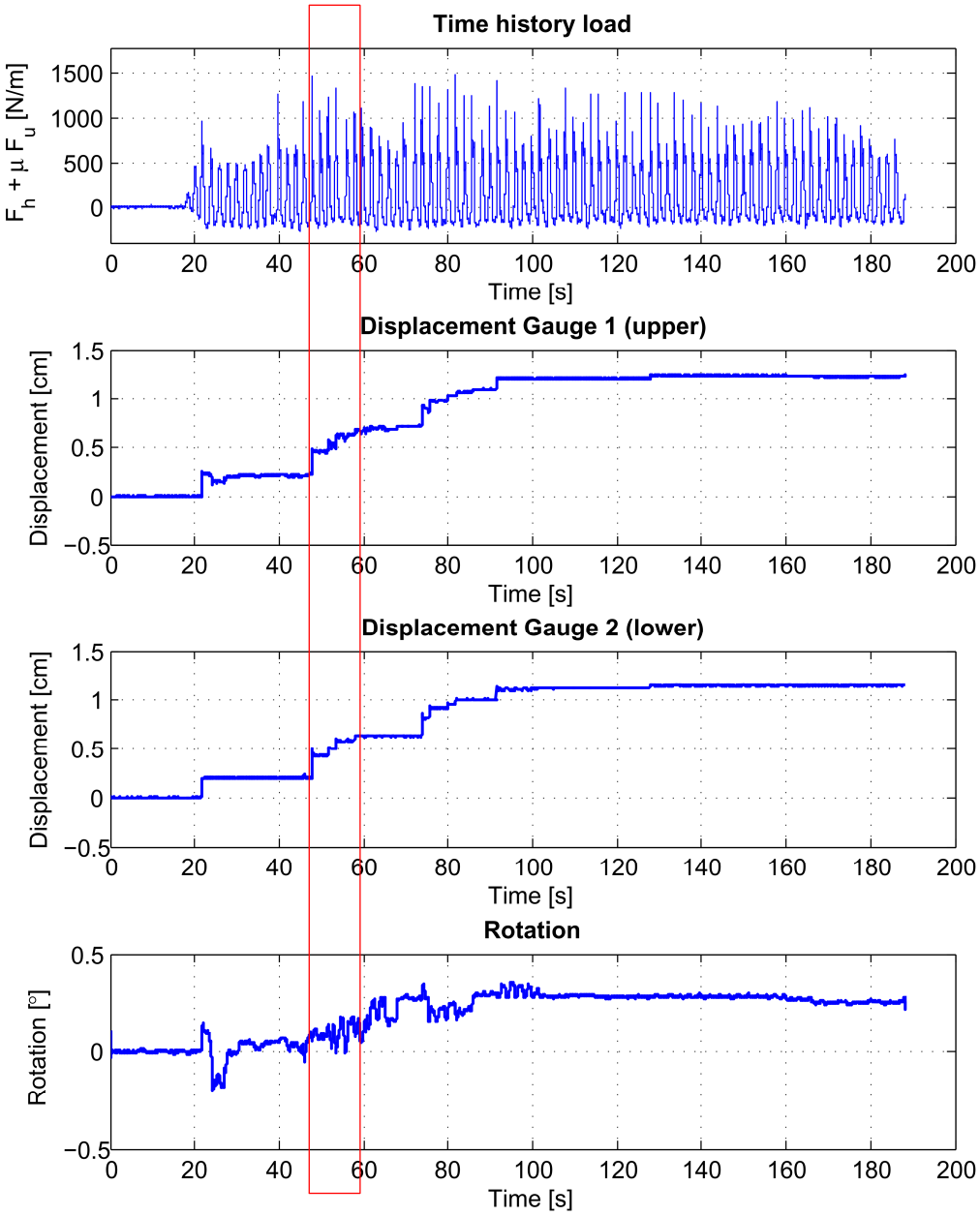

Figure 5.1. Forces, displacements and rotations

The results from Figure 5.1 come from test 3.1.3, with specified wave height (to the wave generator) of 27 cm, a wave period of 2 sec, water depth of 35 cm, and a caisson mass of 103 kg. In this test, a total displacement of 1.15 cm is recorded and a final rotation of 0.26 deg.

5.1 Rocking analysis

In the current section, rocking will be discussed with the aid of the focus area from Figure 5.1, representing the caisson movement for a time segment of 12 seconds. The zoomed area is displayed in Figure 5.2, comparing only the time history load and the rotation.

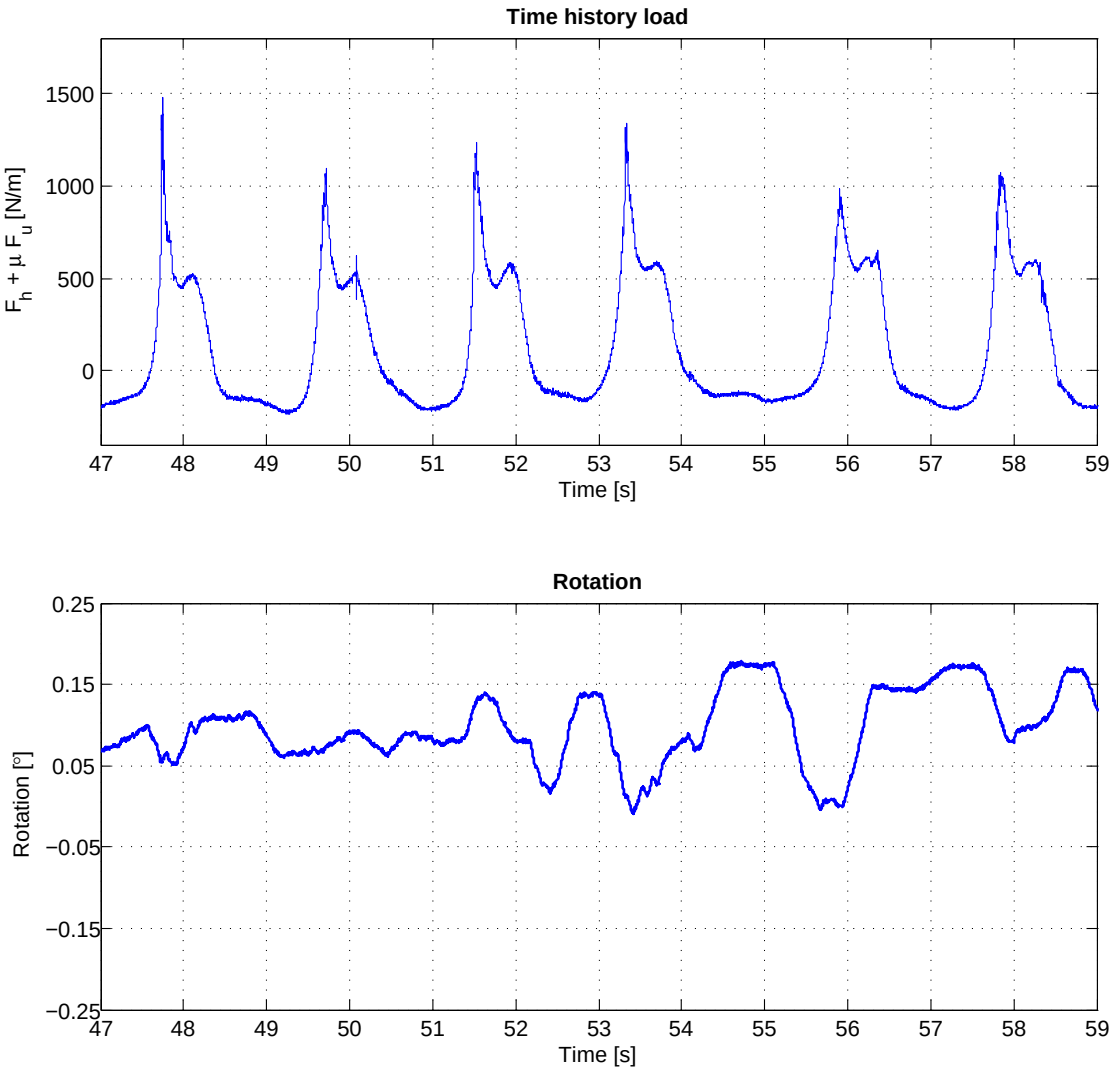

Figure 5.2. Rocking and forces correlation.

It is clear that rocking occurs in phase with the waves, as displayed in Figure 5.2. When a wave hits the caisson, the forces rock it shoreward. After this event, the caisson begins to rock seaward and, at the same time, the next wave hits. The impact between the wave hitting the caisson at the same time as it rotates seaward may account for the increased forces recorded on the caisson face, as mentioned in Section 4.5. (CHECK THIS)

5.2 Sliding analysis

At the same way, Figure 5.3 shows that caisson displacements can be easily recognized for almost all the thrust peaks that appear in the time interval. For the second peak and the penultimate peak, only reversible displacements have been recorded, probably caused by a rocking movement of the caisson.

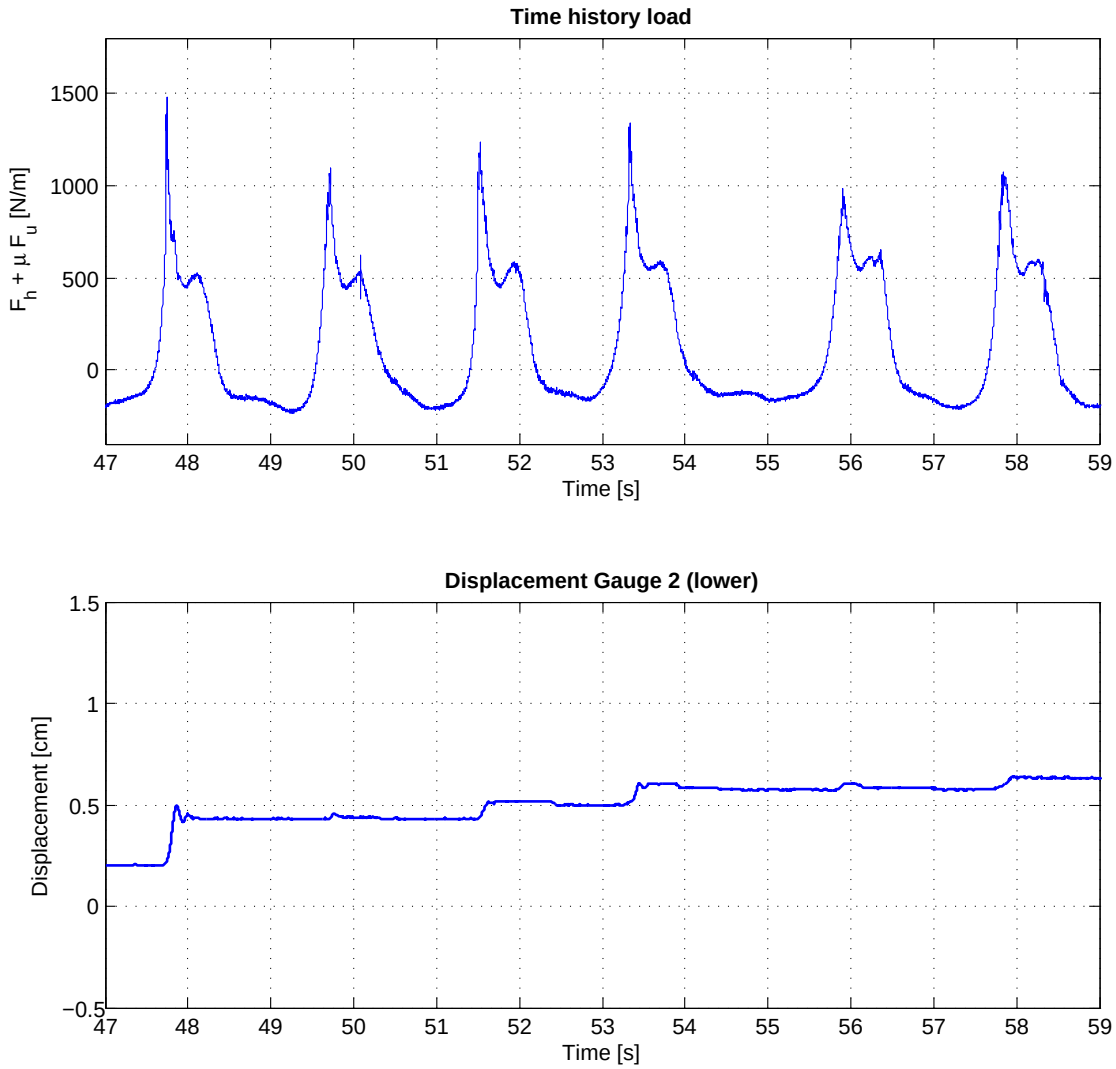

Figure 5.3. Displacements and forces correlation.

However, this is a very particular case, because not always a peak of wave force corresponds to a caisson sliding. As specified above, under static conditions sliding occurs when a strong horizontal force produced by a wave exceeds the difference between the weight of the caisson in water and the uplift force, generated from the same wave, times the friction coefficient. This sentence can be mathematically declared as Equation (5.2):

$$F_h = \mu F_u - \mu W' \tag{5.2}$$

Where:

F_h	horizontal force upon the caisson [N/m]
F_u	uplift force upon the bottom of the caisson [N/m]
μ	friction coefficient
W'	weight of the caisson in water [N/m]

or, in another form, as Equation (5.9)

$$\mu W' = F_h + \mu F_u \tag{5.3}$$

For this reason, it is possible to compare the time history load, given by the sum of horizontal force and uplift force times the friction coefficient, with the threshold represented by the caisson weight in water times the friction coefficient.
The last value is useful for displaying the sliding failure function as it doesn't vary during a single test, because it is constant for a certain water depth and for a given weight of the caisson.
As concluded from Section 2.6, a different friction coefficient is found when dealing with a wet foundation and different weights. However, when using the peak method described in this section, closer matches are found by using a friction coefficient of $\mu = 0.45$.

Thus, the previous graph can be revise adding the sliding threshold, in Figure 5.4. It will be more evident that all the peaks overtake the limit, making the caisson displacement an expected occurrence.

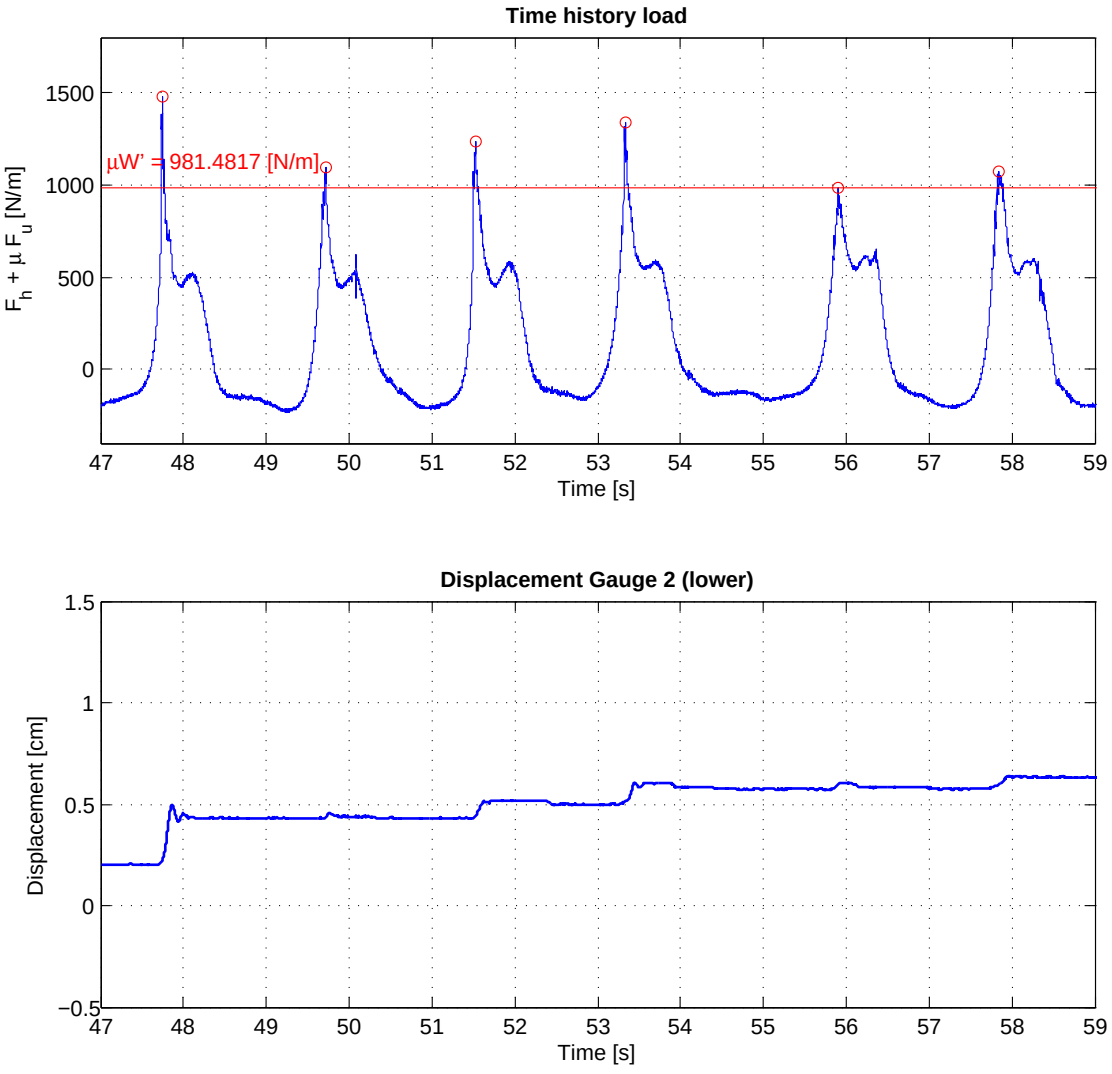

Figure 5.4. Peaks that theoretically cause sliding.

Even so, for certain tests displacement are much lower than the expected values, as it can be seen from the Figure 5.5:

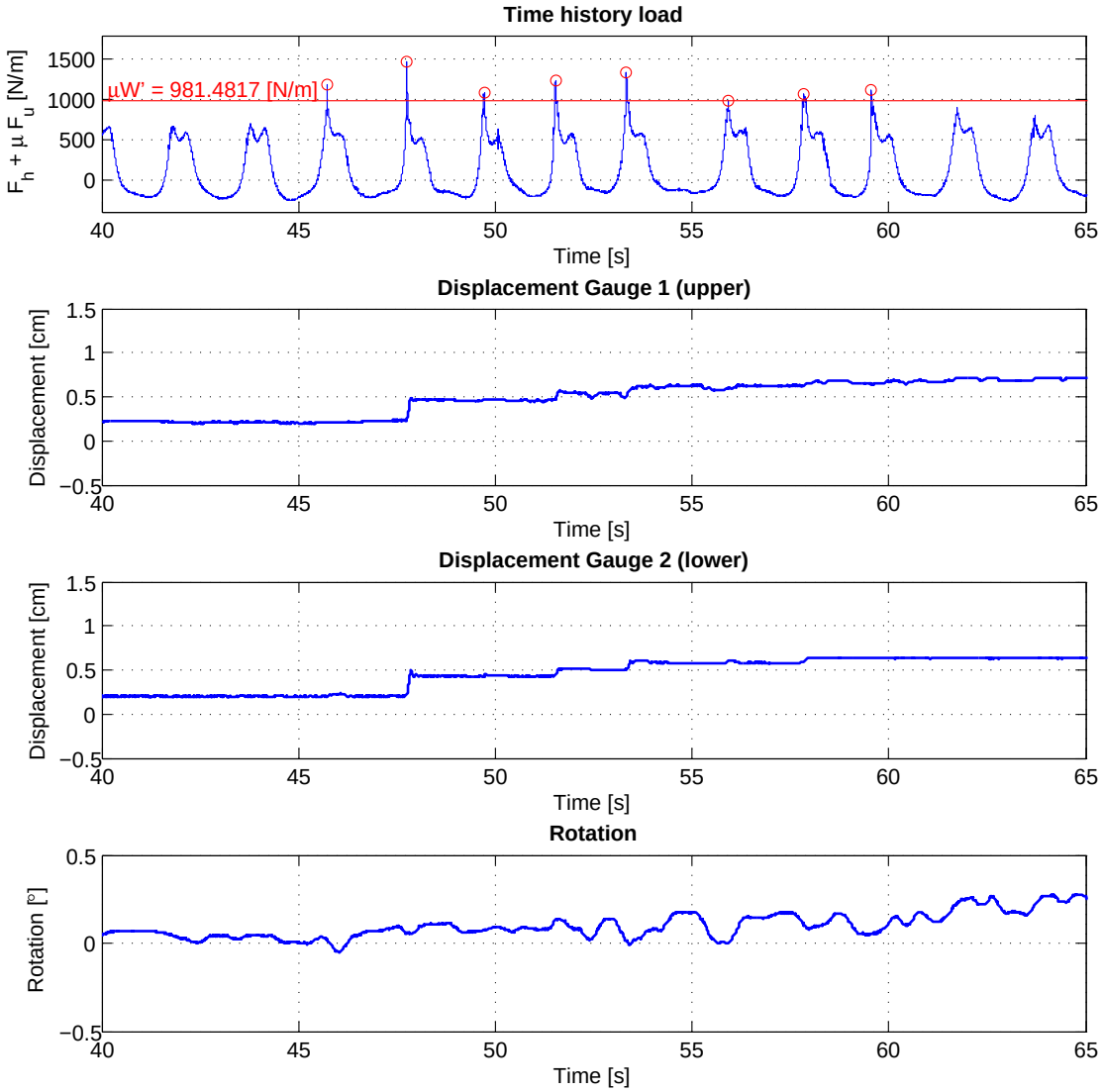

Figure 5.5. Peaks that theoretically cause sliding.

and for other tests, displacements do not occur when they are expected, as it can be examined in the Figure 5.6:

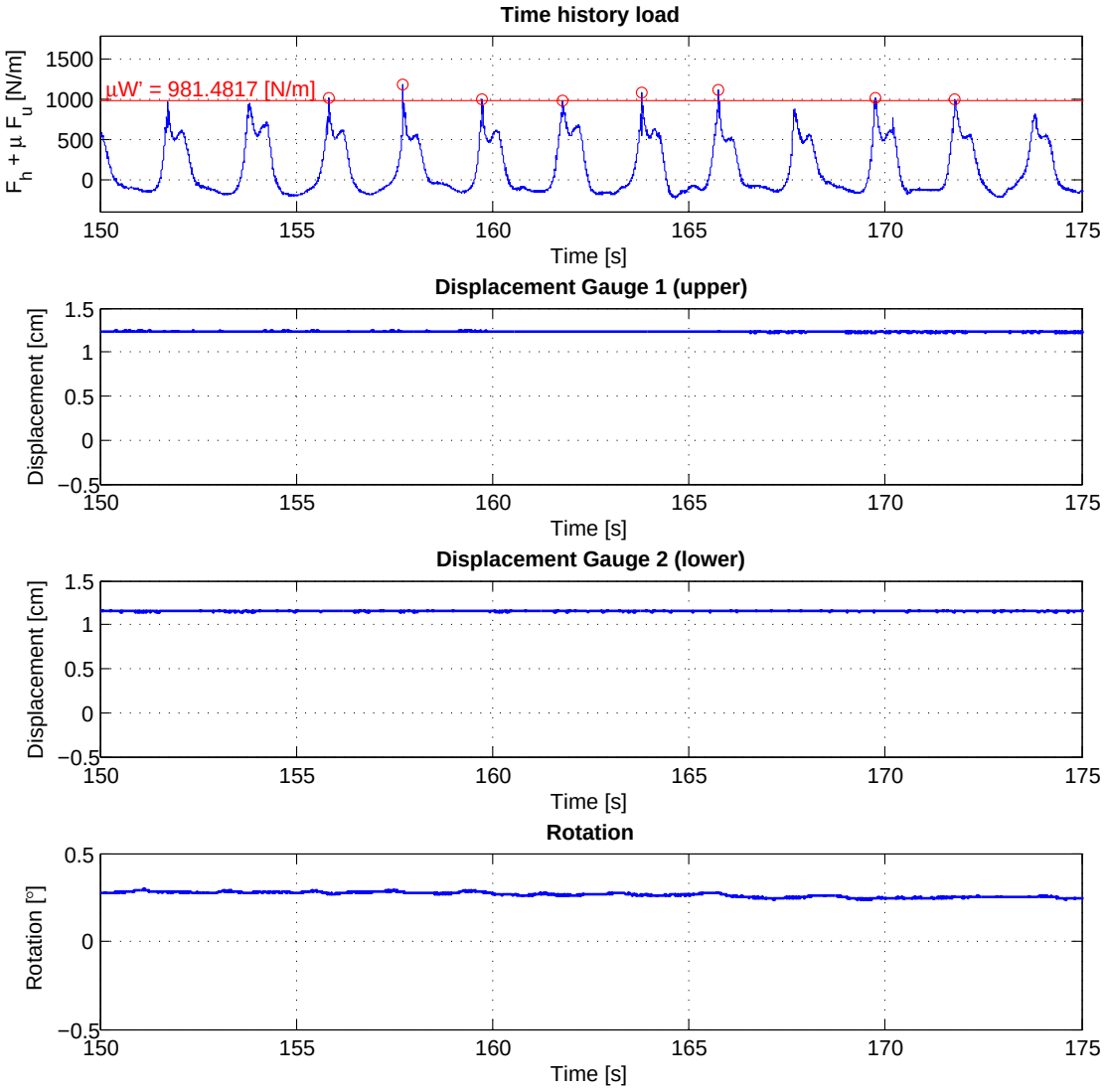

Figure 5.6. Peaks that theoretically cause sliding.

Figures 5.5 and 5.6 show two examples of peak series that are expected to cause displacement, but that not always occur. To better understand the relation between these peaks and the sliding failure mechanism, the static approach is not sufficient.

This two cases belong to the same test that has been cited above, that is the 3.1.3, with specified wave height (to the wave generator) of 27 cm, a wave period of 2 sec, water depth of 35 cm, and a caisson mass of 103 kg.

5.3 Expected sliding distance

The expected sliding distance is calculated using the method described by Shimosako, Takahashi, and Tanimoto [1994]. The authors presented a simplified model for the estimation of distance of caisson sliding that was found to compare satisfactorily well with data from smallscale physical model tests, as pointed out by Cuomo, Lupoi, Shimosako, and Takahashi [2011].
The time history load proposed for this model is quite simple indeed, showing an isosceles triangular shape in Figure 5.7:

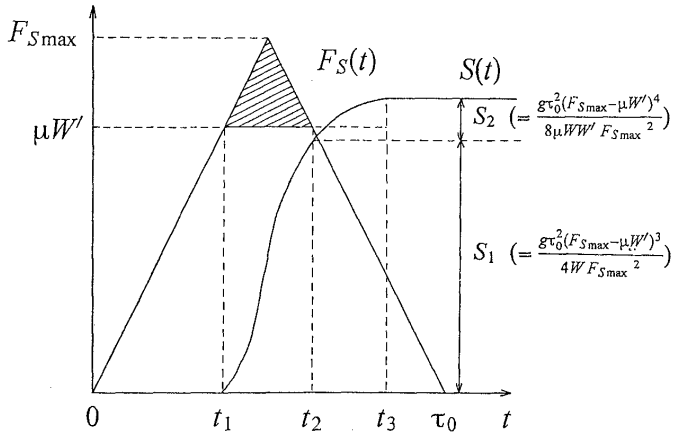

Figure 5.7. Proposed calculation model of the sliding distance for Shimosako et al.

The Equation (5.4) allows to calculate the permanent displacement S as:

$$S = \frac{g{\tau_0}^2(F_{Smax} - \mu W')^3(F_{Smax} + \mu W')}{8\mu WW'{F_{Smax}}^2} \tag{5.4}$$

Where:

τ_0	duration of triangular wave thrust, calculated as explained below [s]
F_{Smax}	$=F_h+\mu F_u$, calculated with pressure formula of Goda [1974] [N/m]
μ	friction coefficient
W	weight of the caisson in air [N/m]
W'	weight of the caisson in water [N/m]

τ_0 is obtained from theoretical analysis and model experiments, and assumes the following values:

$$\tau_0 = k\tau_{0F} \tag{5.5}$$

$$k = \frac{1}{((\alpha^*)^{0.3} + 1)^2} \tag{5.6}$$

$$\alpha^* = max(\alpha_1, \alpha_2) \tag{5.7}$$

$$\tau_{0F} = (0.5 - \frac{H}{8h})T \qquad (0 \leq \frac{H}{h} \leq 0.8) \tag{5.8}$$

Where:

α_1	impulsive pressure coefficient according to Takahashi, Tanimoto, and Shimosako [1993]
α_2	impulsive pressure coefficient in pressure formula of Goda [1974]
H	wave height [m]
h	water depth [m]
T	wave period [s]

Takahashi et al. [1993] have pointed out that for $\frac{d}{h}$>0.7 (where d is the water depth above the berm) α_1 is always nearly zero and smaller than α_2.

This sliding distance must be calculated for all the waves that exert a peak value of wave thrust F_{Smax} larger than the μ W', which represents the sliding failure function, displayed in Equation (5.9):

$$\mu W' = F_h + \mu F_u \tag{5.9}$$

The total permanent displacement will be obtained as the sum of all the single sliding distances.

Using the Goda pressure formula to calculate F_{Smax} the results will be always the same for each wave impact, therefore also the total final sliding distance will be always identical.
In order to obtain comparable results in term of sliding distance, the permanent displacement S (for each wave) has been accounted only for a number of times equal to the number of waves that have experimentally overtaken the sliding threshold.

Furthermore it has been introduced a modification of this formula, applying to F_{Smax} the experimented peak value of wave thrust, for each wave that exceeds the sliding threshold. Also the duration of the triangular wave thrust has been replaced by a mean value of τ_0, having assumed only a qualitative analysis.
As it will be pointed out in Chapter 5.4, τ_0 (called T_d in that chapter) can be reasonably taken as 0.2 s.

These two expected sliding distances (for the two methods) are displayed in Table 5.1 together with the permanent displacement and rotation for each test that have experimented sliding, where d is the water depth, H the wave height, T the wave period, D the recorded displacement, Dc1 the expected displacement as proposed by Shimosako et al. [1994], Dc2 the expected displacement with the modified formula and R the recorded rotation.
For some other tests there was no final rotation or displacement, but only some small temporary displacements and rotations occured.

Table 5.1. Permanent displacements and rotation.

Mass [kg]	d [cm]	H [cm]	T [s]	D [cm]	Dc1 [cm]	Dc2 [cm]	R [deg]
103	33	25	2	0.46	22.81	43.03	-0.20
103	35	27	2	1.15	406.33	60.23	0.26
113	33	25	2	0.03	0	0	-0.08
113	35	27	2	0.11	65.42	115.34	0.22

Results show an over-estimate of sliding distance, ranging from 2 to 3 orders of magnitude.
The reason can be partially found, if using the Shimosako et al. [1994] formula, on the higher value of wave thrust F_{Smax} for Goda [1974] formula, compared to the unconstant and on average lower peak values of wave load experimented in the tests. Moreover, the duration of the wave thrust is over-estimate as well, giving a mean value of 0.35 s.
Therefore it is possible to say that applying this formula we are 'on the safe side'.

5.4 Qualitative dynamic response

From the previous sliding data analysis, it can be easily observed that sometimes, despite the wave forces exceed the sliding threshold, no permanent caisson displacements are recorded, but only some rotations.
Therefore, in order to gain better understanding of the sliding triggering condition, a dynamic approach should be applied.
In fact a quasi-static approach, which has been presented previously, implies that in equilibrium condition, when a wave hits the caisson, there is always the direct transfer of its force to the foundation.
On the other side, impulsive waves require that also caisson stiffness and damping are included in the equilibrium problem, since they can significantly affect the phenomena.

For the purpose of this thesis, the dynamic effects will be take into account only qualitatively. In general this is made using a "dynamic response factor", defined by Martinelli and Lamberti [2010] as the ratio between the maximum effective response and the response to the maximum applied load under stationary conditions.
The "sliding response factor" has the same meaning of the "dynamic response factor", giving the ratio between the maximum sliding force F_S(t) and its maximum horizontal wave force.
This parameter primarily depends on the natural oscillation periods of the caisson. The most important for this analysis is the T_1^+, which represents the in-phase oscillation period, common to all length to width ratios.
Martinelli and Lamberti [2010] suggest to calculate the main eigen-period with the formula (5.10), which is based on the "European average design", a series of researches performed by Larras [1961], by Franco [1994] on Italian structures and by H.Oumeraci et al. [2001] report on representative European structures:

$$T_1^+ = 0.0565 h_c^{0.75} = 0.0353 s \tag{5.10}$$

where h_c is the caisson height [m].

Together with the natural period of the caisson, also the total duration of the triangular load T_d is needed. This value can vary with the different shape of the time history load associated to a wave, as it can be observed below:

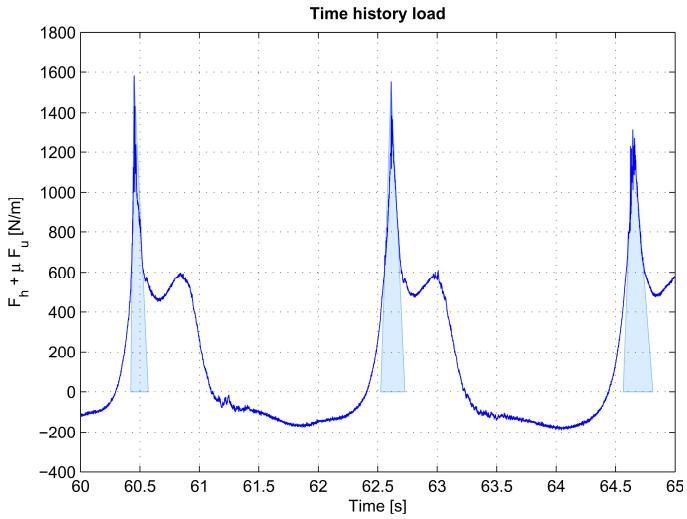

Figure 5.8. Duration of the triangular load T_d for different waves.

Since only a qualitative analysis of the dynamic response of the caisson is here presented, it is possibile to choose an order of magnitude for T_d.
Reasonably, this value can be assumed between 0.15 and 0.3 s.

Once the two periods are obtained, the relative frequency of triangular force (unit impulse) can be calculated as the ratio in-phase oscillation period T_1^+ over total duration of the triangular load T_d.
The result is approximately a range between 0.4 and 1.

At this point the "European average design" diagram will be used.

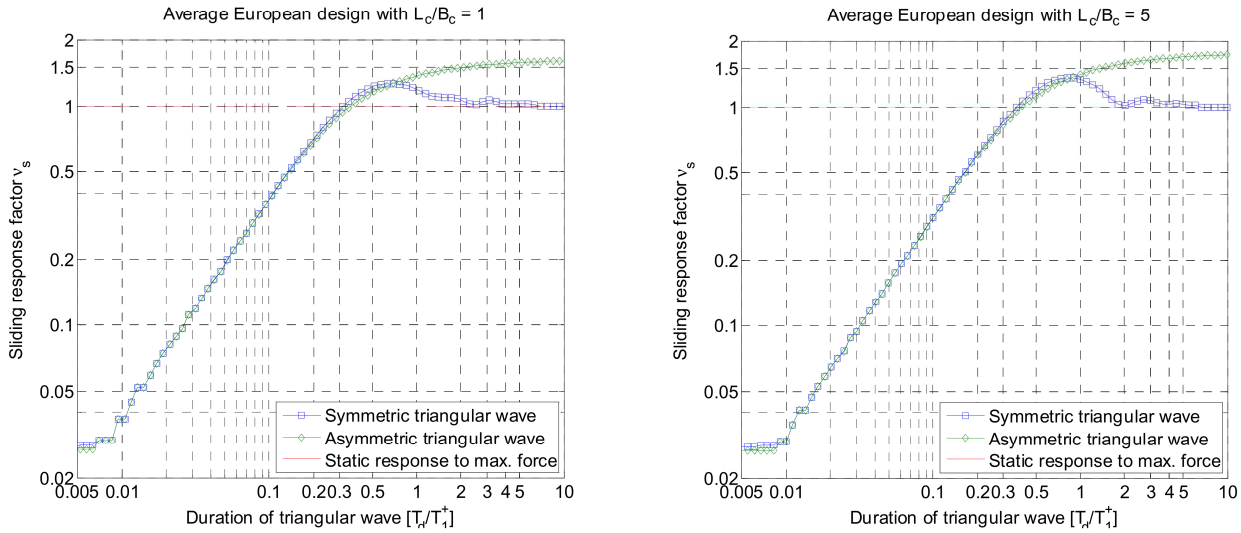

Figure 5.9. Assessment of the sliding response factor through the "Average European design".

As it can be seen, different diagrams are proposed depending on the ratio length over width of the caisson. In this case L/B is close to 1, so the attention will be put on the first graph.

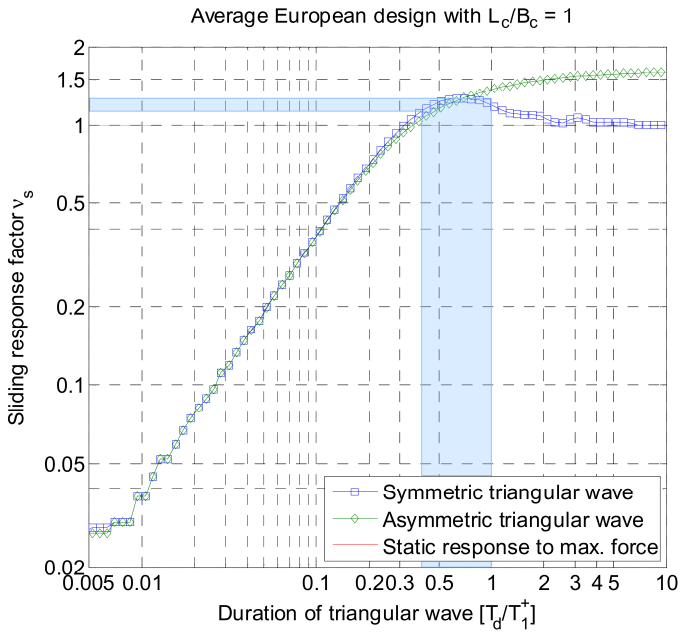

Figure 5.10. Assessment of the sliding response factor through the "Average European design" in the present case.

Having set a range between 0.4 and 1 for the relative frequency of triangular force, the sliding response factor assumes values between 1.1 and 1.25, supposing a response to symmetric triangular wave. In any case the result is independent from the shape in that range and this is positive for our study.

As it has been presented before, sliding not always occur when the static threshold is overtaken. This is quite clear observing the Figure 5.11:

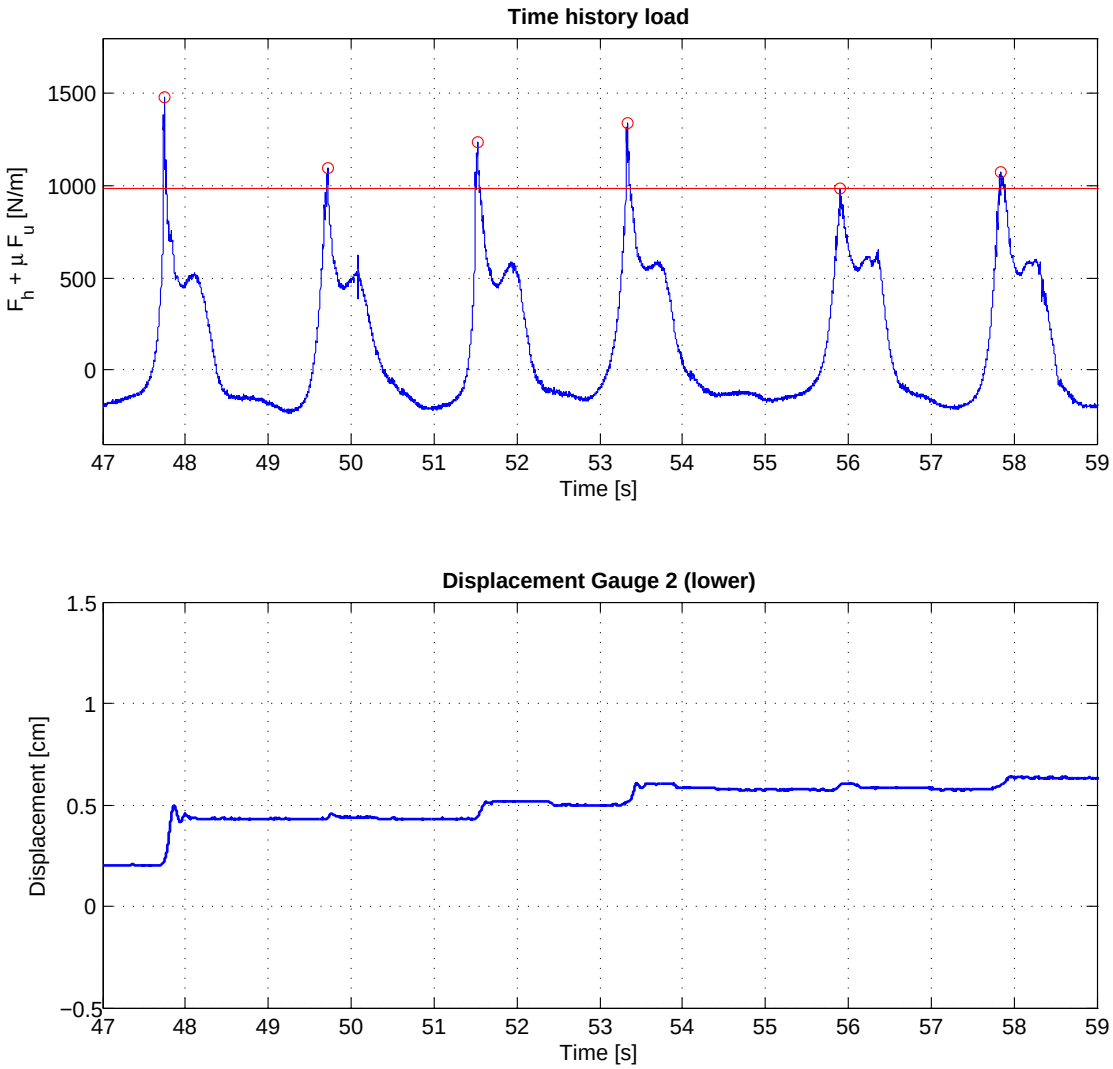

Figure 5.11. Peaks that theoretically cause sliding, according to a static analysis.

If the sliding response factor is applied, a better explanation of the phenomena can be done.
In fact, it is possible to look at the previous figure, modified with the red stripe that represents the new sliding threshold, in Figure 5.12.
Only when the acting force is upper than the red stripe, the sliding is expected. While if we are inside the red stripe, sliding is only a possible occurrence, sometimes happens, sometimes no. Under the lower threshold of the red stripe sliding is not expected.

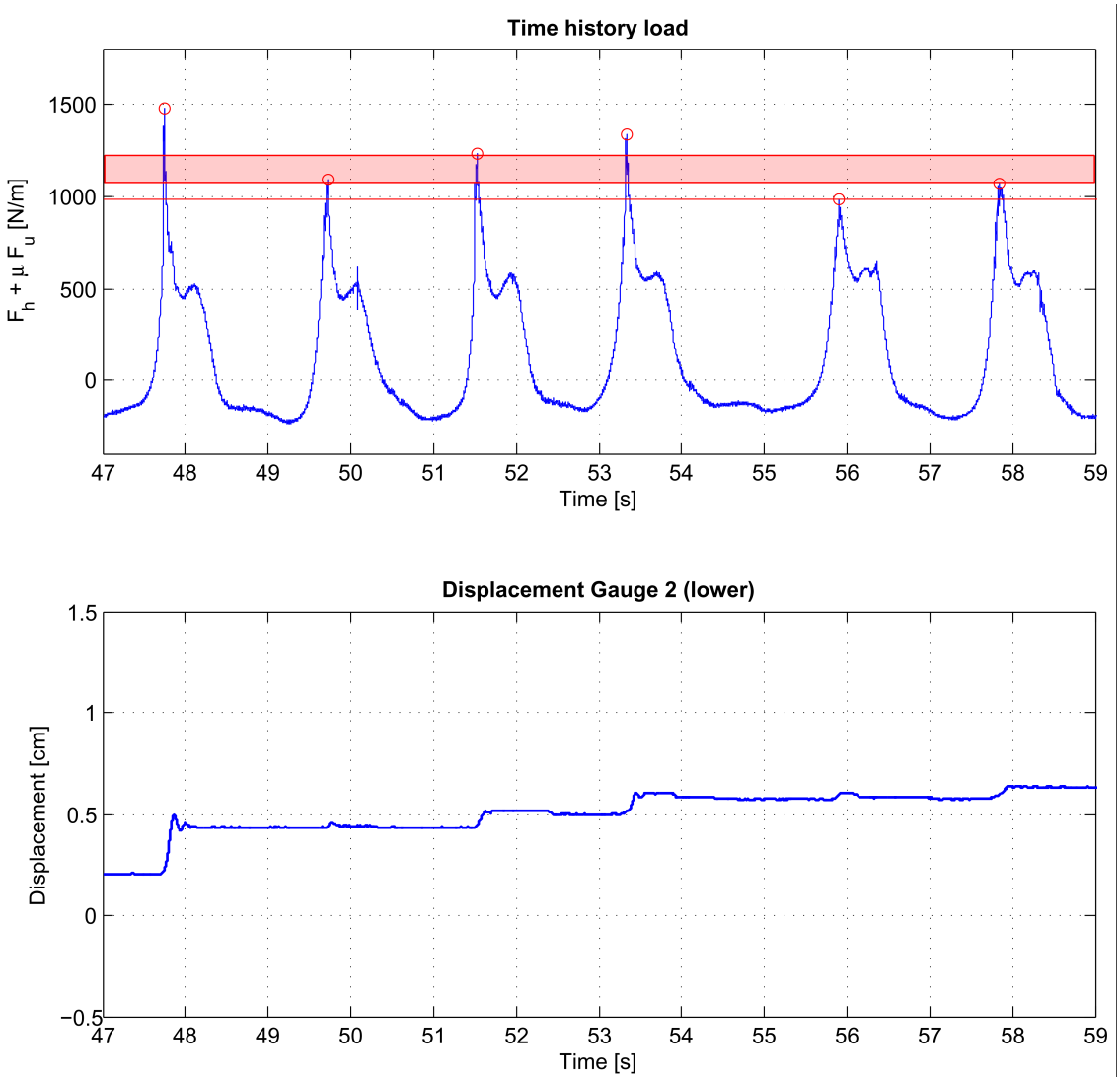

Figure 5.12. Peaks that theoretically cause sliding, according to a dynamic analysis.

The correction proposed with the sliding response factor interprets effectively the measurements in a better way. The difference between the dynamic analysis and the static analysis is up to 25% in this case, so the static approach can be widely considered as 'on the safe side'.

The dynamic aspect can become essential when the sliding response factor assumes values lower than one. In that case a static approach would be too cautelative, especially when violent impactc are expected. Tipically this cases occur when there are huge berms and not neglictable slope in front of the caisson, which were not the situation of the present study.
Now it is clear that a dynamic analysis can give a better explanation of the phenomena.

Part IV

Conclusions

6 Uncertainties and Errors

In this section the possible sources for errors are investigated, and the measures against them described. The uncertainties will also be presented and discussed.

Sources of errors include the factors that can lead to compromising the reliability of data. A list of those factors is presented in the following list. The factor of 'Human Error', which is usually considered a primary cause of errors, is divided among more than one source of errors.

1. Test procedure. A test plan has been layed out in Chapter 2. Also a procedure was established and closely followed for the conducting of each test. A reflection-absorbtion test for wave generator every 4^{th} test, with every change in water level. Recalibration of wave gauges was made after each change in water level and at the start of a new day of testing.
2. Changes in water conductivity. This is a factor that can influence the signals coming from wave gauges. Conductivity changes can occur due to changes in temperature or the mineral content of the water. To account for this, frequent recalibration of gauges was done. Before a calibration, the generator was run for a short time, in order to mix the water with the minerals that might have deposited on the bottom of the flume.
3. Old or defective equipment. At first investigation, the equipment available at the flume used for model testing was deemed adequate. However, some errors could have been made during operation due to lack of familiarity with the equipment. During testing, it was noted that the reflection absorption function of the generator was not fully effective even after several self-tests. The error was considered within a margin and accepted. After investigations using the reflection analysis capabilities of WaveLab, it was discovered that some of the tests had significant reflection and poor reliability. This item was described in more detail in 3
4. Errors in the setup. The positioning of the model in the flume was done precisely, the pressure transducers were carefully positioned and calibrated, the positioning of the wave gauges was done according to 2.5. Due to the large amounts of electronic equipment, there was the risk of interference, which was eliminated by use of a 'voltage stabilizer'.
5. Calibration errors. To eliminate errors due to poor calibration, the procedure was simplified, like described in Section 2.4. The readings were compared to theoretical values for validation and a perfect match was obtained.
6. Wrong input. A test schedule was made and a procedure established and closely followed during each test in order to eliminate the risk of confusion during programming of the wave generator. When possible, programs developed in MatLab where checked by manual calculations and compared to WaveLab.

Although a thorough investigation of the error sources was made, there is always a small posibility of unidentified sources of error. Considering the measures taken by the research group, the risk of errors has been minimized. Where errors were noticed after occurrence, measured were taken in order to correct or compensate them.

Sources for uncertainty are the assumptions made during calculation, that can cause the output to be less reliable. In this project there is the assumption that there are no elastic deformations of the foundation and structure. The structure and foundation

are considered infinitely stiff and there is the assumption of no dynamic damping and amplification. These assumptions can be considered adequate for the model testing in this project. Burcharth, Andersen, and Andersen [2009] concludes that the analysis using this simple method 'is expected to give reasonable estimates on caisson displacements' while mentioning that the results might be slightly on the unsafe side due to the assumption of no elastic deformations in the soil and no rocking. Andersen, Burcharth, and Andersen [2010] aims to validate this study by comparison with a numerical model that accounts for the response of the soil. Considering the results of this study, it has been concluded that, for the purpose of this research, the simplified model wil be used.

Rocking has been observed during testing. The analytical model used in this report fails to predict this behavior, because it is only one-dimensional.

Another important source of uncertainty is the foundation, which has not been investigated. No response of the foundation was considered in the analytical model, and thus it was not studied during testing. As numerical and physical tests have shown, the foundation plays an important role in the behavior of the breakwater. Including foundation response in the calculation would lead to more accurate results and can be the object of future study.

As detailed in Chapter 2.2, two gauges were mounted for the measurement of displacements and rotation. For a full picture of the movement of the structure, a third gauge to measure the vertical displacement should have been used.

7 Conclusion

The aim of this project, as described in the Chapter 1, has been to investigate the behavior of a caisson breakwater through scaled model testing.
In Chapter 2 a test plan is established and detailed specifications for model testing are presented in Section 2.2. The data gathered in the laboratory was processed in Chapter III, and the results analyzed considering the research purpose. Before and during the testing, as well as when analyzing data, sources of errors and uncertainties have been considered and investigated. The results of this investigation can be found in Chapter 6 of the Conclusion. Some suggestions for improvements and further study proposals are stated later in this chapter.
Finally, based on the research done, a conclusion in drawn.

7.1 Answers to the research questions

Before starting wave tests, the friction coefficient has been experimentally evaluated, keeping the foundation completely wet. It has been estimated 0,45 for the two tests with the smallest masses of the caisson, the ones that later showed sliding. It is a lower value than 0,5 or 0,6 (the later one is proposed by Goda), suggested tipically for the design of the caissons.

The theory used in this project to predict the pressures is the one formulated by Goda, and detailed by H.Oumeraci et al. [2001]. A short description of assumptions, and equations are found in Appendix A.2. The forces calculated using Goda's formula are comparable to the ones obtained by integration of pressures measured in the lab, except for some breaking waves. It is found that the equations used for prediction are on the safe side for no-breaking waves. For the three tests with breaking waves, the theory did not apply, and its use leaded to underestimation of wave forces.
Therefore, if breaking waves are expected for a caisson breakwater project, a series of phisical model tests are suggested.

Due to the limited time available, not enough wave types were generated in order to have a more conclusive answer to the question if different wave types influence the sliding distance. Still some conclusions can be drawn.
Several types of waves were generated during testing. Irregular waves have been found to have a less severe influence on sliding distance than regular waves, because rocking return motion can be in phase with the incident waves. Steeper waves create larger forces, but with shorter duration. Such waves produce a larger response of the caisson (displacement, as well as rotation).
In any case, a dynamic analysis has been proved to be more reliable for predicting the sliding triggering conditions, as pointed out in Chapter 5.4. This aspect can be extremely important if the sliding response factor assumes values lower than one, because sliding can occur even before the static sliding threshold. Hence the need of using a bigger safety coefficient when the sliding failure function has to be verified.

Regarding the sliding distance, the comparison between a predictiong formula (in this case it has been chosen the one of Shimosako et al. [1994]) and the measured data has given a low correlation, showing more than one or two orders of magnitude of difference. A better investigation into this aspect should be made.

If sliding is allowed, it can help optimize the construction costs, at first glance. However

a study of the optimization of construction costs is a complex matter and it can be the potential focus of future researches. The forces used in the current design for caisson breakwaters, described in H.Oumeraci et al. [2001] are on the safe side. The design of caissons that allow for no sliding requires considering a larger design force.
Due to small duration of the impact of breaking waves, the dynamic response of a lighter, less costly structure and foundation might absorb the impact and it is possible for no permanent displacement to occur. Also some allowable displacement over the lifetime of the structure can be evaluated in order to reduce costs.

Finally a sampling frequency analysis has been made, considering a certain wave-type. It has been observed that, reducing the sampling frequency, also the measured force over the caisson has lowered, but with acceptable results until about 300 Hz (less than 1% of difference). Therefore it is possible to use frequencies lower than 1000Hz without loosing data accuracy. On the other hand, using higher sampling frequencies there is the risk of recording water drops hitting the caisson at very high pressure, but that do not represent the effective pressure of the wave acting on the caisson wall.

7.2 Suggestions for improvement

As with any scientific investigation, there are certain limitations due to assumptions, equipment and time available, and targeted level of detail. While aiming to do the best possible within the limitations of the study, there are some items that can be better investigated.

The following suggestions for improvement and future study have been formulated:

- More wave heights and periods can be used in order to have more variety in the data, and thus more reliability of the results. More breaking wave tests should be conducted. At each water level, wave heights can be increased with each test.
- Inclusion of the foundation in the calculations. The importance of the foundation response is highlighted by the study of Andersen et al. [2010]. A more thorough investigation would require a look into the influence of the foundation in the analysis chapter, and inclusion of foundation investigation within the model testing.
- Fixing another displacement gauge on the vertical direction, thus constructing a full view of the movements of the structure during interaction with waves. As observed in this project, rocking is present, and a permanent rotation is noted.
- Conducting a numerical study on a computer model that includes the structure and foundation response and soil behavior, and comparing the results.

Part V

Literature

Bibliography

Andersen, Burcharth, and Andersen, 2010. Lars Andersen, Hans Falk Burcharth, and T. Lykke Andersen. *Validity pf Simplified Analysis of Stability of Caisson Breakwaters on Rubble Foundation Exposed to Impulsive Loads.* Coastal Engineering, 2010.

Andersen and Frigaard, 2011. Thomas Lykke Andersen and Peter Frigaard. *Lecture notes for the course in water wave mechanics*. ISSN: 1901-7286, DCE Lecture Notes No. 24. Aalborg University, Department of Civil Engineering, 2011.

Burcharth, Andersen, and Meinert, 2008. H.F. Burcharth, T. Lykke Andersen, and P. Meinert. *The Importance of Pressure Sampling Frequency in Models for Determination of Critical Wave Loadings on Monolithic Structures.* Coastal Engineering Journal, 2008.

Burcharth, Andersen, and Andersen, 2009. H.F. Burcharth, L. Andersen, and T. Lykke Andersen. *Analyses of Stability of Caisson Breakwaters on Rubble Foundation Exposed to Impulsive Loads.* Coastal Engineering Journal, 2009.

CEM, 2012. CEM. *Coastal Engineering Manual*, 2012.

Cuomo, Lupoi, Shimosako, and Takahashi, 2011. Giovanni Cuomo, Giorgio Lupoi, Ken-Ihiro Shimosako, and Shigeo Takahashi. *Dynamic Response and sliding distance of composite breakwaters under breaking and non-breaking wave attack.* Coastal Engineering, 2011.

DNV, 2011. DNV. *DNV-OS-J101: Design of Offshore Wind Turbine Structures*, 2011.

Franco, 1994. L Franco. *Analysis of the dynamic response of caisson breakwaters*. Coastal Engineering Journal, 1994.

Goda, 1974. Yoshimi Goda. *New wave pressure formulae for composite breakwaters*. 14th Conference of Coastal Engineering, 1974.

Goda and Suzuki, 1976. Yoshimi Goda and Yasumasa Suzuki. *Estimation of incident and reflected waves in random wave experiments.* 1976.

Goda and Takagi, 2000. Yoshimi Goda and Hiroshi Takagi. *A reliability design method of caisson breakwaters with optimal wave heights.* 2000.

H.Oumeraci, A.Kortenhaus, Allsop, Groot, Crouch, Vrijling, and Voortman, 2001. H.Oumeraci, A.Kortenhaus, William Allsop, Maarten de Groot, Roger Crouch, Han Vrijling, and Hessel Voortman. *Probabilistic design tools for vertical breakwaters.* ISBN: 90-5809-249-6. 2001.

Kisacik, Troch, and Bogaert, 2012. Dogan Kisacik, Peter Troch, and Philippe Van Bogaert. *Experimental study of violent wave impact on a vertical structure with an overhanging horizontal cantilever slab.* 2012.

Larras, 1961. J Larras. *Cours d'hydraulique maritime et du travaux maritimes*. 1961.

Liu, Niu, and Yu, 2011. Yu Liu, Xiaojing Niu, and Xiping Yu. *A new predictive formula for the inception of wave breaking.* Coastal Engineering, 2011.

Martinelli and Lamberti, 2010. Luca Martinelli and Alberto Lamberti. *Dynamic response of caisson breakwaters: suggestions for the equivalent static analysis of a single caisson in the array*. Coastal Engineering Journal, 2010.

Shimosako, Takahashi, and Tanimoto, **1994**. Kenichiro Shimosako, Shigeo Takahashi, and Katsutoshi Tanimoto. *Estimating the Sliding Distance of Composite Breakwaters due to Wave Forces Inclusive of Impulsive Forces.* 1994.

Takahashi, Tanimoto, and Shimosako, **1993**. S. Takahashi, K. Tanimoto, and K. Shimosako. *Experimental study of impulsive pressures on composite breakwaters*. Rept. of Port and Harbour Research Institute, Vol.31, No.5, 1993.

Part VI

Appendix

A Analytical models

Figure A.1 shows some parameters used in this chapter, as well as throughout the project.

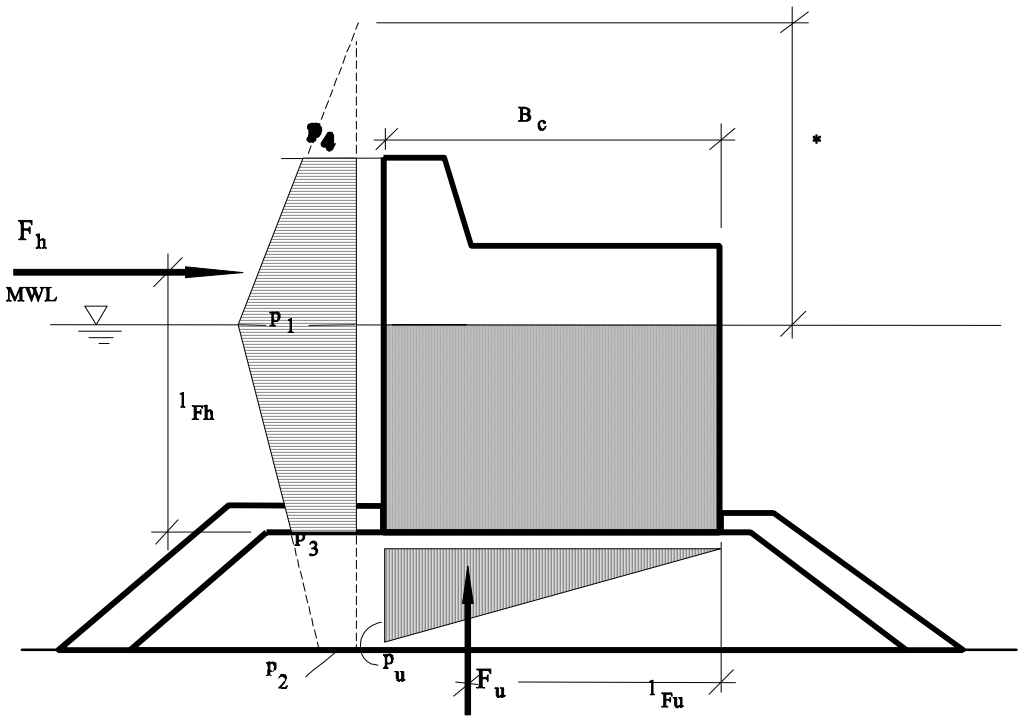

Figure A.1. Loading of caisson [H.Oumeraci et al., 2001].

A.1 Breaking wave height

A MatLab program was used to obtain the breaking wave height and period. A short description of the theory used in the program will be done in this section. The theory is taken from DNV [2011], H.Oumeraci et al. [2001], Liu, Niu, and Yu [2011], and the lecture notes for Water Wave Mechanics by Andersen and Frigaard [2011].

Wave breaking depends on steepness (A.1) and water depth. The theory developed by Miche gives an estimation of the maximum steepness that can be seen in Equation (A.2) (reduced to Equation (A.3) in shallow water).

$$\lambda = \frac{H}{L} \tag{A.1}$$

$$\lambda = 0.142 \cdot \tanh(kd) \tag{A.2}$$

$$H \leq 0.88 \cdot d \tag{A.3}$$

$$k = \frac{2\pi}{L}$$

λ_b	steepness
H	wave height
L	wave length
d	water depth
k	wave number

Breaking limits for shallow and deep water are defined by Equations (A.4) and (A.5) respectively.

$$\frac{H}{d} = 0.78 \tag{A.4}$$

$$\frac{H}{L} = 0.14 \tag{A.5}$$

The MatLab program takes into consideration these limits to calculate the maximum wave height for a specific water depth. Parameter d/L is calculated to determine weather the water is considered shallow ($d/L < 1/2$), intermediate ($1/20 < d/L < 1/2$), or deep ($1/2 < d/L$).

A wave is simulated and tested against the breaking conditions. An itterative procedure is used to calculate L, using Equation (A.6). The corresponding period of the obtained wave is obtained through Equation (A.8).

$$L = L_0 \cdot \tanh\left(2\pi\frac{h}{L}\right) \tag{A.6}$$

$$L_0 = \frac{gT^2}{2\pi} \tag{A.7}$$

$$11.1\sqrt{\frac{H}{g}} \leq T \leq 14.3\sqrt{\frac{H}{g}} \tag{A.8}$$

The type of breaking depends on steepness, but also also on the bottom slope. The type of breaking is obtained using the Iribarren number, which is defined in Equation (A.9), where $\tan\alpha$ is the bottom slope [Andersen and Frigaard, 2011].

$$\xi = \frac{\tan\alpha}{\sqrt{\lambda}} \tag{A.9}$$

Liu et al. [2011] proposes a new fromula for wave breaking inception, which aims to cover a wider range of bottom slopes than Goda and Ostendorf and Madsen. This is done by using an index called $\Psi_b^{'}$, defined in Equation (A.10). Wave breaking is considered to begin for parameter $\Psi_b^{'} = 0.69$.

$$\Psi_b^{'} = (1.21 - 3.30\lambda_b)\,(1.48 - 0.5\gamma_b)\,\Psi_b \tag{A.10}$$

$$\Psi_b = \frac{gH_b}{H_b}$$

λ_b	breaking wave steepness
γ_b	relative breaking wave height
g	gravity acceleration
H_b	breaking wave height
C_b	breaking wave celerity

Breaking wave celerity is calculated using Equation (A.11).

$$C_b = \sqrt{\frac{gL_b}{2\pi}\tanh\frac{2\pi}{L}\left(h + \frac{H_b}{2}\right)} \tag{A.11}$$

The breaking wave heights obtained from Liu et al. [2011] differ to some extent from the ones obtained using DNV [2011]. Table A.1 shows the different heights obtained by using the formulas, for three different SWL. The values in the table are in meters.

Table A.1. Breaking heights obtained by the different methods.

SWL	DNV	New formula
19	14.82	14.46
16	12.48	12.18
15	11.7	11.42

A.2 Forces acting on the caisson

The horizontal and vertical forces acting on the caisson (F_h and F_u in Figure A.1) are obtained using the method described in H.Oumeraci et al. [2001]. The method to obtained the pressures will be detailed in this section.

$$\eta^* = 0.75(1+\cos\beta)\lambda_1 H \tag{A.12}$$
$$p_1 = 0.5(1+\cos\beta)(\lambda_1\alpha_1 + \lambda_2\alpha_2\cos^2\beta)\rho g H \tag{A.13}$$
$$p_3 = \alpha_3 p_1 \tag{A.14}$$
$$p_4 = \alpha_4 p_1 \tag{A.15}$$
$$p_u = 0.5(1+\cos\beta)\lambda_3\alpha_1\alpha_3\rho g H \tag{A.16}$$

Where:

$\lambda_1, \lambda_2, \lambda_3$	multiplication factors depending on structure geometry
$\alpha_1, \alpha_2, \alpha_3, \alpha_4,$	multiplication factors depending on wave conditions

$$\alpha_1 = 0.6 + 0.5\left(\frac{4\pi h_s/L}{\sinh(4\pi h_s/L)}\right) \tag{A.17a}$$
$$\alpha_2 = min\left(\frac{\left(1-\frac{d}{H}\right)\left(\frac{H}{d}\right)^2}{3}, \frac{2d}{H}\right) \tag{A.17b}$$
$$\alpha_3 = 1 - \left(\frac{d+d_c}{h}\right)\left(1 - \frac{1}{\cosh(2\pi h/L)}\right) \tag{A.17c}$$
$$\alpha_4 = 1 - \frac{R_c^*}{\eta^*} \tag{A.17d}$$

Where:

h_s	water depth in front of the whole structure
L	wavelength
R_c^*	minimum of the freeboard and the notional run-up elevation
d_c	height over which the caisson protrudes in the rubble mound

The horizontal force is then caclulated using Formula (A.18), and the vertical force using Equation (A.19)

$$F_{h,Goda} = \frac{1}{2}(p_1+p_4)R_c^* + \frac{1}{2}(p_1+p_3)(d+d_c) \tag{A.18}$$

$$F_{u,Goda} = \frac{1}{2} p_u B_c \tag{A.19}$$

A.3 Scaling

An analogy to a prototype can be made. The scale considered for this project is 1:42.5. The scales used are calculated in Equations (A.20a) to (A.20f).

$$\text{Length: } \lambda_L = 42.5 \tag{A.20a}$$

$$\text{Velocity: } \lambda_V = \sqrt{\lambda_L} = 6.51 \tag{A.20b}$$

$$\text{Time: } \lambda_T = \frac{\lambda_L}{\lambda_V} = 6.51 \tag{A.20c}$$

$$\text{Specific weight: } \lambda_\rho = \frac{\rho_P}{\rho_M} = 0.97 \tag{A.20d}$$

$$\text{Force: } \lambda_F = \lambda_\rho \lambda_L^3 = 7.45 \cdot 10^4 \tag{A.20e}$$

$$\text{Mass: } \lambda_M = \lambda_L^3 \rho = 7.45 \cdot 10^4 \tag{A.20f}$$

Where:

ρ_P	Secific weight for water in prototype
ρ_M	Secific weight for water in model

B Result Plots

	Name		Name	Mass	SWL	H	T	Observations
Tests for fixed part	fixed-d25h20t153	Tests for moving part	initial-d25h20t153	113	0.25	0.2	1.53	theoretical breaking
	fixed-d25h10t112		initial-d25h10t112			0.1	1.12	quasi-static
	fixed-d25h20t2		Initial-d25h20t2			0.2	2	breaking
	fixed-d25hs18tp153		initial-d25hs18tp153			Hs = 0.18	1.53	irregular
	fixed-d33h20t153		initial-d33h20t153		0.33	0.2	1.53	quasi-static
	fixed-d33h10t112		initial-d33h10t112			0.1	1.12	quasi-static
	fixed-d33h25t2		initial-d33h25t2			0.257	2	breaking
	fixed-d33hs18tp153		initial-d33hs18tp153			Hs = 0.18	1.53	irregular
	fixed-d35h20t153		initial-d35h20T153		0.35	0.2	1.53	quasi-static
	fixed-d35h10t112		initial-d35h10T112			0.1	1.12	quasi-static
	fixed-d35h27t2		initial-d35h27T2			0.27	2	breaking
	fixed-d35hs18tp153		initial-d35hs18tp153			Hs = 0.18	1.53	irregular
	fixed-d25h20t153		plus10-d25h20tp153	123	0.25	0.2	1.53	theoretical breaking
	fixed-d25h10t112		plus10-d25h10tp112			0.1	1.12	quasi-static
	fixed-d25h20t2		plus10-d25h20tp153stream			0.2	2	breaking
	fixed-d25hs18t153		plus10-d25hs18tp153			Hs = 0.18	1.53	irregular
	fixed-d33h20t153		plus10-d33h20t153		0.33	0.2	1.53	quasi-static
	fixed-d33h10t112		plus10-d33h10t112			0.1	1.12	quasi-static
	fixed-d33h25t2		plus10-d33h25t2			0.257	2	breaking
	fixed-d33hs18tp153		plus10-d33hs18tp153			Hs = 0.18	1.53	irregular
	fixed-d35h20t153		plus10-d35h20t153		0.35	0.2	1.53	quasi-static
	fixed-d35h10t112		plus10-d35h10t112			0.1	1.12	quasi-static
	fixed-d35h27t2		plus10-d35h27t2			0.27	2	breaking
	fixed-d35hs18tp153		plus10-d35hs18tp153			Hs = 0.18	1.53	irregular
	fixed-d25h20t153		minus10-d25h20t153	103	0.25	0.2	1.53	theoretical breaking
	fixed-d25h10t112		minus10-d25h10t112			0.1	1.12	quasi-static
	fixed-d25h20t2		minus10-d25h20t2			0.2	2	breaking
	fixed-d25hs18t153		minus10-d25hs18tp153			Hs = 0.18	1.53	irregular
	fixed-d33h20t153		minus10-d33h20t153		0.33	0.2	1.53	quasi-static
	fixed-d33h10t112		minus10-d33h10t112			0.1	1.12	quasi-static
	fixed-d33h25t2		minus10-d33h20t2			0.257	2	breaking
	fixed-d33hs18tp153		minus10-d33hs18tp153			Hs = 0.18	1.53	irregular
	fixed-d35h20t153		minus10-d35h20t153		0.35	0.2	1.53	quasi-static
	fixed-d35h10t112		minus10-d35h10t112			0.1	1.12	quasi-static
	fixed-d35h27t2		minus10-d35h27t2			0.27	2	breaking
	fixed-d35hs18tp153		minus10-d35hs20tp153			Hs = 0.18	1.53	irregular

Figure B.1. Test table

Maximum F_u

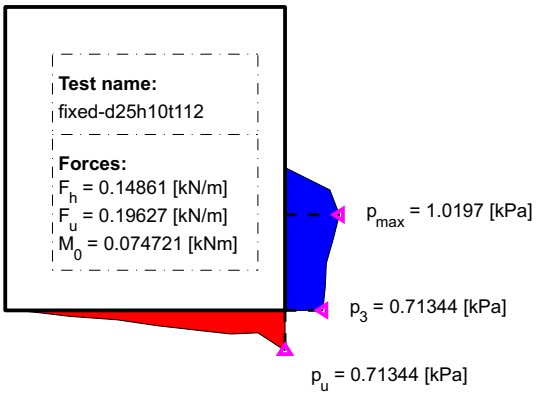

Maximum F_h

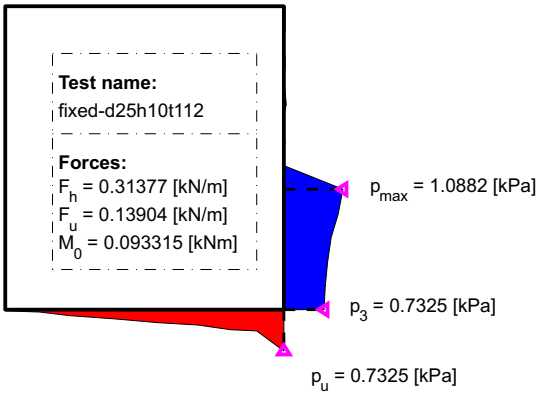

Maximum F_u

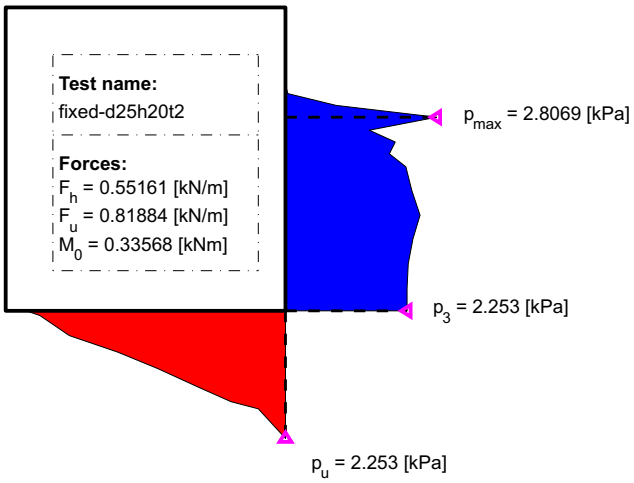

Maximum F_h

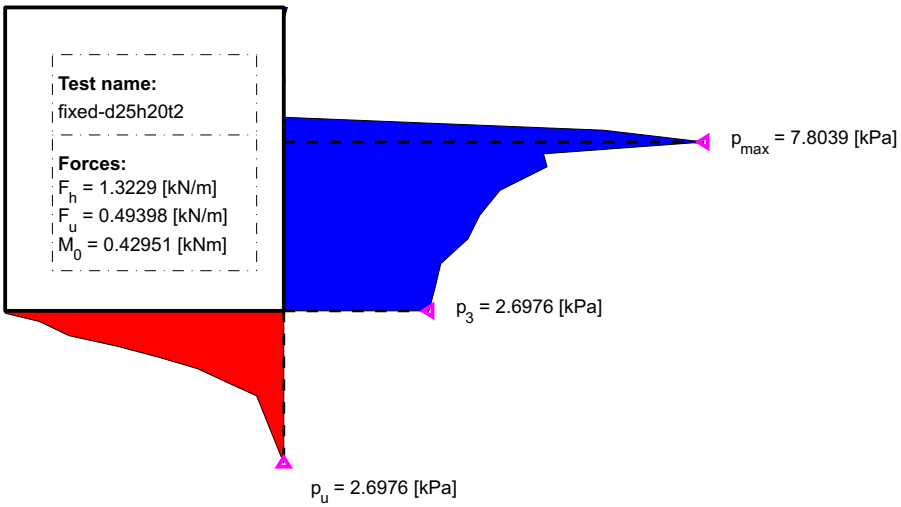

Maximum F_u

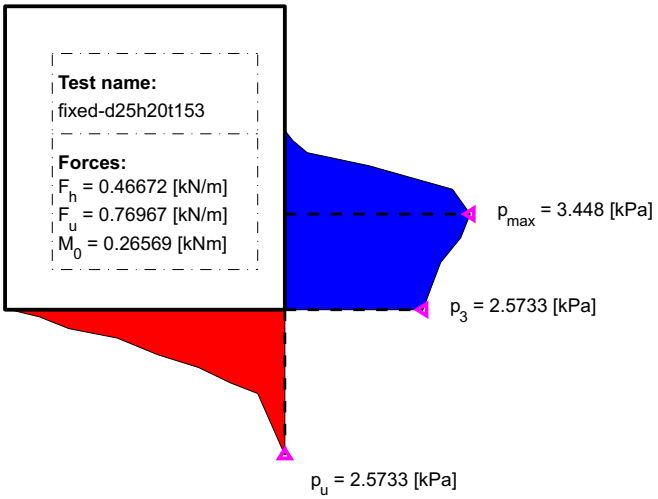

Maximum F_h

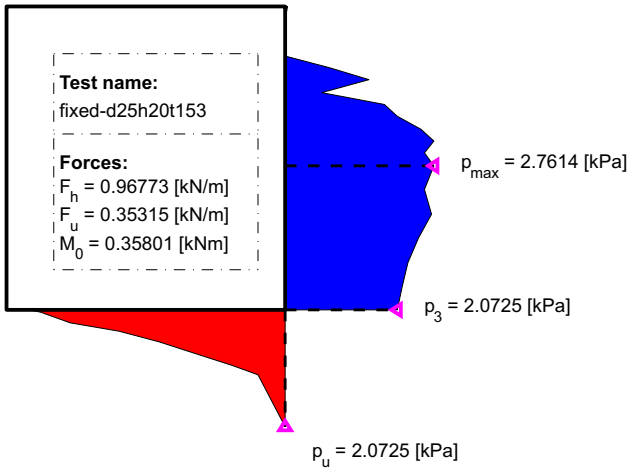

Maximum F_h

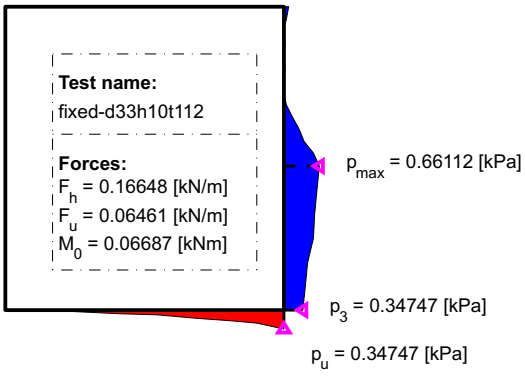

Maximum F_u

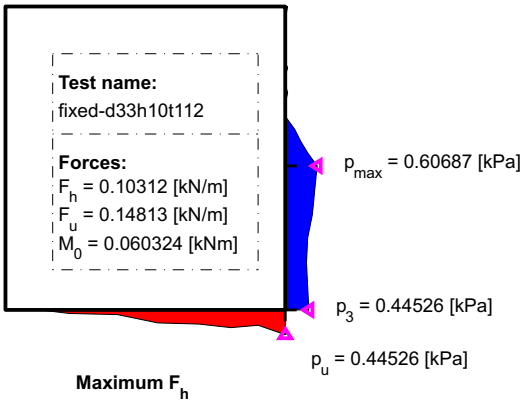

Maximum F_h

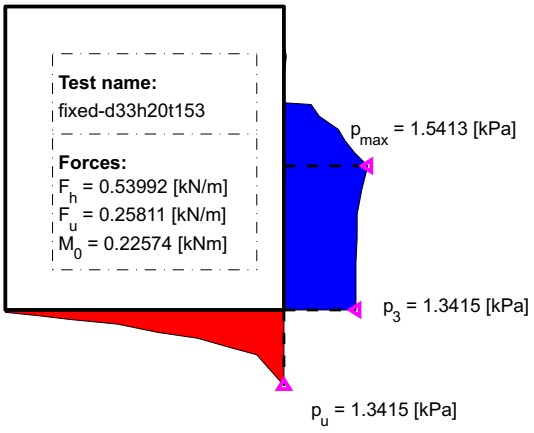

Maximum F_u

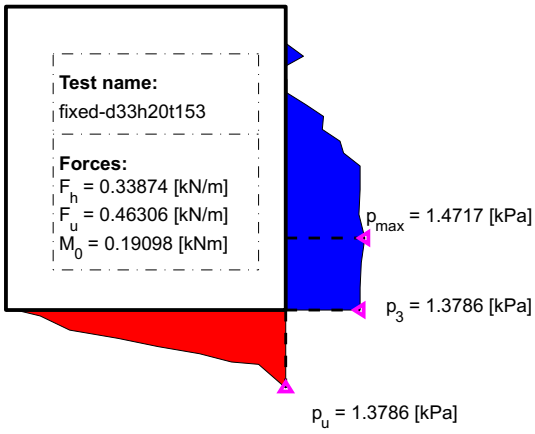

Maximum F_h

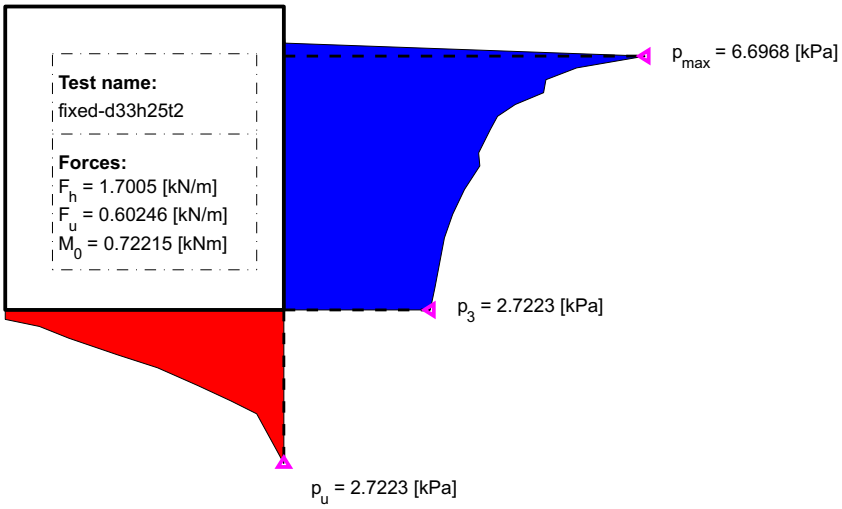

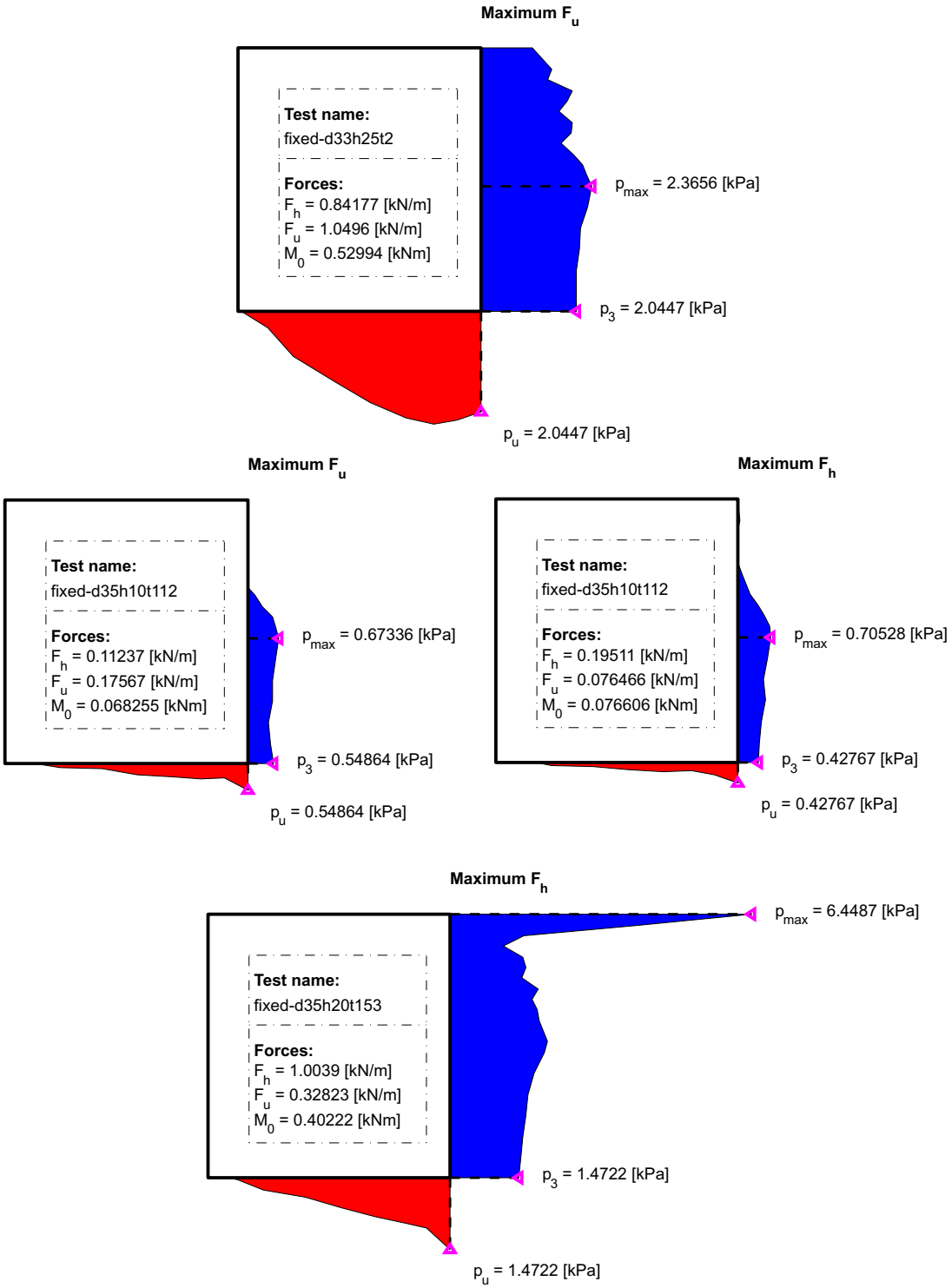
Maximum F_u
Test name:
fixed-d33h25t2
Forces:
F_h = 0.84177 [kN/m]
F_u = 1.0496 [kN/m]
M_0 = 0.52994 [kNm]
p_{max} = 2.3656 [kPa]
p_3 = 2.0447 [kPa]
p_u = 2.0447 [kPa]
Maximum F_u
Test name:
fixed-d35h10t112
Forces:
F_h = 0.11237 [kN/m]
F_u = 0.17567 [kN/m]
M_0 = 0.068255 [kNm]
p_{max} = 0.67336 [kPa]
p_3 = 0.54864 [kPa]
p_u = 0.54864 [kPa]
Maximum F_h
Test name:
fixed-d35h10t112
Forces:
F_h = 0.19511 [kN/m]
F_u = 0.076466 [kN/m]
M_0 = 0.076606 [kNm]
p_{max} = 0.70528 [kPa]
p_3 = 0.42767 [kPa]
p_u = 0.42767 [kPa]
Maximum F_h
Test name:
fixed-d35h20t153
Forces:
F_h = 1.0039 [kN/m]
F_u = 0.32823 [kN/m]
M_0 = 0.40222 [kNm]
p_{max} = 6.4487 [kPa]
p_3 = 1.4722 [kPa]
p_u = 1.4722 [kPa]

Maximum F_u

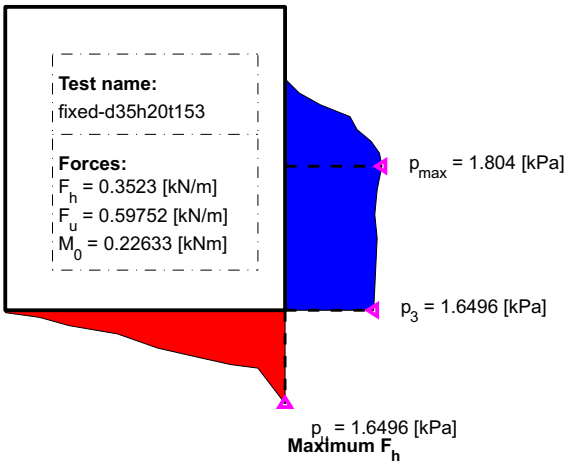

Maximum F_h

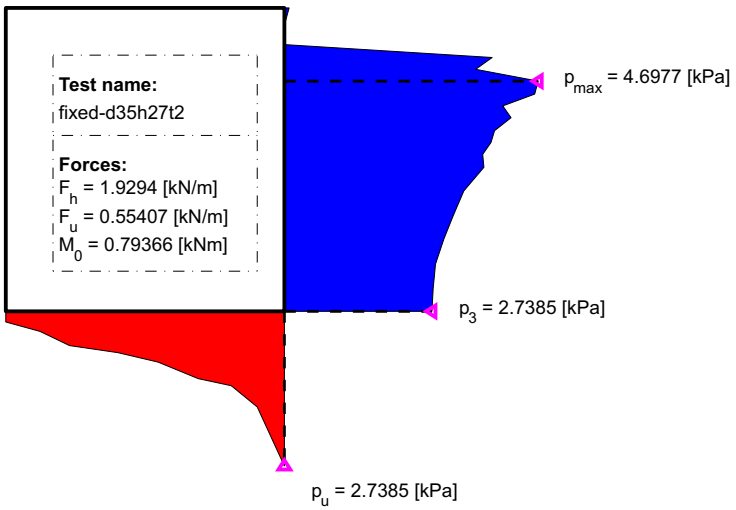

Maximum F_u

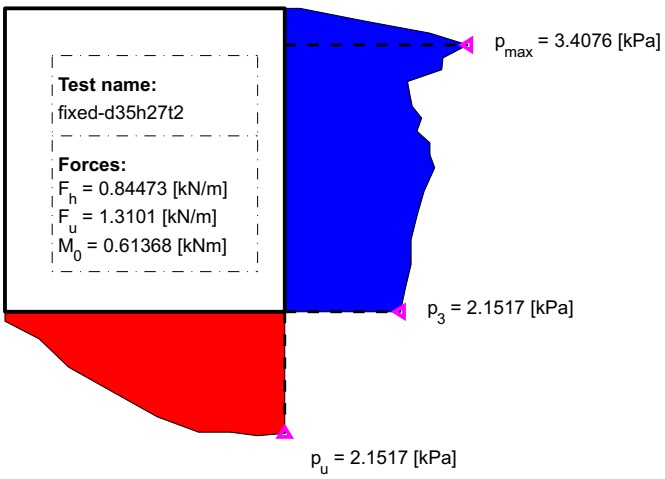

Maximum F_h

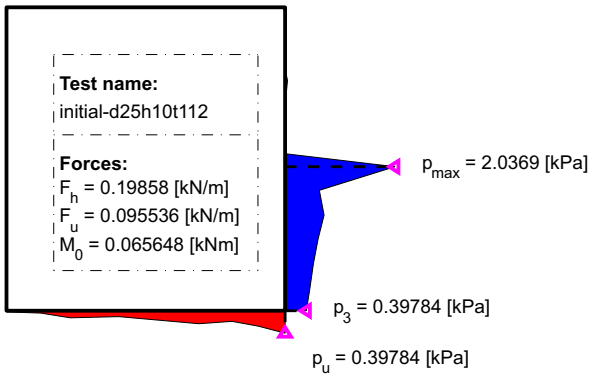

Maximum F_u

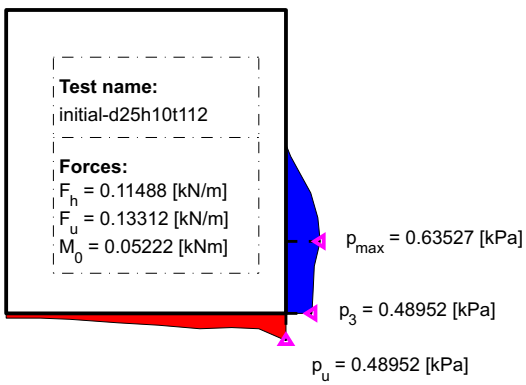

Maximum F_u

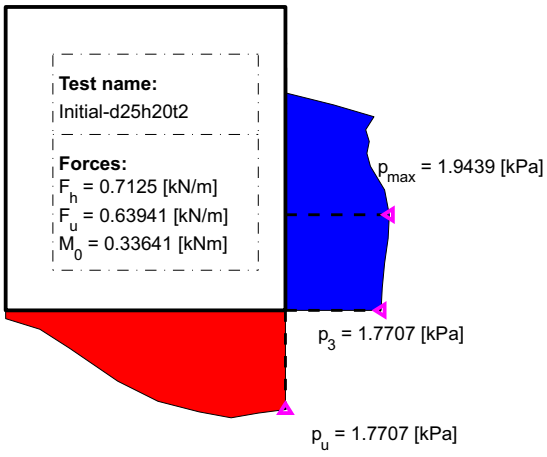

Maximum F_h

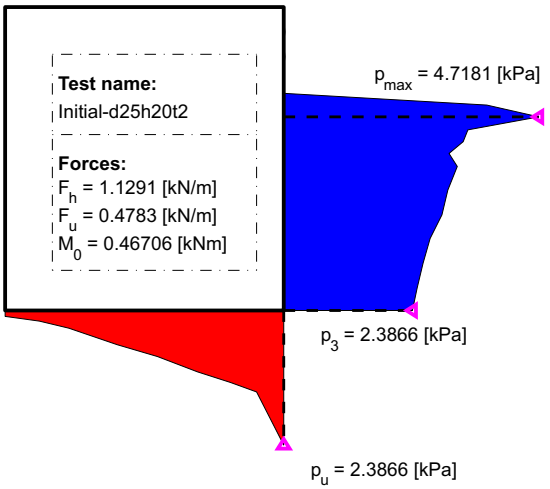

Maximum F_u

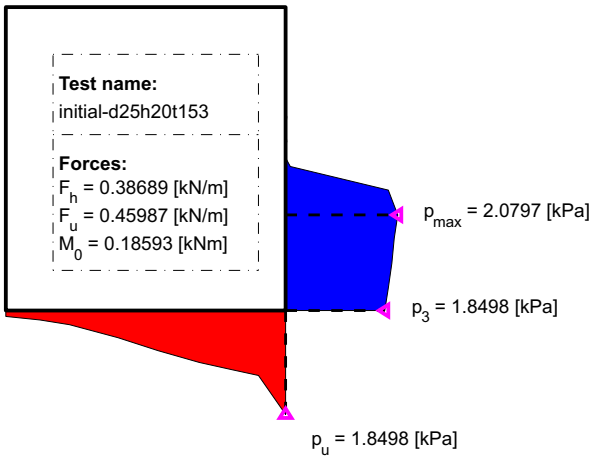

Maximum F_h

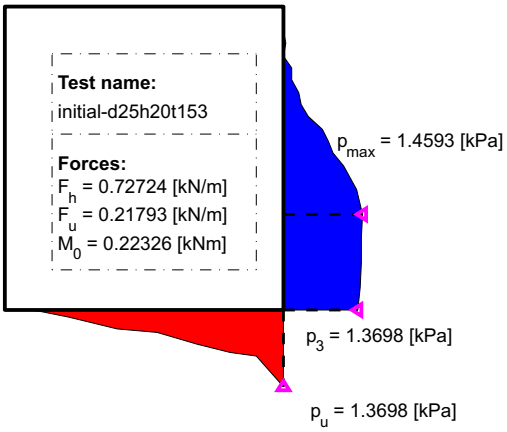

Maximum F_u

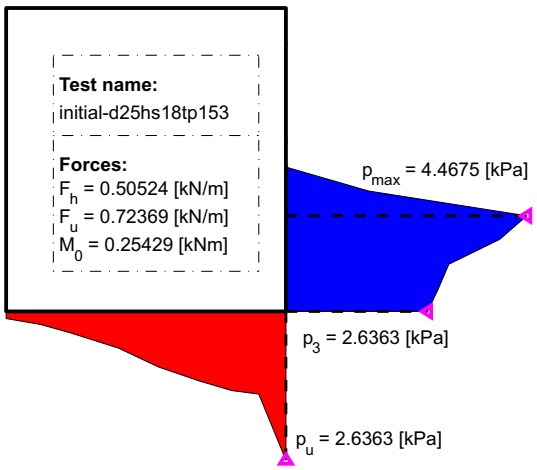

Maximum F_h

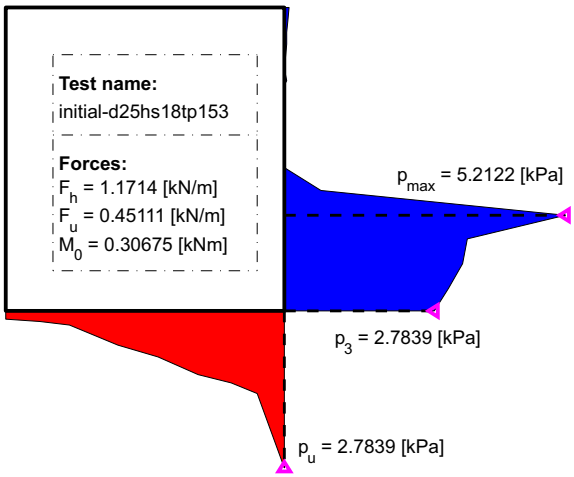

Maximum F_u

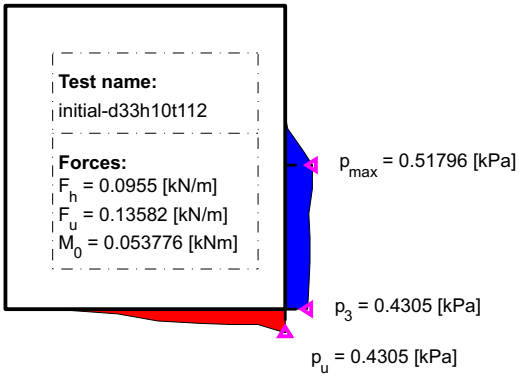

Maximum F_h

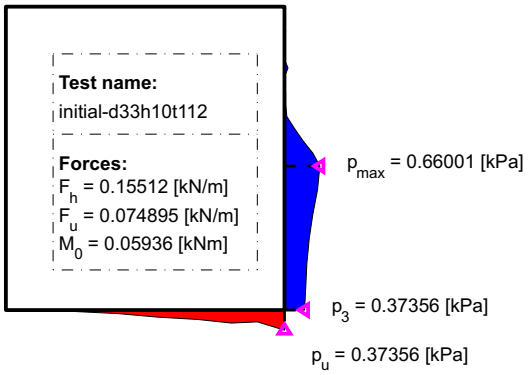

Maximum F_u

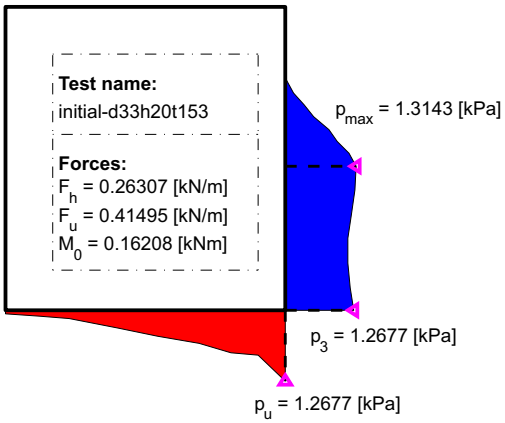

Maximum F_h

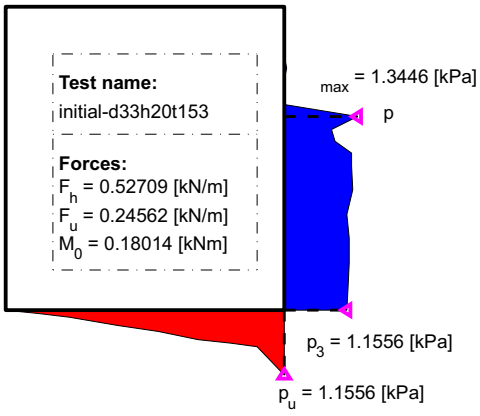

Maximum F_u

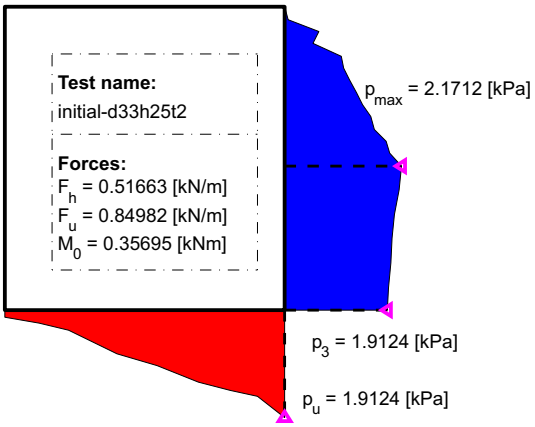

Maximum F_h

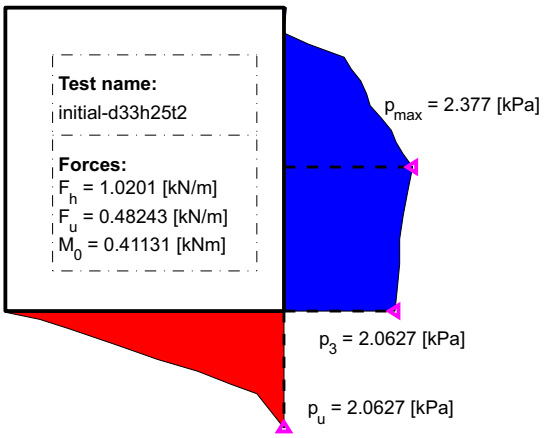

Maximum F_u

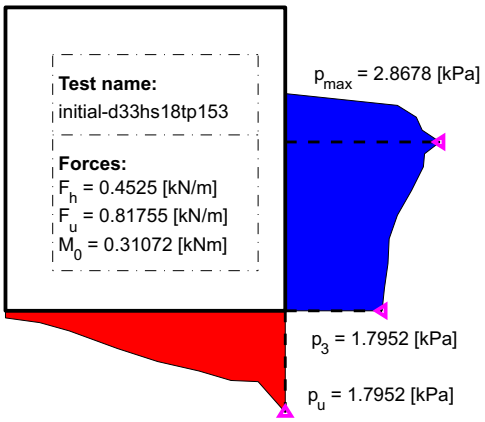

Maximum F_h

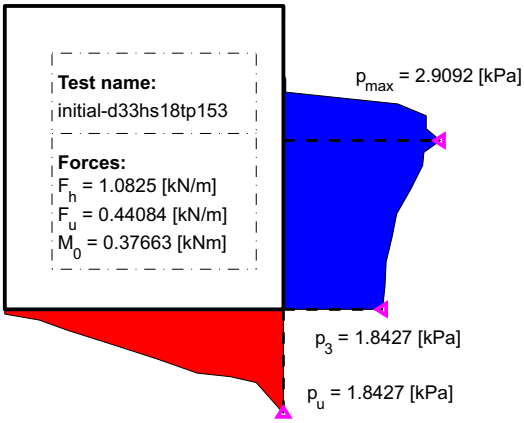

Maximum F_u

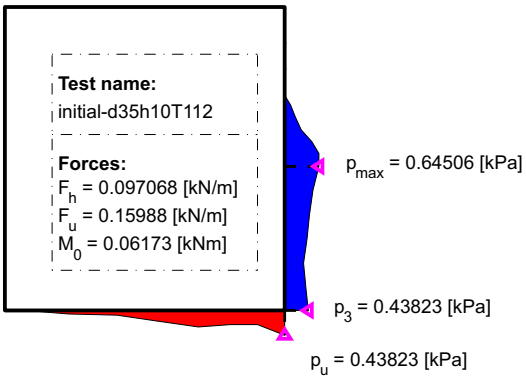

Maximum F_h

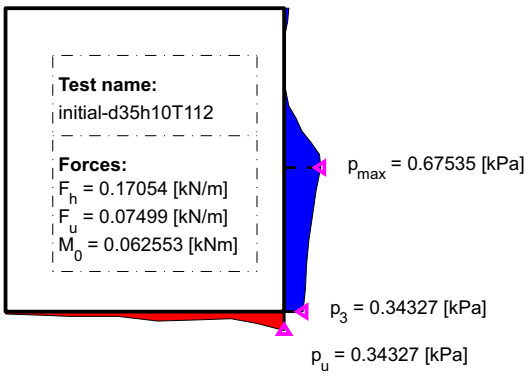

Maximum F_u

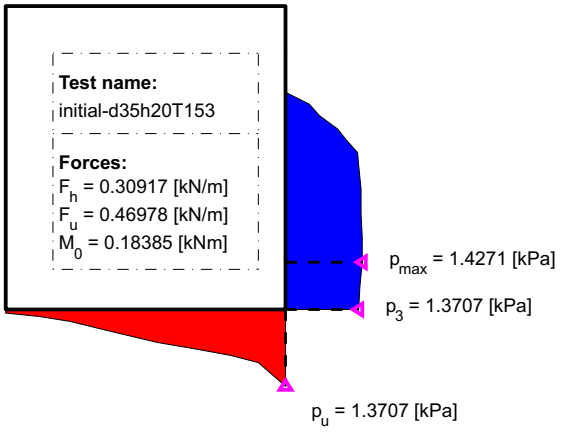

Maximum F_h

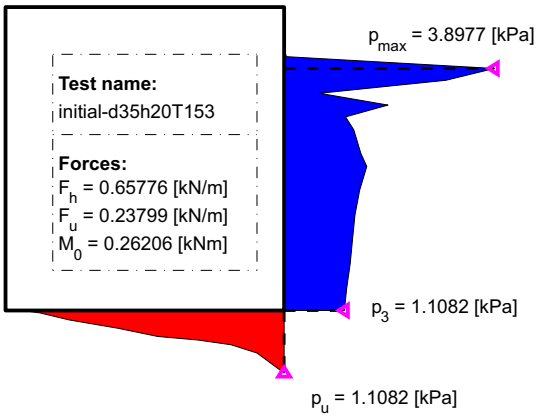

Maximum F_h

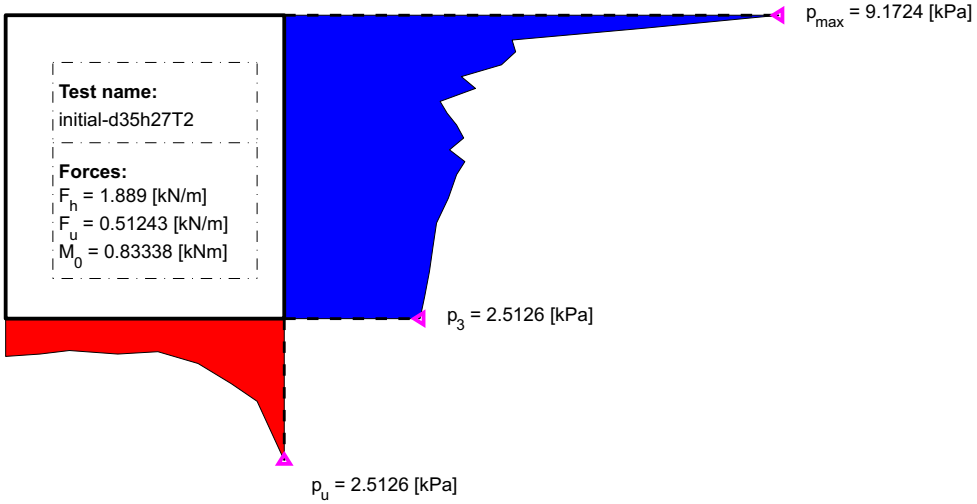

Maximum F_u

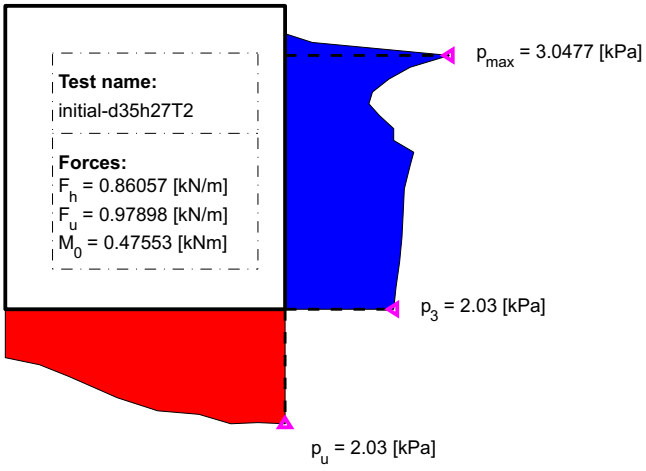

Maximum F_u

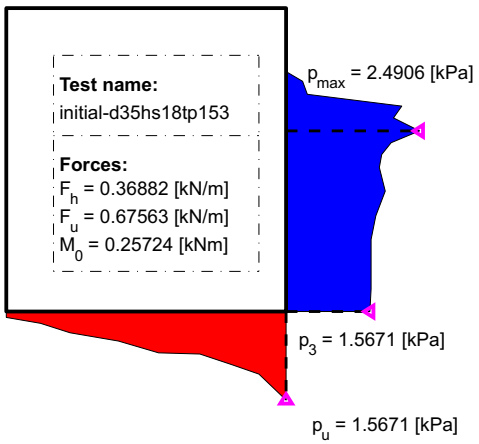

Maximum F_h

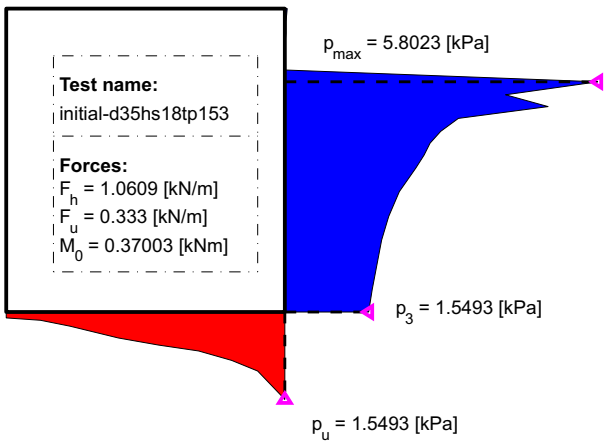

Maximum F_u

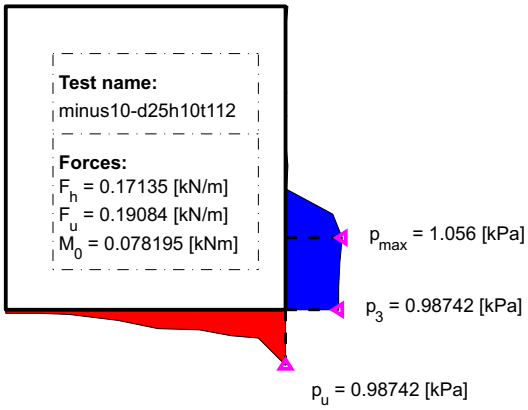

Maximum F_h

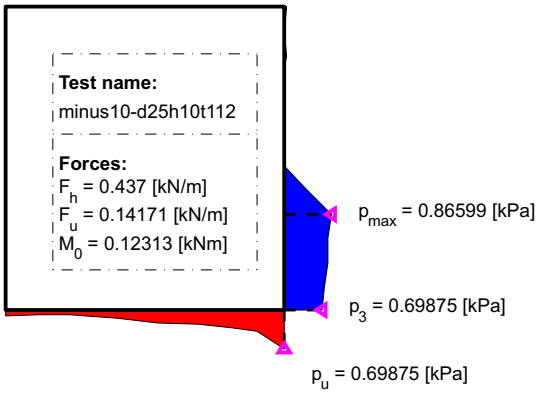

Maximum F_u

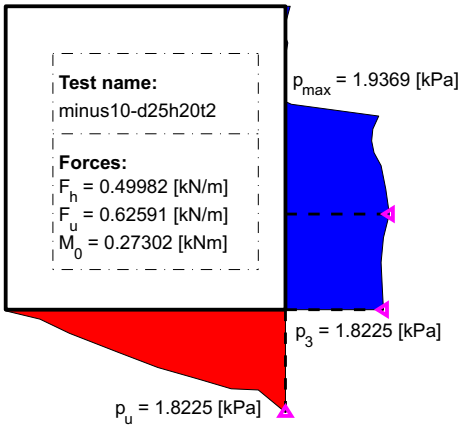

Maximum F_h

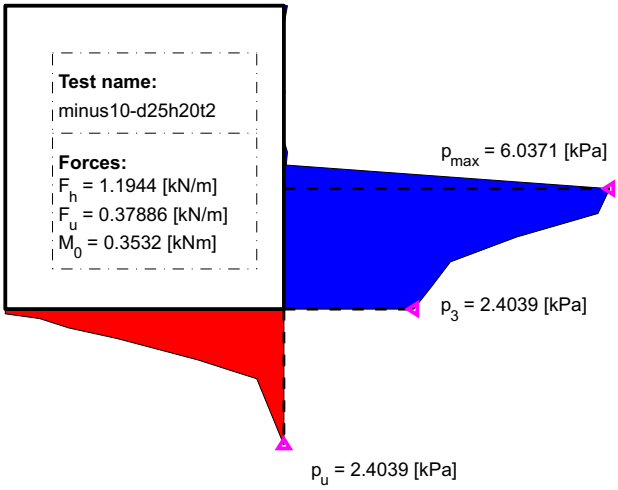

Maximum F_u

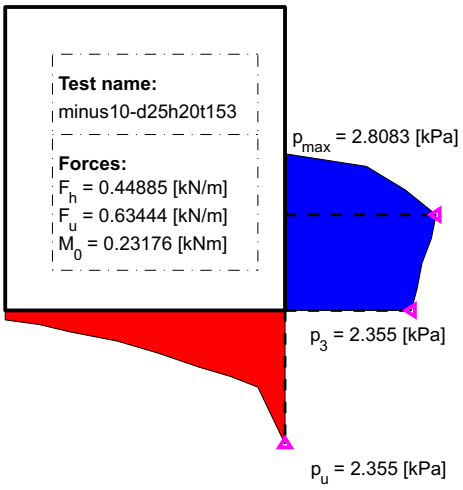

Maximum F_h

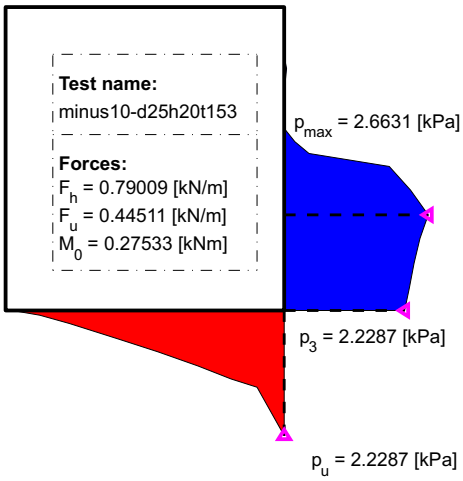

Maximum F_u

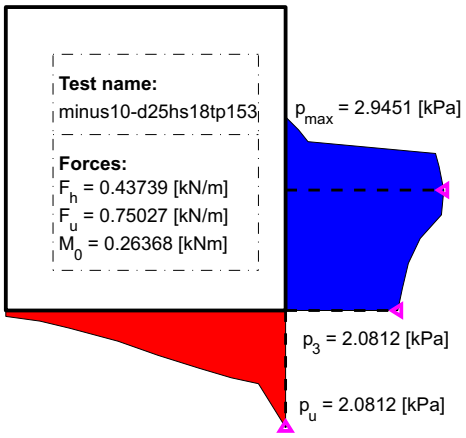

Maximum F_h

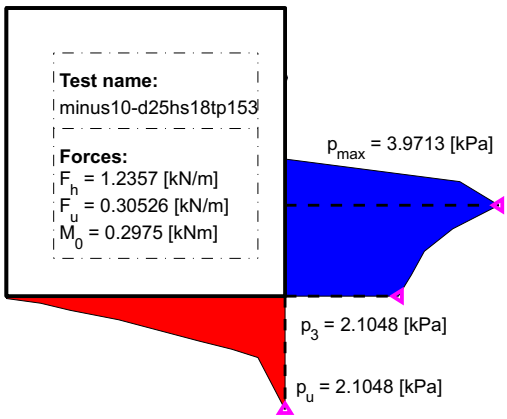

Maximum F_u

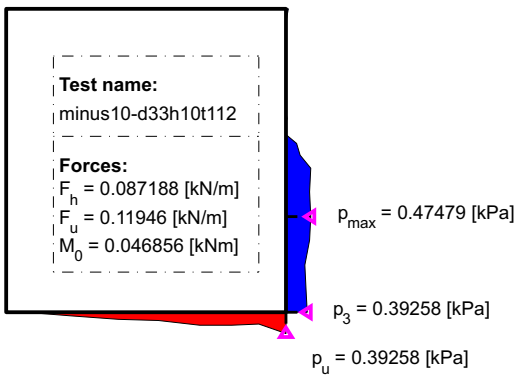

Maximum F_h

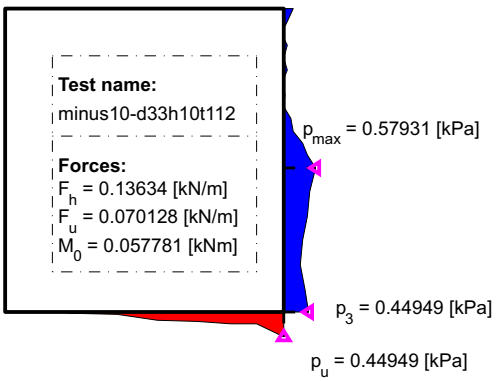

Maximum F_u

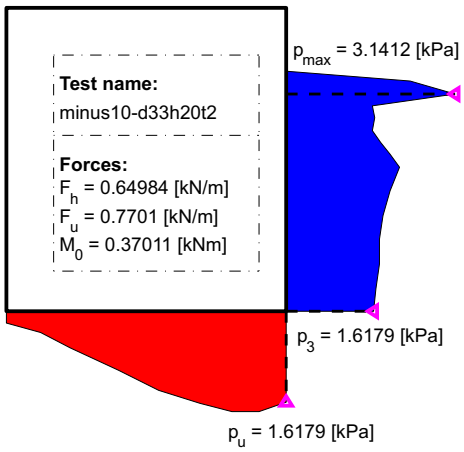

Maximum F_h

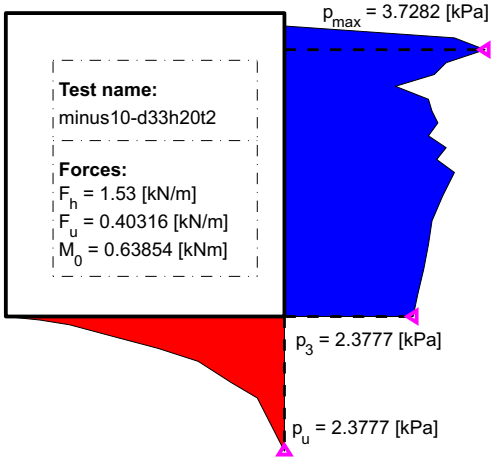

Maximum F_u

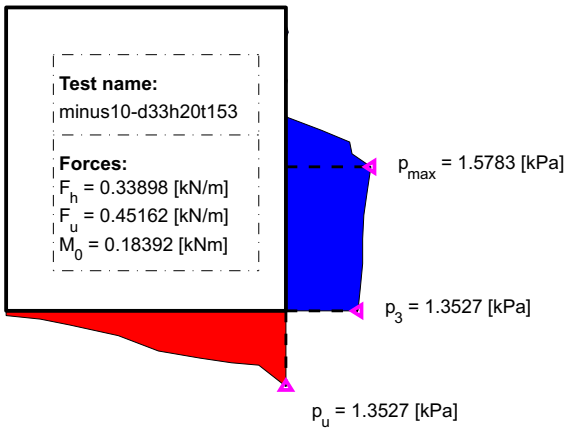

Maximum F_h

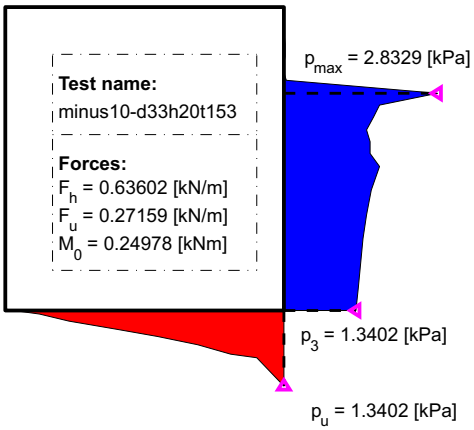

Maximum F_u

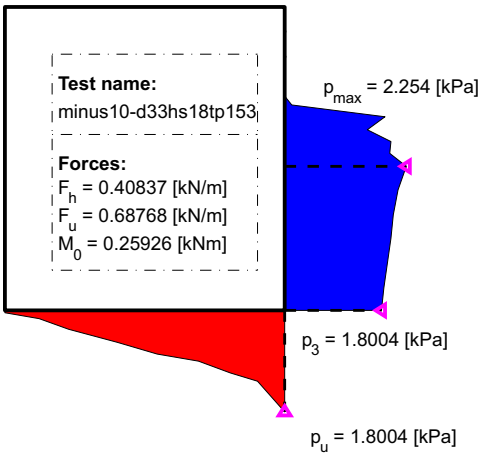

Maximum F_h

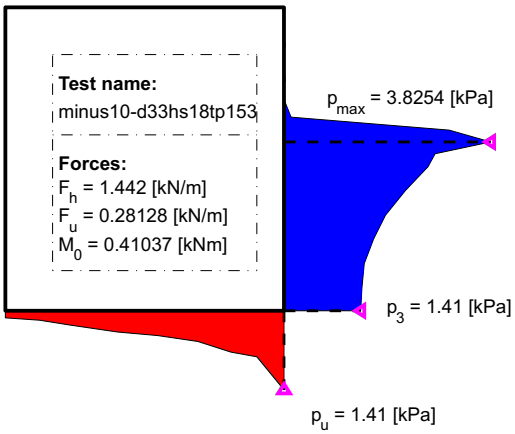

Maximum F_u

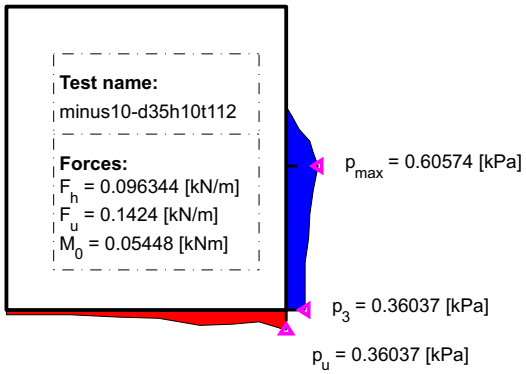

Maximum F_h

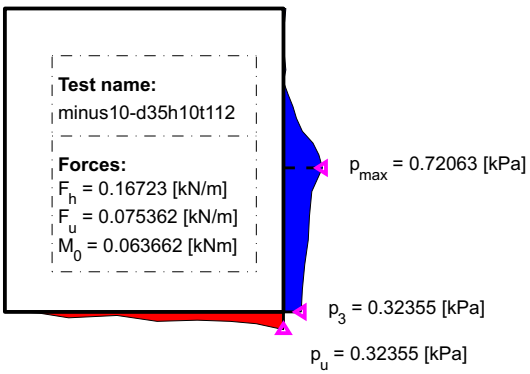

Maximum F_u

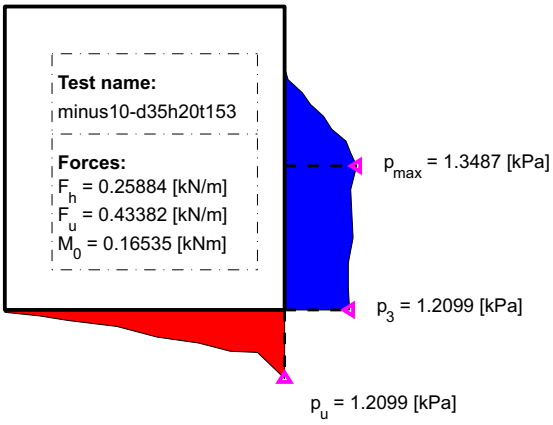

Maximum F_h

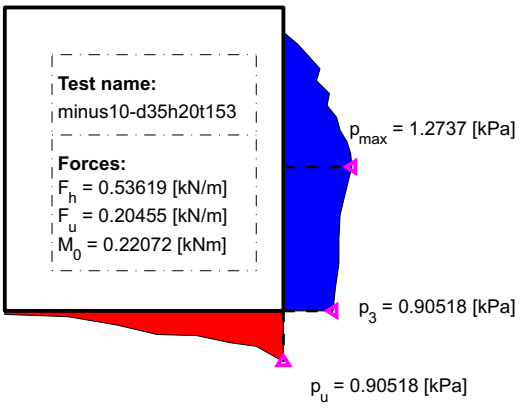

Maximum F_h

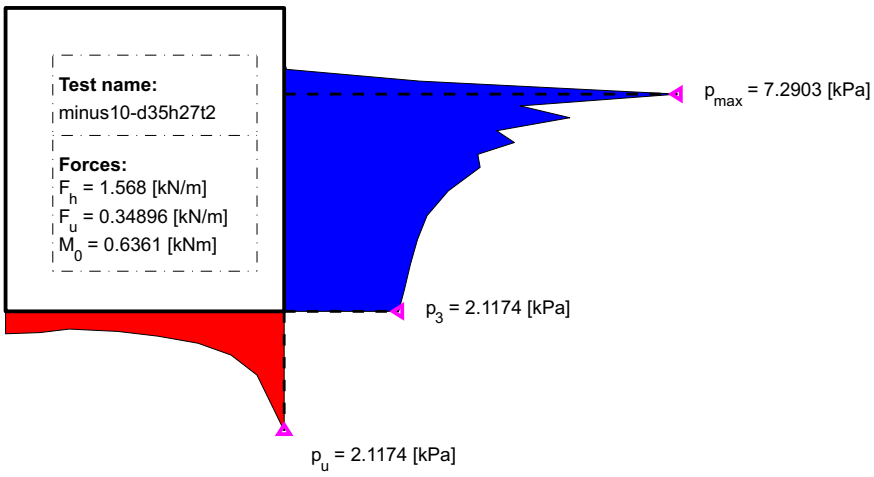

Maximum F_u

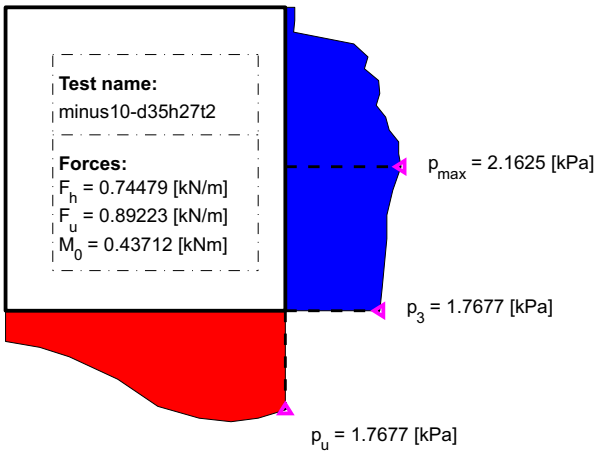

Maximum F_h

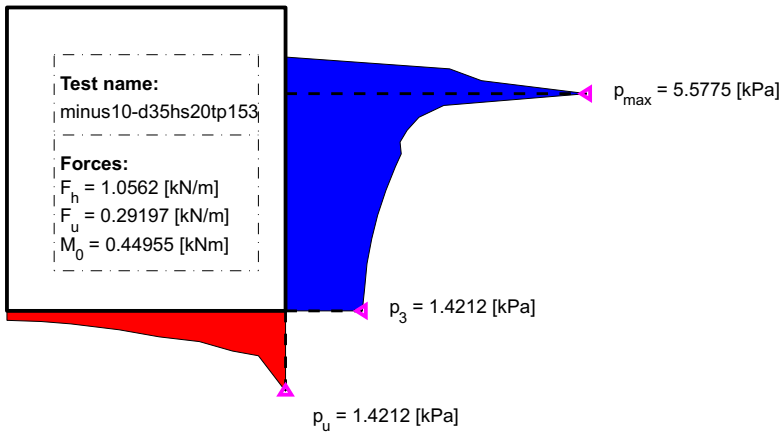

Maximum F_u

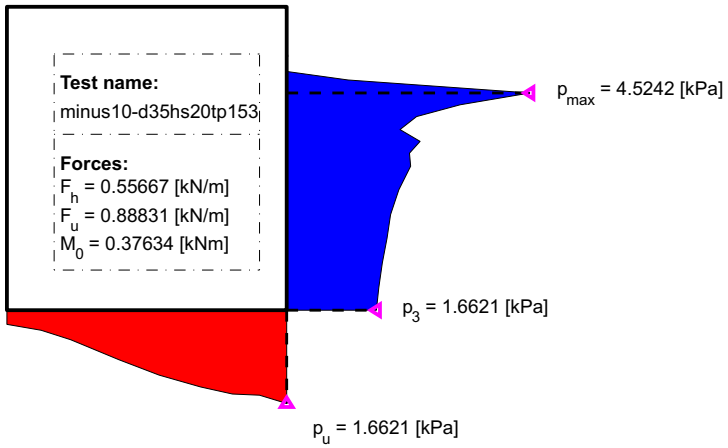

Maximum F_u

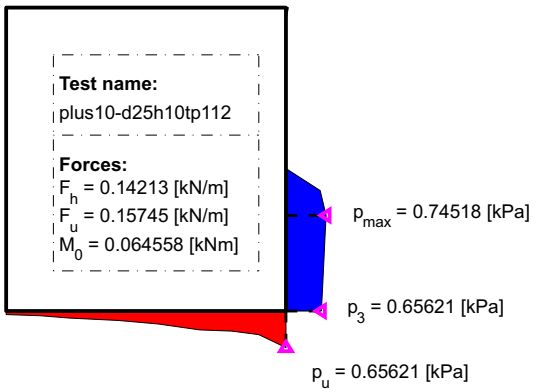

Maximum F_h

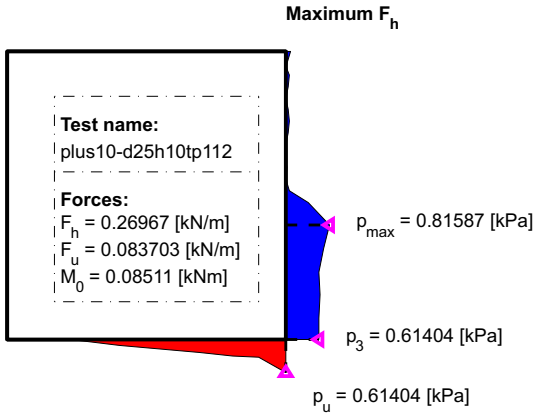

Maximum F_u

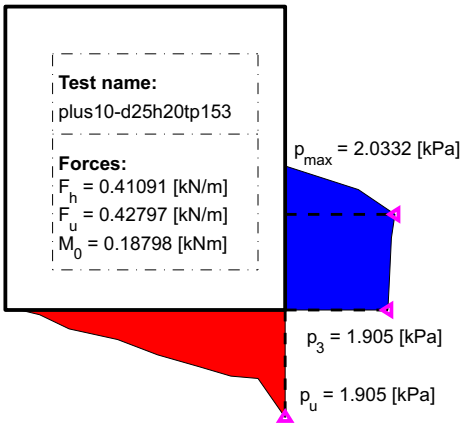

Maximum F_h

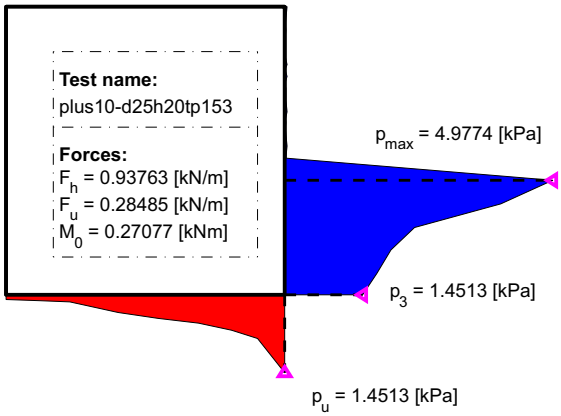

Maximum F_u

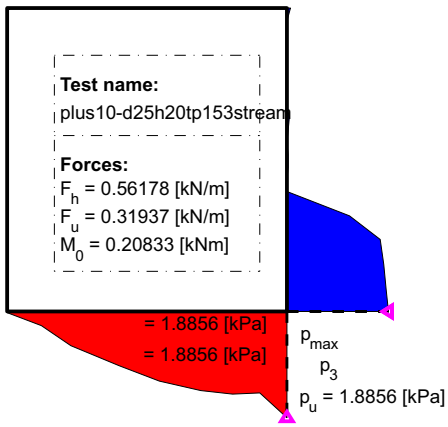

Maximum F_h

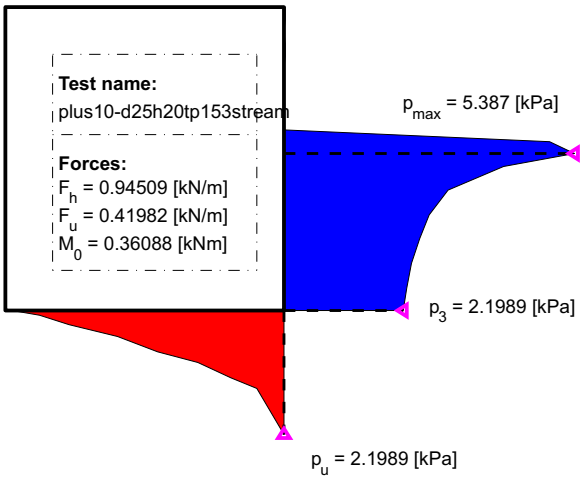

Maximum F_u

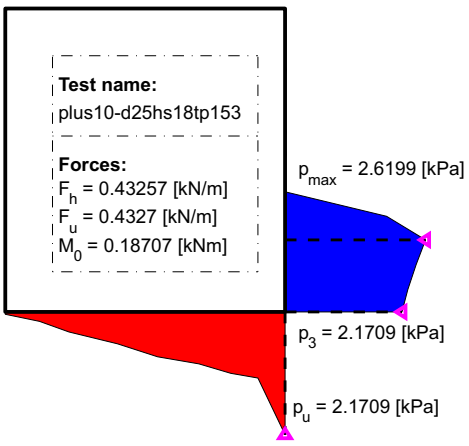

Maximum F_h

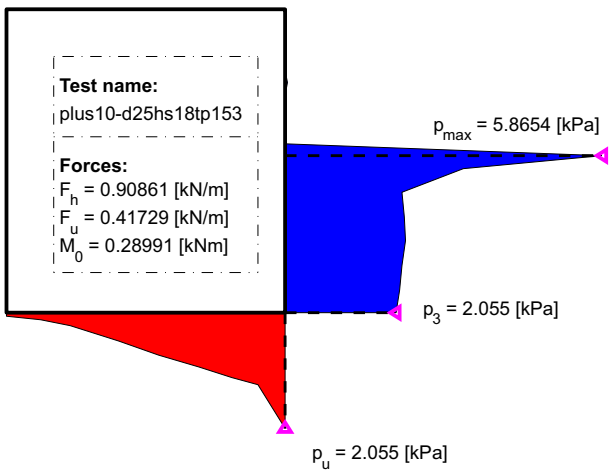

Maximum F_u

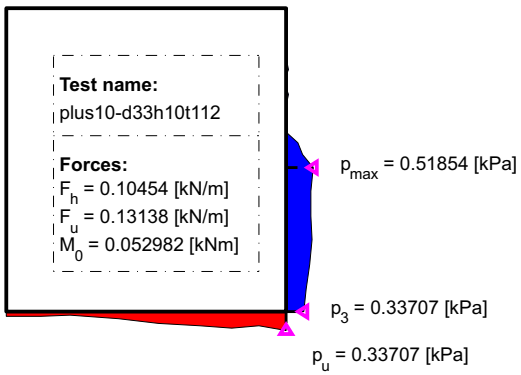

Maximum F_h

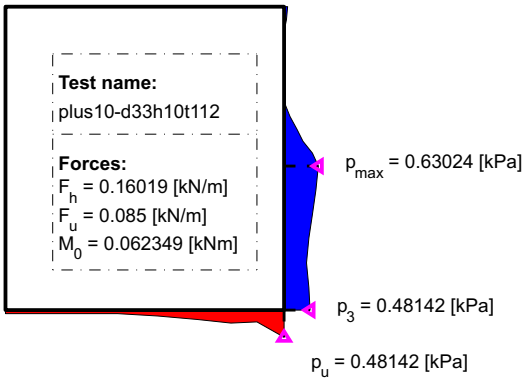

Maximum F_u

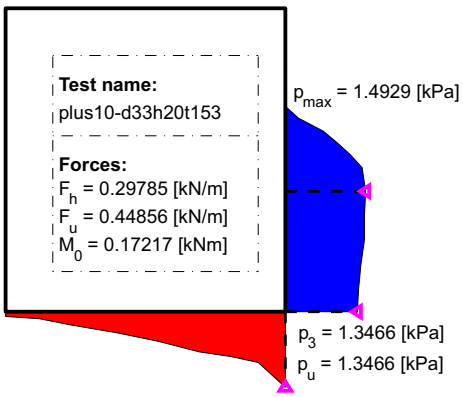

Maximum F_h

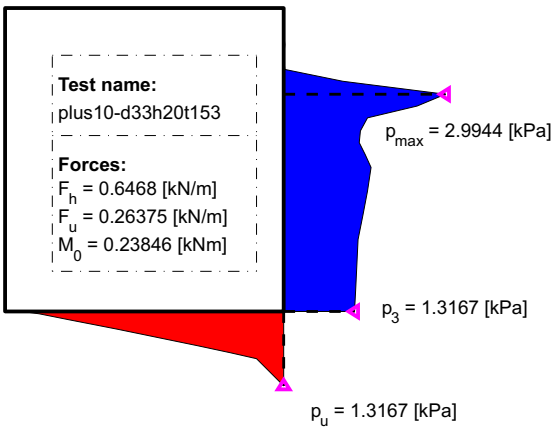

Maximum F_h

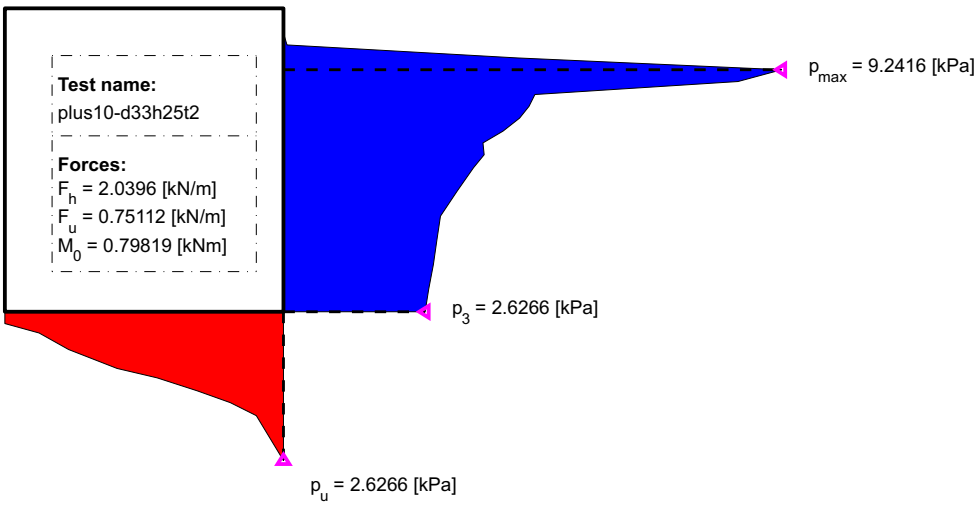

Maximum F_u

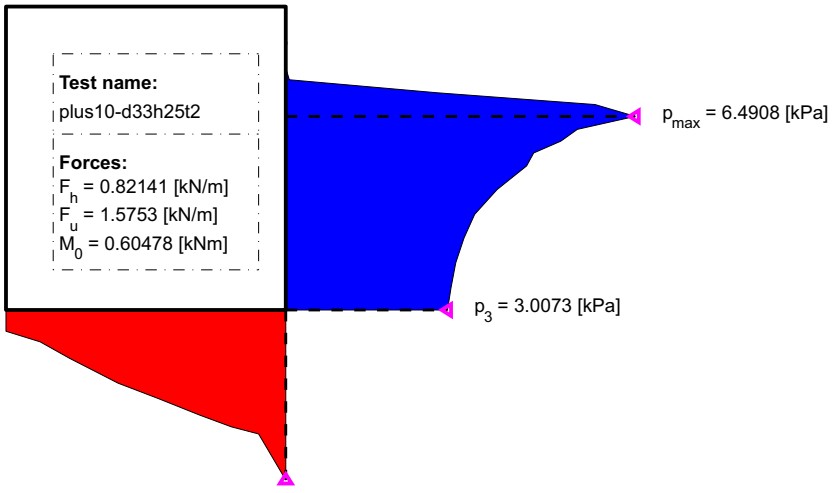

Maximum F_h

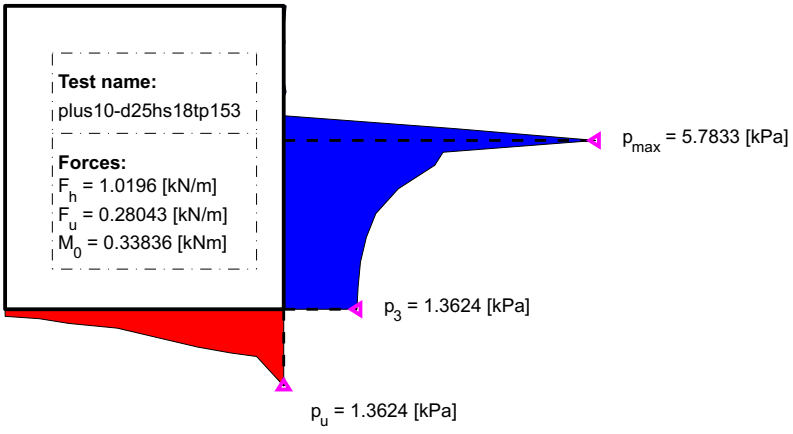

Maximum F_u

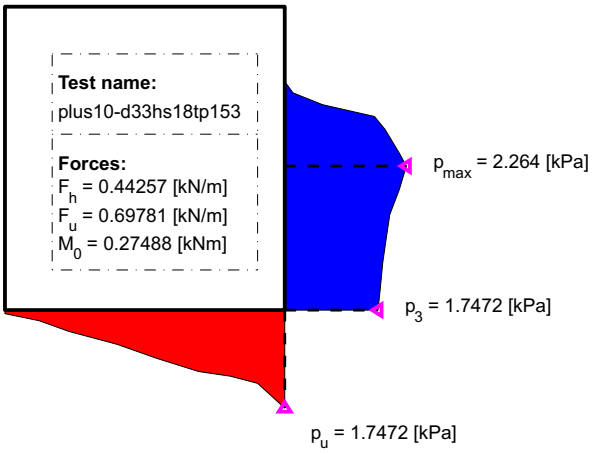

Maximum F_u

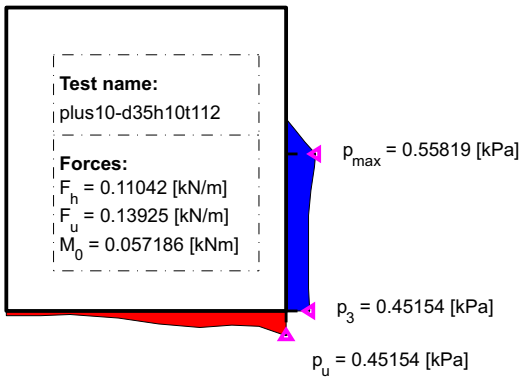

Maximum F_h

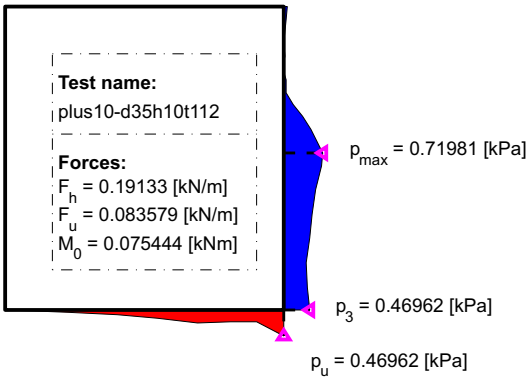

Maximum F_u

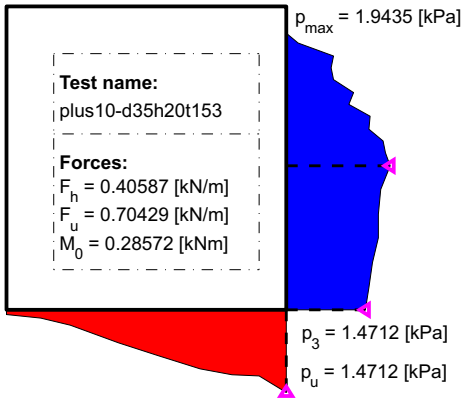

Maximum F_h

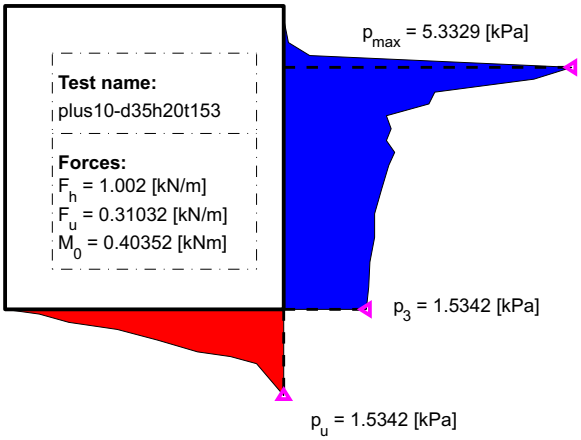

Maximum F_h

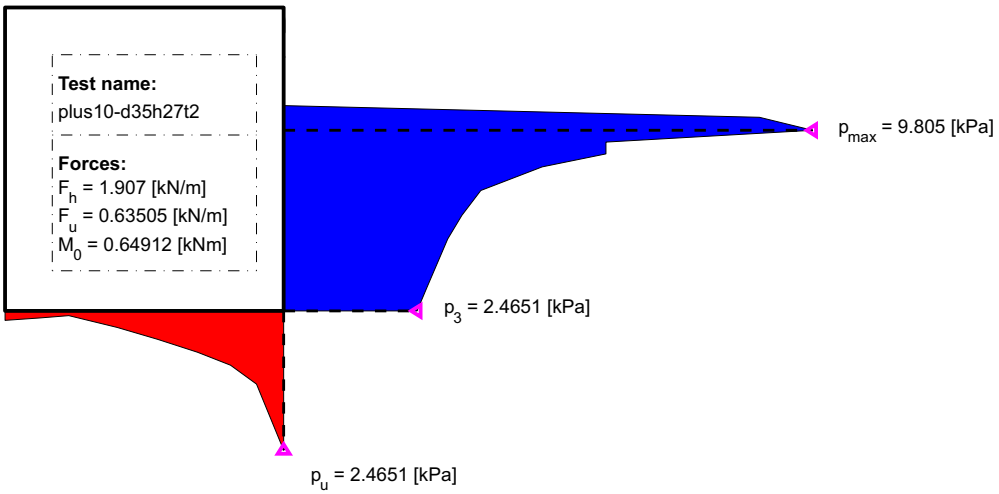

Maximum F_u

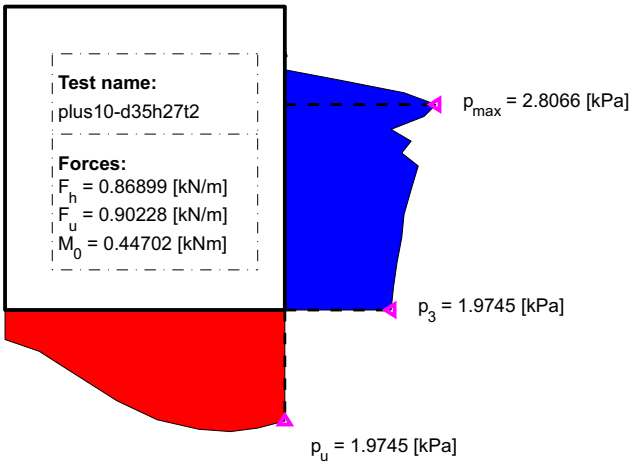

Maximum F_u

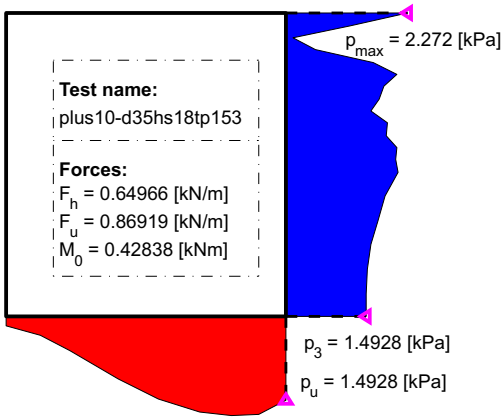

Maximum F_h

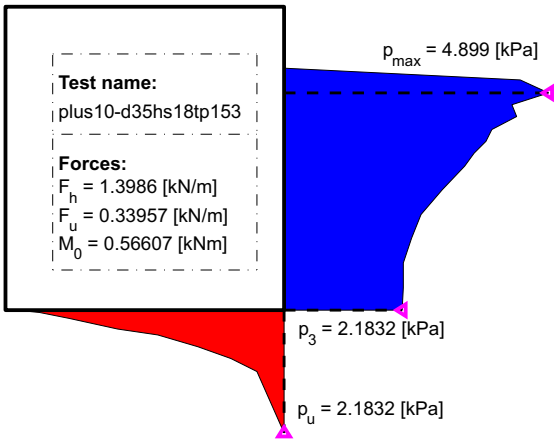

C MATLAB scripts

This appendix includes main MATLAB codes used for the thesis.

C.1 Main program

```
%%% Aalborg University & Università di Padova
%%% Department of Civil Engineering
%%% Fall semester 2012 – Spring semester 2013
%%% Group B107

close all
clear all
clc
clf
tic


%% GENERAL IMPUT PARAMETERS

fs=1000;     % [Hz] sampling frequency
m=103;       % [kg] mass of caisson (for displacements calculation)
g=9.81;      % [m/s^2]
gamma=9810; % [N/m] specific weight water 4°C
mu=0.45;     % friction coefficient (from experiments)

h=0.35;      % [m] water depth in front of structure
H=0.27;      % [m] wave height specified
T=2;         % [s] wave period specified

d=h-0.092;   % [m] depth in front of caisson
hc=0.534;    % [m] height of the caisson
b=0.3;       % [m] width of the movable part of the caisson (front view)
l=0.469;     % [m] width of the movable part of the caisson (lateral view)
bm=0.174;    % [m] distance from the top of the berm (seaward) to the wall

air0=1;      % SUBTRACT AIR PRESSURE? (air0=1)
% only for obtaining the hydrostatic pressure profile
% i.e. when loading load calibration_setup2_+XX


%% CLACULATING OFFSET IN AIR

if air0==1
load calibration_setup2_air
for i=1:30
    zero_offset(i)=mean(PGM(:,i));
end
end


%% LOADING SAVED DATA (MATLAB VARIABLE FORMAT) AND ASSIGNING

% load initial_d33h25t2_sheet2
% load initial_d35h20t153_sheet2
% load initial_d35h27t2_sheet2
% load minus10_d25h20t2_sheet1
```

```
% load minus10_d33h25t2_sheet1
% load minus10_d35h20t153_sheet1
load minus10_d35h27t2_sheet1

if air0==1;
for i=1:30
    PGM(:,i)=PGM(:,i)-zero_offset(i);
end
end

PG1=PGM(:,1);
PG2=PGM(:,2);
PG3=PGM(:,3);
PG4=PGM(:,4);
PG5=PGM(:,5);
PG6=PGM(:,6);
PG7=PGM(:,7);
PG8=PGM(:,8);
PG9=PGM(:,9);
PG10=PGM(:,10);

PG11=PGM(:,11);
PG12=PGM(:,12);
PG13=PGM(:,13);
PG14=PGM(:,14);
PG15=PGM(:,15);
PG16=PGM(:,16);
PG17=PGM(:,17);
PG18=PGM(:,18);
PG19=PGM(:,19);
PG20=PGM(:,20);

PG21=PGM(:,21);
PG22=PGM(:,22);
PG23=PGM(:,23);
PG24=PGM(:,24);
PG25=PGM(:,25);
PG26=PGM(:,26);
PG27=PGM(:,27);
PG28=PGM(:,28);
PG29=PGM(:,29);
PG30=PGM(:,30);

pwall=[PG12 PG11 PG10 PG9 PG8 PG7 PG18 PG6 PG17 PG5 PG16 PG4 PG15 PG3 PG14...
    PG2 PG13 PG1]; %from bottom,up
pbottom=[PG19 PG20 PG21 PG22 PG23 PG24 PG25]; % from seaward to shoreward


%% CONVERTING VOLTS TO PRESSURES

% the increment is not included in the calibration because it is
% subtracted when subtracting hydrostatic pressure (next step in program)
[S,I]=signal_to_pressure;
for i=1:18
%     if i==1 && i==20
%         Pressures(:,i) = 0;
%     else
     Pressures(:,i)=pwall(:,i)*S(i)+I(i);
end
```

```
[Sup,Iup]=signal_to_uplift;
for i=1:7
%     if i==1 && i==9
%         Upressures(:,i) = 0;
%     else
     UPressures(:,i)=pbottom(:,i)*Sup(i)+Iup(i);
end


%% SUBTRACTING HYDROSTATIC PRESSURE (offset for the first 10 seconds)

% either this subtraction or the subtraction in volts
if air0==1
    for i=1:18
        zr=Pressures(:,i);
        zr=zr(1:10*fs);
        Pressures(:,i)=Pressures(:,i)-mean(zr);
    end

    for i=1:7
        zr=UPressures(:,i);
        zr=zr(1:10*fs);
        UPressures(:,i)=UPressures(:,i)-mean(zr);
    end
end


%% ADDING 4 TRANSDUCERS BY EXTRAPOLATION

Pressures = [zeros(1,length(Pressures(:,1)))' Pressures zeros(1,length...
    (Pressures(:,1)))'];
UPressures = [zeros(1,length(UPressures(:,1)))' UPressures zeros(1,length...
    (UPressures(:,1)))'];

Pressures(:,1)  = Pressures(:,2) - ((Pressures(:,3)-Pressures(:,2))/4.3)...
    *3.9 ;    % Vertical Bottom Pressure transducer due to extrapolation
Pressures(:,20) = Pressures(:,19) - ((Pressures(:,18)-Pressures(:,19))/2.15)...
    *2.2;     % Vertical Top Pressure transducer due to extrapolation
UPressures(:,1) = Pressures(:,2) - ((Pressures(:,3)-Pressures(:,2))/4.3)...
    *3.9;     % Horizontal Right Pressure transducer due to extrapolation
UPressures(:,9) = UPressures(:,8) - ((UPressures(:,7)-UPressures(:,8))/10.0)...
    *6.3;     % Horizontal Left Pressure transducer due to extrapolation

for i=1:length(Pressures(:,1))
    if Pressures(i,1)<0
        Pressures(i,1)=0;
    end
end
for i=1:length(Pressures(:,20))
    if Pressures(i,20)<0
        Pressures(i,20)=0;
    end
end
for i=1:length(UPressures(:,1))
    if Pressures(i,1)<0
        Pressures(i,1)=0;
    end
end
```

```
for i=1:length(UPressures(:,9))
    if Pressures(i,9)<0
        Pressures(i,9)=0;
    end
end

PG31 = PG12 - ((PG11-PG12)/4.3)*3.9;% Vertical Bottom Pressure transducer
                                    % due to extrapolation
PG32 = PG1 - ((PG13-PG1)/2.15)*2.2; % Vertical Top Pressure transducer
                                    % due to extrapolation
PG33 = PG19 - ((PG20-PG19)/5.0)*5.0;% Horizontal Seaward Pressure transducer
                                    % due to extrapolation
PG34 = PG25 - ((PG24-PG25)/5.5)*6.3;% Horizontal Shoreward Pressure transducer
                                    % due to extrapolation

pwall=[PG31 PG12 PG11 PG10 PG9 PG8 PG7 PG18 PG6 PG17 PG5 PG16 PG4 PG15 PG3...
    PG14 PG2 PG13 PG1 PG32];        % from bottom,up
pbottom=[PG33 PG19 PG20 PG21 PG22 PG23 PG24 PG25 PG34];
                                    % from seaward to shoreward


%% PRESSURES PLOT

% % static pressure plot
% k=10000;
% pressure_plot(Pressures(k,:)*10^-3, UPressures(k,:)*10^-3);
%
% movie plot
% k=25000; % n° of frames skipped from the beginning of the recording
% %            (due to still water)
%
% for i=1:70000
%     pressure_plot(Pressures(k,:)*10^-2, UPressures(k,:)*10^-2);
%     axis ([-100 50 -50 100])
%     Film(i)=getframe;
%     clf
%     k=k+50;
% end
%
% movie(Film,2,20);


%% FORCES INTEGRATION

F=1:length(PGM);
Fu=1:length(PGM);
for i=1:length(PGM)
    [F(i),Fu(i),yF(i),xFu(i)]=pressure_integration(Pressures(i,:),...
        UPressures(i,:));
end

% forces plot
xF=linspace(0,(length(F)/fs),length(F));

figure(2)

subplot(2,1,1)
plot(xF,F)
xlabel('Time [s]')
```

```
ylabel('Horizontal  force [N/m]')
xlim([40 140])
ylim([-400 1500])
title('Horizontal force','FontWeight','bold')
grid on
box on

subplot(2,1,2)
plot(xF,Fu)
xlabel('Time [s]')
ylabel('Uplift  force [N/m]')
xlim([40 140])
ylim([-400 1500])
title('Uplift force','FontWeight','bold')
grid on
box on

Fmaxrec=max(F+mu*Fu)


%% PEAK OVER THRESHOLD

Fpot=F+mu*Fu;
thr=(m*g/b-d*l*gamma)*mu;

% find peaks separated by more than 1 second (=fs) and return their locations
[pks,locs]=findpeaks(Fpot,'MINPEAKDISTANCE',fs);
locs(pks<thr)=[];
pks(pks<thr)=[];

figure(3)
xFpot=linspace(0,(length(Fpot)/fs),length(Fpot));
hold on
plot(xFpot,Fpot)
plot(locs/fs,pks,'ro');                 % add POTs and highlight them with
                                        % a red (r) circle (o)
plot([0 length(Fpot)]/fs,[thr thr],'r') % add a line for the threshold
                                        % [f.e.: line('XData',[0 200],
grid on                                 % 'YData',[1 1],'LineStyle','-',...,
box on                                  % 'LineWidth',2,'Color','m')]
xlabel('Time [s]')
ylabel('F_h + \mu F_u [N/m]')
ylim([-400 1800])
text(0,thr,[' \muW'' = ',num2str(thr),' [N/m]'],'VerticalAlignment','bottom',...
    'HorizontalAlignment','left','Color','red')
hold off


%% GODA FORCES AND MOMENTS, TOTAL TIME OF WAVE THRUST

[L] = wave_length(T,h); % Calculates wavelenght (Diego's Lecture 4)
tau0F=(0.5-H/(8*h))*T;
hb=h;                   % hb is the water depth at a distance of 5*Hs (which
                        % is smaller than H), which is always shorter than
                        % the beginning of the sloping part in the flume
if H/d<=2
    alfaI0=H/d;
else
    alfaI0=2;
```

```
end

delta11=0.93*(bm/L-0.12)+0.36*((h-d)/h-0.6);
delta22=-0.36*(bm/L-0.12)+0.93*((h-d)/h-0.6);

if delta11<=0
    delta1=20*delta11;
else
    delta1=15*delta11;
end

if delta22<=0
    delta2=4.9*delta22;
else
    delta2=3*delta22;
end

if delta2<=0
    alfaI1=cos(delta2)/cosh(delta1);
else
    alfaI1=1/(cosh(delta1)*(cosh(delta2))^2);
end

alfaS=alfaI0*alfaI1;

if d/h>0.7
    alfastar=min(((hb-d)/(3*hb)*((H/d)^2)),(2*d/H)); % alfa 2 of Goda formula
else
    alfastar=max((min(((hb-d)/(3*hb)*((H/d)^2)),(2*d/H))),alfaS);
end

k=1/(((alfastar^0.3)+1)^2);
tau0=tau0F*k

beta=0;  % calculating Fmax with Goda
alfa1=0.6+0.5*(((4*pi*h/L)/(sinh(4*pi*h/L)))^2);
alfa2=min(((hb-d)/(3*hb)*((H/d)^2)),(2*d/H));
alfa3=1-d/h*(1-1/(cosh(2*pi*h/L)));
p1=gamma*H*(alfa1+alfa2*(cos(beta))^2);
p2=p1/(cosh(2*pi*h/L));
p3=alfa3*p1;
pu=alfa1*alfa3*gamma*H;

% horizontal force
if (1.5*H)>(hc-d)
    Fhmax=((p3+p1)*d/2)+(((p1*(1.5*H-(hc-d))/(1.5*H))+p1)*(hc-d)/2)
else
    Fhmax=((p3+p1)*d/2)+(p1*1.5*H/2)
end

if (1.5*H)>(hc-d)
    paolo=1
else
    paolo=2
end

% moment of horizontal force (rotating around the foot of the caisson shoreward)
if (1.5*H)>(hc-d)
    MFhmax=(p1*(1.5*H-(hc-d))/(1.5*H))*(hc-d)*(d+(hc-d)/2)+(p1-(p1*(1.5*H-...
```

```
        (hc-d))/(1.5*H)))*(hc-d)/2*(d+(hc-d)/3)+(p3*d*d/2)+(p1-p3)*d/2*2/3*d
else
    MFhmax=p1*1.5*H/2*(1.5*H/3)+(p3*d*d/2)+(p1-p3)*d/2*2/3*d
end

% uplift force
Fumax=pu*l/2

% moment of uplift force (rotating around the foot of the caisson shoreward)
MFumax=Fumax*l*2/3

% overturning moment
Mtot=MFhmax+MFumax

% horizontal force + uplift force
Fmax=Fhmax+mu*Fumax


%% PREDICTED DISPLACEMENTS CALCULATION

% displacement prediction using Shimosako (1994)
TOTdispl=(g*(tau0^2)*((Fmax-thr)^3)*(Fmax+thr)/(8*thr*m*(Fmax)^2));

thr1=thr; % same threshold 'thr', placed for counting the # of waves of the test
[pks1,locs1]=findpeaks(Fpot,'MINPEAKDISTANCE',fs);
locs1(pks1<thr1)=[];
pks1(pks1<thr1)=[];
nw=length(pks1) % # of waves during the test

% total permanent displacement
TOTdispl1=TOTdispl*nw

% displacement prediction using Shimosako (1994) modfified using pks (measured)
% and tau0 measured (approximate mean value)

tau0=0.2;

for i=1:length(pks)
     TOTdispl2=(g*(tau0^2)*((pks(i)-thr)^3)*(pks(i)+thr)/(8*thr*m*(pks(i))^2));
end

TOTdispl2=0;
for i=1:length(pks)
     TOTdispl2=TOTdispl2+(g*(tau0^2)*((pks(i)-thr)^3)*(pks(i)+thr)/...
         (8*thr*m*(pks(i))^2));
end

% total permanent displacement
TOTdispl2


%% DISPLACEMENT ANALYSIS

b=17.5/100; % [m] distance between displacement gauges
% offset subtraction for displacement gauges
DG1=DG1-mean(DG1(1:10*fs));
DG2=DG2-mean(DG2(1:10*fs));
% filtering
% DG1=smooth(DG1,50); % by moving average
```

```
% DG2=smooth(DG2,50);

DG1=smooth(DG1,'sgolay'); % by Savitzky–Golay
DG2=smooth(DG2,'sgolay'); % preserves peak hights and width better

% conversion from volts to meters 1 V = 0.104331 m\
% and multiplication by –1 gives positive values
D1=DG1*0.104331;
D2=DG2*0.104331;

if mean(D1(end–fs:end))<0
    D1=–D1;
end

if mean(D2(end–fs:end))<0
    D2=–D2;
end

%permanent displacement
D1_p=mean(D1(end–fs:end))–mean(D1(1:fs));
D2_p=mean(D2(end–fs:end))–mean(D2(1:fs))
D_perm=(D1_p+D2_p)/2;

% calculating rotation
ROT=radtodeg(atan((D1–D2)/b));
% permanent rotation
ROT_perm=mean(ROT(end–fs:end))–mean(ROT(1:fs))


%% PLOTTING DISPLACEMENTS AND ROTATION

% smoothing the data for plotting by moving average
D1=smooth(D1,70);%200
D2=smooth(D2,70);%200
ROT=smooth(ROT,350);%500
xF=linspace(0,(length(F)/fs),length(F));
xD1=linspace(0,(length(D1)/fs),length(D1));
xD2=linspace(0,(length(D2)/fs),length(D2));
xROT=linspace(0,(length(ROT)/fs),length(ROT));

figure(4)

subplot(2,1,1)
xFpot=linspace(0,(length(Fpot)/fs),length(Fpot));
hold on
plot(xFpot,Fpot)
plot(locs/fs,pks,'ro');                  % add POTs and highlight them with
                                         % a red (r) circle (o)
plot([0 length(Fpot)]/fs,[thr thr],'r')  % add a line for the threshold
                                         % [f.e.: line('XData',[0 200],
grid on                                  % 'YData',[1 1],'LineStyle','–',...,
box on                                   % 'LineWidth',2,'Color','m')]
xlabel('Time [s]')
ylabel('F_h + \mu F_u [N/m]')
title('Time history load','FontWeight','bold')
xlim([47 59])
ylim([–400 1800])
text(0,thr,[' \muW'' = ',num2str(thr),' [N/m]'],'position',[40 (thr+100)]...
    ,'Color','red') %'VerticalAlignment','bottom','HorizontalAlignment','left'
```

```
hold off

% subplot(4,1,2)
% plot(xD1,D1*100,'LineWidth',1.2)
% xlabel('Time [s]')
% ylabel('Displacement [cm]')
% title('Displacement Gauge 1 (upper)','FontWeight','bold')
% xlim([47 59])
% ylim([-0.5 1.5])
% grid on
% box on

subplot(2,1,2)
plot(xD2,D2*100,'LineWidth',1.2)
xlabel('Time [s]')
ylabel('Displacement [cm]')
title('Displacement Gauge 2 (lower)','FontWeight','bold')
xlim([47 59])
ylim([-0.5 1.5])
grid on
box on

% subplot(4,1,4)
% plot(xROT,ROT,'LineWidth',1.2)
% xlabel('Time [s]')
% ylabel('Rotation [\circ]')
% title('Rotation','FontWeight','bold')
% xlim([40 65])
% ylim([-0.5 0.5])
% grid on
% box on

figure(5)
xFpot=linspace(0,(length(Fpot)/fs),length(Fpot));
% hold on
plot(xFpot,Fpot)
set(gcf, 'PaperPositionMode', 'auto');
% plot(locs/fs,pks,'ro');                 % add POTs and highlight them with
                                          % a red (r) circle (o)
% plot([0 length(Fpot)]/fs,[thr thr],'r') % add a line for the threshold
                                          % [f.e.: line('XData',[0 200],
grid on                                   % 'YData',[1 1],'LineStyle','-',...,
box on                                    % 'LineWidth',2,'Color','m')]
xlabel('Time [s]')
ylabel('F_h + \mu F_u [N/m]')
title('Time history load','FontWeight','bold')
xlim([47 59])
ylim([-400 1800])
% text(0,thr,[' \mu(G-W) = ',num2str(thr),' [N/m]'],'position',[40 (thr+150)]...
% ,'Color','red') %'VerticalAlignment','bottom','HorizontalAlignment','left'
% hold off

toc
```

C.2 Wave length calculation

```
function [L] = wave_length(T,h)
```

```
% WAVELENGTH
% Calculates wavelenght (Vicinanza's Lecture 4, AAU)

g=9.81;
Len=(g*(T^2)*0.5/pi)*sqrt(tanh(4*pi*pi*h/(T*T*g)));  % 1984 SPM, p.2—7
L1=Len;
for k=1:250
    L2=(g*(T^2)*0.5/pi)*tanh(2*pi*h./L1);
    L1=L2;
end
L=L2;
end
```

C.3 Convertion from Volts to Pressure for the front wall of the caisson

```
function [S,I]=signal_to_pressure

% calibration for volts to pressure, for the front wall.

% D1 = [0 3.9 8.2 12.5 16.8 21.1 25.4 27.55 27.55 29.7 31.85 34 36.15 38.3...
    % 40.45 42.6 44.75 46.9 49.05 51.2 53.4]
D0=[2 4.15 6.3 8.45 10.6 12.75 14.90 17.05 19.20 21.35 23.50 25.65 27.80...
    32.1 36.4 40.7 45 49.3];
D1=D0*0;               % 1st test: air pressure
D2=D0+0.7;             % 2nd test: SWL at 7 mm above the edge of the caisson
D3=D0+10;              % 3rd test: SWL at 10 cm above the edge of the caisson
D=[D1' D2' D3']*10^—2; % from [cm] to [m]

g=9.81;                % [m/s^2]
rho=1000;              % [kg/m^3]

PH=g*rho*D;            % [m/s^2]*[kg/m^3]*[m]=[N/m^2]

load calibration_setup2_air

PG1=PGM(:,1);
PG2=PGM(:,2);
PG3=PGM(:,3);
PG4=PGM(:,4);
PG5=PGM(:,5);
PG6=PGM(:,6);
PG7=PGM(:,7);
PG8=PGM(:,8);
PG9=PGM(:,9);
PG10=PGM(:,10);

PG11=PGM(:,11);
PG12=PGM(:,12);
PG13=PGM(:,13);
PG14=PGM(:,14);
PG15=PGM(:,15);
PG16=PGM(:,16);
PG17=PGM(:,17);
PG18=PGM(:,18);
% PG19=PGM(:,19);
% PG20=PGM(:,20);
```

```
%
% PG21=PGM(:,21);
% PG22=PGM(:,22);
% PG23=PGM(:,23);
% PG24=PGM(:,24);
% PG25=PGM(:,25);
% PG26=PGM(:,26);
% PG27=PGM(:,27);
% PG28=PGM(:,28);
% PG29=PGM(:,29);
% PG30=PGM(:,30);

pwall=[PG12 PG11 PG10 PG9 PG8 PG7 PG18 PG6 PG17 PG5 PG16 PG4 PG15 PG3 PG14...
    PG2 PG13 PG1];%from bottom,up
% pbottom=[PG19 PG20 PG21 PG22 PG23 PG24 PG25];
V0=fliplr(mean(pwall));% change the order, now from the top to the bottom,
                       % and do the average for each column (for each PG),
                       % so that now the matrix is a vector (one row).
% V0u=mean(pbottom);

load calibration_setup2_+07

PG1=PGM(:,1);
PG2=PGM(:,2);
PG3=PGM(:,3);
PG4=PGM(:,4);
PG5=PGM(:,5);
PG6=PGM(:,6);
PG7=PGM(:,7);
PG8=PGM(:,8);
PG9=PGM(:,9);
PG10=PGM(:,10);

PG11=PGM(:,11);
PG12=PGM(:,12);
PG13=PGM(:,13);
PG14=PGM(:,14);
PG15=PGM(:,15);
PG16=PGM(:,16);
PG17=PGM(:,17);
PG18=PGM(:,18);
% PG19=PGM(:,19);
% PG20=PGM(:,20);
%
% PG21=PGM(:,21);
% PG22=PGM(:,22);
% PG23=PGM(:,23);
% PG24=PGM(:,24);
% PG25=PGM(:,25);
% PG26=PGM(:,26);
% PG27=PGM(:,27);
% PG28=PGM(:,28);
% PG29=PGM(:,29);
% PG30=PGM(:,30);

pwall=[PG12 PG11 PG10 PG9 PG8 PG7 PG18 PG6 PG17 PG5 PG16 PG4 PG15 PG3 PG14...
    PG2 PG13 PG1];%from bottom,up
% pbottom=[PG19 PG20 PG21 PG22 PG23 PG24 PG25];
V1=fliplr(mean(pwall));% change the order, now from the top to the bottom,
```

```
                        % and do the average for each column (for each PG),
                        % so that now the matrix is a vector (one row).
% V1u=mean(pbottom);

load calibration_setup2_+10

PG1=PGM(:,1);
PG2=PGM(:,2);
PG3=PGM(:,3);
PG4=PGM(:,4);
PG5=PGM(:,5);
PG6=PGM(:,6);
PG7=PGM(:,7);
PG8=PGM(:,8);
PG9=PGM(:,9);
PG10=PGM(:,10);

PG11=PGM(:,11);
PG12=PGM(:,12);
PG13=PGM(:,13);
PG14=PGM(:,14);
PG15=PGM(:,15);
PG16=PGM(:,16);
PG17=PGM(:,17);
PG18=PGM(:,18);
% PG19=PGM(:,19);
% PG20=PGM(:,20);
%
% PG21=PGM(:,21);
% PG22=PGM(:,22);
% PG23=PGM(:,23);
% PG24=PGM(:,24);
% PG25=PGM(:,25);
% PG26=PGM(:,26);
% PG27=PGM(:,27);
% PG28=PGM(:,28);
% PG29=PGM(:,29);
% PG30=PGM(:,30);

pwall=[PG12 PG11 PG10 PG9 PG8 PG7 PG18 PG6 PG17 PG5 PG16 PG4 PG15 PG3 PG14...
    PG2 PG13 PG1];%from bottom,up
% pbottom=[PG19 PG20 PG21 PG22 PG23 PG24 PG25];
V2=fliplr(mean(pwall));% change the order, now from the top to the bottom,
                        % and do the average for each column (for each PG),
                        % so that now the matrix is a vector (one row).
% V2u=mean(pbottom);

%V0=0*V1;
V=[V0' V1' V2'];        % the apostrophe change rows for coloums, now the
                        % matrix has 3 columns and 18 rows (each row has the
                        % three values calculated for three water depths)
% Vu=[V0u' V1u' V2u'];

% cc=hsv(18);
for i=1:length(V)
    x=V(i,:);
    y=PH(i,:);
    pfit=polyfit(x,y,1); % 1 grade because it has to be a line (pressure
                          % depends only on depth)
```

```
    S(i)=pfit(1);        % S(i) is a row vector containing the slopes
                         % (1 row, 18 columns)
    I(i)=pfit(2);        % I(i) is a row vector containing the intercepts
                         % (1 row, 18 columns)

%     y2=polyval(pfit,x);
%     hold on
%     figure(1)
%     plot(x,y,'x','color', cc(i,:),'LineWidth',1.2)
%     plot(x,y2,'color', cc(i,:),'LineWidth',1.2)
%     hold off
end

% for j=1:length(Vu)
%     i=i+1;
%     x=Vu(j,:);
%     y=PHu;
%     pfit=polyfit(x,y,1);
%     S(i)=pfit(1);
%     I(i)=pfit(2);
% end

S=fliplr(S);           % change the order, now from the bottom to the top,
                       % as it is in the main program
I=fliplr(I);           % change the order, now from the bottom to the top,
                       % as it is in the main program
end
```

C.4 Convertion from Volts to Pressure for the bottom surface of the caisson

```
function [S,I] = signal_to_uplift

% calibration for volts to pressure, for the bottom surface of the caisson.

D1=49.3;
D1=D1+0.7;  % there were 7 mm of water above the edge of the caisson
D0=D1*0;
D2=D1+10;
D=[D0' D1' D2']*10^-2;  % from [cm] to [m]

rho=1000;    % [kg/m^3]
g=9.81;      % [m/s^2]

PH=D*rho*g; % [m/s^2]*[kg/m^3]*[m]=[N/m^2]

load calibration_setup2_air

% PG1=PGM(:,1);
% PG2=PGM(:,2);
% PG3=PGM(:,3);
% PG4=PGM(:,4);
% PG5=PGM(:,5);
% PG6=PGM(:,6);
% PG7=PGM(:,7);
% PG8=PGM(:,8);
% PG9=PGM(:,9);
```

```
% PG10=PGM(:,10);
%
% PG11=PGM(:,11);
% PG12=PGM(:,12);
% PG13=PGM(:,13);
% PG14=PGM(:,14);
% PG15=PGM(:,15);
% PG16=PGM(:,16);
% PG17=PGM(:,17);
% PG18=PGM(:,18);
PG19=PGM(:,19);
PG20=PGM(:,20);

PG21=PGM(:,21);
PG22=PGM(:,22);
PG23=PGM(:,23);
PG24=PGM(:,24);
PG25=PGM(:,25);
% PG26=PGM(:,26);
% PG27=PGM(:,27);
% PG28=PGM(:,28);
% PG29=PGM(:,29);
% PG30=PGM(:,30);

% pwall=[PG12 PG11 PG10 PG9 PG8 PG7 PG18 PG6 PG17 PG5 PG16 PG4 PG15 PG3...
    % PG14 PG2 PG13 PG1];   % from bottom, up
pbottom=[PG19 PG20 PG21 PG22 PG23 PG24 PG25];
% V0=fliplr(mean(pbottom));
V0=mean(pbottom);
% V0u=mean(pbottom);

load calibration_setup2_+07

% PG1=PGM(:,1);
% PG2=PGM(:,2);
% PG3=PGM(:,3);
% PG4=PGM(:,4);
% PG5=PGM(:,5);
% PG6=PGM(:,6);
% PG7=PGM(:,7);
% PG8=PGM(:,8);
% PG9=PGM(:,9);
% PG10=PGM(:,10);
%
% PG11=PGM(:,11);
% PG12=PGM(:,12);
% PG13=PGM(:,13);
% PG14=PGM(:,14);
% PG15=PGM(:,15);
% PG16=PGM(:,16);
% PG17=PGM(:,17);
% PG18=PGM(:,18);
PG19=PGM(:,19);
PG20=PGM(:,20);

PG21=PGM(:,21);
PG22=PGM(:,22);
PG23=PGM(:,23);
PG24=PGM(:,24);
```

```
PG25=PGM(:,25);
% PG26=PGM(:,26);
% PG27=PGM(:,27);
% PG28=PGM(:,28);
% PG29=PGM(:,29);
% PG30=PGM(:,30);

% pwall=[PG12 PG11 PG10 PG9 PG8 PG7 PG18 PG6 PG17 PG5 PG16 PG4 PG15 PG3...
    % PG14 PG2 PG13 PG1];   % from bottom, up
pbottom=[PG19 PG20 PG21 PG22 PG23 PG24 PG25];
% V1=fliplr(mean(pbottom));    % from the top, down
V1=mean(pbottom);
% V1u=mean(pbottom);

load calibration_setup2_+10

% PG1=PGM(:,1);
% PG2=PGM(:,2);
% PG3=PGM(:,3);
% PG4=PGM(:,4);
% PG5=PGM(:,5);
% PG6=PGM(:,6);
% PG7=PGM(:,7);
% PG8=PGM(:,8);
% PG9=PGM(:,9);
% PG10=PGM(:,10);
%
% PG11=PGM(:,11);
% PG12=PGM(:,12);
% PG13=PGM(:,13);
% PG14=PGM(:,14);
% PG15=PGM(:,15);
% PG16=PGM(:,16);
% PG17=PGM(:,17);
% PG18=PGM(:,18);
PG19=PGM(:,19);
PG20=PGM(:,20);

PG21=PGM(:,21);
PG22=PGM(:,22);
PG23=PGM(:,23);
PG24=PGM(:,24);
PG25=PGM(:,25);
% PG26=PGM(:,26);
% PG27=PGM(:,27);
% PG28=PGM(:,28);
% PG29=PGM(:,29);
% PG30=PGM(:,30);

% pwall=[PG12 PG11 PG10 PG9 PG8 PG7 PG18 PG6 PG17 PG5 PG16 PG4 PG15 PG3...
    % PG14 PG2 PG13 PG1];   % from bottom, up
pbottom=[PG19 PG20 PG21 PG22 PG23 PG24 PG25];
% V2=fliplr(mean(pbottom));    % from the top, down
V2=mean(pbottom);
% V2u=mean(pbottom);

%V0=0*V1;
V=[V0' V1' V2'];
% Vu=[V0u' V1u' V2u'];
```

```
y=PH;
% cc=hsv(8);
for i=1:length(V)
    x=V(i,:);
    pfit=polyfit(x,y,1);
    S(i)=pfit(1);
    I(i)=pfit(2);

%     y2=polyval(pfit,x);
%     hold on
%     figure(1)
%     plot(x,y,'x','color', cc(i,:),'LineWidth',1.2)
%     plot(x,y2,'color', cc(i,:),'LineWidth',1.2)
%     hold off
end
% S=fliplr(S);
% I=fliplr(I);
end
```

C.5 Goda forces compared with measured forces

```
clear all
close all
clc

% Horizontal forces
godaH=[166.4    681.6   163.6   535.6   193.1   460.2];
godaH2=[679.8   663.3   628.3];

meaH=[136       544.6   138.7   406.7   153.9   553.1];
meaH2=[930.4    853.8   1561.1];

% Uplift forces
godaU=[130.8    364.4   93.9    271.7   98.8    233.4];
godaU2=[403.7   352.1   326.5];

meaU=[72.8      141.0   51.2    174.4   55.7    171.3];
meaU2=[334.4    352.6   346.4];

% Overturning moments
godaO=[52.7     177.5   46.7    144.1   53.2    126.1];
godaO2=[187.4   183.8   175.5];

meaO=[40.2      133.8   41.4    120     42.9   189.0];
meaO2=[320.5    293.9   589.9];


% P=polyfit(mea,goda,1);
% x=0:1600;
% y=polyval(P,x);

figure(1)
hold on
plot(meaH,godaH,'bo','LineWidth',1.2)
plot(meaH2,godaH2,'ro','LineWidth',1.2)
xlabel('measured [N/m]')
ylabel('Goda [N/m]')
```

```
xlim([0 1600])
ylim([0 1600])
plot([0 1600],[0 1600],'k')
%plot(x,y,'r')
legend('Non-Breaking','Breaking','45\circ line')
grid off

figure(2)
hold on
plot(meaU,godaU,'bo','LineWidth',1.2)
plot(meaU2,godaU2,'ro','LineWidth',1.2)
xlabel('measured [N/m]')
ylabel('Goda [N/m]')
xlim([0 600])
ylim([0 600])
plot([0 600],[0 600],'k')
%plot(x,y,'r')
legend('Non-Breaking','Breaking','45\circ line')
grid off

figure(3)
hold on
plot(meaO,godaO,'bo','LineWidth',1.2)
plot(meaO2,godaO2,'ro','LineWidth',1.2)
xlabel('measured [Nm/m]')
ylabel('Goda [Nm/m]')
xlim([0 600])
ylim([0 600])
plot([0 600],[0 600],'k')
%plot(x,y,'r')
legend('Non-Breaking','Breaking','45\circ line')
grid off

pl_11=meaH;
pl_12=meaH2;
pl_21=meaH/godaH;
pl_22=meaH2/godaH2;

figure(4)
hold on
plot(pl_11,pl_21,'ro','LineWidth',1.2)
plot(pl_12,pl_22,'bo','LineWidth',1.2)
xlabel('measured [N/m]')
ylabel('measured / predicted with Goda [-]')
plot([0 1600],[1 1],'k')
%plot(x,y,'r')
%legend('Non-Breaking','Breaking')
xlim([0 1600]);
ylim([0.5 2])
box on
grid on
hold off
```